



Aalborg Universitet

AALBORG UNIVERSITY  
DENMARK

## Multispot fiber laser welding

Schutt Hansen, Klaus

DOI (link to publication from Publisher):  
[10.5278/vbn.phd.engsci.00043](https://doi.org/10.5278/vbn.phd.engsci.00043)

Publication date:  
2015

Document Version  
Publisher's PDF, also known as Version of record

[Link to publication from Aalborg University](#)

Citation for published version (APA):  
Schutt Hansen, K. (2015). *Multispot fiber laser welding*. Aalborg Universitetsforlag. Ph.d.-serien for Det Teknisk-Naturvidenskabelige Fakultet, Aalborg Universitet <https://doi.org/10.5278/vbn.phd.engsci.00043>

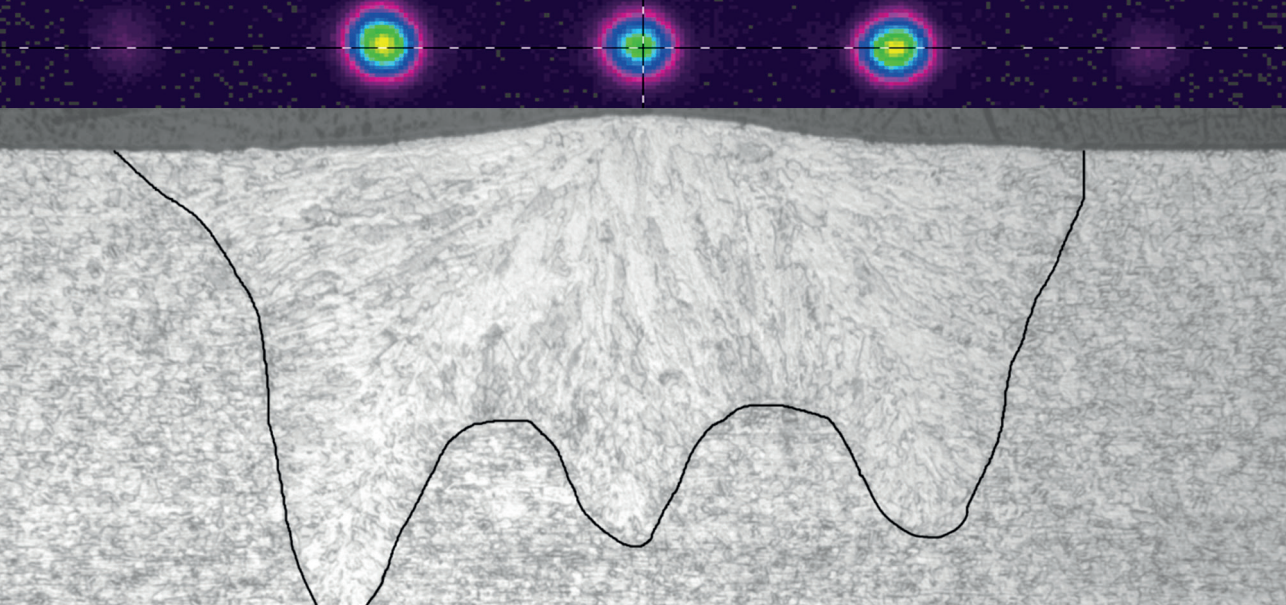
### General rights

Copyright and moral rights for the publications made accessible in the public portal are retained by the authors and/or other copyright owners and it is a condition of accessing publications that users recognise and abide by the legal requirements associated with these rights.

- Users may download and print one copy of any publication from the public portal for the purpose of private study or research.
- You may not further distribute the material or use it for any profit-making activity or commercial gain
- You may freely distribute the URL identifying the publication in the public portal -

### Take down policy

If you believe that this document breaches copyright please contact us at [vbn@aub.aau.dk](mailto:vbn@aub.aau.dk) providing details, and we will remove access to the work immediately and investigate your claim.



# **MULTISPOT FIBER LASER WELDING**

INDUSTRIAL PHD PROJECT

BY  
**KLAUS SCHÜTT HANSEN**

DISSERTATION SUBMITTED 2015



**AALBORG UNIVERSITY**  
DENMARK



# MULTISPOT FIBER LASER WELDING

INDUSTRIAL PHD PROJECT

by

Klaus Schütt Hansen



Dissertation submitted 23-12-2015

Thesis submitted: December 23, 2015

PhD supervisors: Professor Ole Madsen  
Aalborg University  
Associate professor Morten Kristiansen  
Aalborg University

Industrial supervisor: Senior engineer Flemming Ove Olsen  
IPU

PhD committee: Associate professor Benny Ørtoft Endelt (chair.)  
Aalborg University  
Professor Alexander F. H. Kaplan  
Luleå Tekniska Universitet  
Project coordinator Claus Bagger  
Novo Nordisk A/S

PhD Series: Faculty of Engineering and Science, Aalborg University

ISSN (online): 2246-1248  
ISBN (online): 978-87-7112-291-6

Published by:  
Aalborg University Press  
Skjernvej 4A, 2nd floor  
DK – 9220 Aalborg Ø  
Phone: +45 99407140  
aauf@forlag.aau.dk  
forlag.aau.dk

© Copyright: Klaus Schütt Hansen

Printed in Denmark by Rosendahls, 2015



## CV

In 2008, I graduated as a mechanical engineer from the Technical University of Denmark. Since then I have been working at IPU. My work here consists of providing expertise on thermal processes with a particular focus on laser processes. In addition I have worked with equipment development for laser processes.

In 2011 I began working on my PhD entitled: "Multi-fiber laser beam welding" in cooperation with the Department of Mechanical and Manufacturing Engineering at Aalborg University. The purpose of this project is to establish methods for the optimisation of beam patterns during laser welding.



# ENGLISH SUMMARY

This dissertation presents work and results achieved in the field of multi spot fiber laser welding. The project has had an empirical approach, and simulations and modelling have been kept at a minimum.

It is assumed, that laser welding with multiple spots can provide new tools for laser welding. First different methods to produce spot patterns with high power single mode fiber lasers have been examined and evaluated. It is found that both diamond turned DOE's (Diffractive Optical Elements) in zinc sulphide and multilevel etched DOE's in fused silica have a good performance. In addition it is found that both also will be good candidates for implementation in an industrial setup. Further tests, to ensure that thermal drift won't be a problem, are needed.

For implementation of spot patterns in industrial setups it will often be necessary to rotate the pattern. Hence, an example of a DOE rotator have been specified and developed in cooperation with the Robocut project, which aims to improve laser cutting by applying beam patterns.

Also welding with multiple spots in a butt joint configuration has been tested. Results are presented, showing it has been possible to control the welding width in incremental steps by adding more spots in a row. The laser power was used to independently control the keyhole and consequently the depth of fusion.

An example of inline repair of a laser weld in a butt joint configuration was examined successfully. Zinc powder was placed in the weld causing expulsion of the melt pool. Trailing beams were applied to melt additional material and ensure a melt pool.

High speed recording of multibeam laser welding was tested. The purpose was to get knowledge about the process during multi spot fiber laser welding, especially information on flow patterns and behaviour of the individual keyholes and their interaction. Unfortunately, the details in the recordings were either overexposed or too dark to obtain any useful information.

Last equipment for measuring and analysing high power laser beam patterns has been developed in the project. It is built around a CCD camera, where beam splitters and proper attenuation are placed in front of the CCD chip. If full attenuation is used, it is possible to measure laser beams with up to 3 kW of laser power focused to a spot with a diameter of 50  $\mu\text{m}$ . A simple approach for comparing and evaluating measured beams patterns with the chosen design has been established, and it is applied in the evaluation of the different spot pattern



designs and in the evaluation of the four different beam shaping techniques tested. It is found that diamond turned DOE's, multi-level etched DOE's and the flexible beam shaping platform used provide sufficient quality in the produced patterns.

**Keywords:** Laser welding; beam shaping; multi beam laser welding; diffractive optics; DOE; single mode fiber laser; multispot laser welding.

# DANSK RESUMÉ

I denne afhandling præsenteres det arbejde og de resultater, som er opnået inden for flerstråle lasersvejsning med fiber laser. Projektet har haft en empirisk tilgang, og simulerings- og modelleringsarbejde er holdt på et minimum.

Det er grundlæggende antaget, at lasersvejsning med flere spots kan give nye værktøjer til brug i lasersvejsning. Først er der testet forskellige metoder til at producere strålemønstre med højeffekt single mode fiber lasere. Ud fra de testede metoder er det konkluderet, at diamantdrejede DOE'er (Diffraktive Optiske Elementer) fremstillet i zinksulfid og flertrins ætsede DOE'er i kvartsglas fungerer godt. Testen viser også, at de begge er gode kandidater til brug i et industrielt miljø. Der er dog behov for yderligere tests for at sikre, at DOE'erne ikke bliver termisk belastet og forårsager termisk drift af strålemønstret.

For at kunne anvende flerstråle løsninger i en industriel produktion vil det ofte være nødvendigt at kunne rotere mønstret. Der er derfor specificeret og udviklet en DOE rotator i samarbejde med Robocut projektet. I Robocut projektet arbejdes der på at forbedre laserskæring ved at anvende strålemønstre.

Der er også udført tests med svejsninger med et flerstrålemønster, hvor strålerne placeres på en række, som er vinkelret på svejseretningen. Svejsningen blev udført som en længde/stød samling. Resultaterne viste, at det var muligt at kontrollere svejsebredden trinvis ved at tilføje flere stråler i rækken. Laserenergien blev brugt til – uafhængigt af svejsebredden – at kontrollere nøglehullet og dermed svejsedybden.

Der er succesfuldt gennemført forsøg med en kontinuert reparationssvejsning på en længdesamling ved at anvende et langt strålemønster. I samlingen var der placeret zinkpulver, som ved opvarmning fordampede og blæste smeltebadet væk. De efterfølgende stråler sørgede for, at der blev smeltet nyt materiale, hvorved smeltebadet kunne opretholdes.

Højhastighedsoptagelser af flerstråle lasersvejsning blev testet. Formålet med optagelserne var at få viden om multistråle fiberlaser svejseprocessen og især blive klogere på flowmønstre og de enkelte nøglehullers opførsel og interaktion med hinanden. Desværre er det ikke muligt i disse optagelser at se detaljerne i flowmønstrene tydeligt nok, da detaljerne enten er overeksponerede eller for mørke i samme billede til at kunne bruges til at se flowmønstrene.

Sidst er der udviklet udstyr til måling og analyse af højeffekts laserstråler som en del af projektet. Udstyret er bygget omkring et CCD kamera, hvor der foran CCD-

chippen er placeret et antal strålesplittere og -dæmpere. Systemet tillader brug af laserenergi på op til 3 kW fokuseret til en plet med en diameter på 50  $\mu\text{m}$ . Der er defineret en simpel tilgang til analyse og sammenligning af de målte strålemønstre med de designede strålemønstre. Denne tilgang har været anvendt til evaluering af fire forskellige stråleomformningsteknikker, som har været testet. Resultaterne viste, at diamantdrejede DOE'er, flertrins ætsede DOE'er og IPUs fleksible platform til produktion af strålemønstre leverede høj nok kvalitet i de producerede mønstre.

**Nøgleord:** Lasersvejsning; stråleomformning; flerstråle lasersvejsning; diffraktiv optik; DOE; single mode fiber laser; lasersvejsning med flere spots

# ACKNOWLEDGEMENTS

During the course of this project I have received a lot of assistance and support from supervisors, family and friends.

An industrial PhD thesis such as this one has several interests, thus it is a challenge to balance it and keep the project on its track. For help with this I would like to express a special thanks to my supervisors: My colleague and supervisor Flemming Olsen, whom has always provided great input and support, whenever unforeseen problems and challenges have occurred. Ole Madsen, whom has provided academic supervision, and Morten Kristiansen, whom has given invaluable feedback on papers and experiments.

The cooperation with the Robocut project has allowed producing and testing expensive optical parts and equipment, which otherwise would not have been possible.

Veli Kujanpää and Petri Laakso from VTT Lappeenranta deserve special thanks for hosting a two month stay, providing lab access and lending out high speed recording equipment.

Grundfos and Danfoss deserve acknowledgement for their support and input about industrial cases and feedback on these.

I need to pay special thanks to IPU and Mogens Arentoft for providing me with the flexibility to spend four years completing the project. Forsknings- og Innovationsstyrelsen are acknowledged for co-financing the project.

I have not mentioned all the assistance, I have received from various lab employees, colleagues, workshops and family. You all know who you are. Thank you!

Finally a special thanks to Nina and my children for the support and accept of all the extra working hours. I love you.

Winter 2015

Klaus Schütt Hansen

# MANDATORY PAGE

Thesis title: Multispot fiber laser welding

Name of PhD student: Klaus Schütt Hansen

Name and title of supervisor and any other supervisors:

Professor Ole Madsen

Associate professor Morten Kristiansen

Senior engineer Flemming Ove Olsen

Papers:

- Paper A: Design of measurement equipment for high power laser beam shapes  
Authors: Klaus Schütt Hansen, Flemming Ove Olsen, Morten Kristiansen, Ole Madsen  
Outlet: NOLAMP 14, 2013
- Paper B: Beam shaping to control of weldpool size in width and depth  
Authors: Klaus Schütt Hansen, Morten Kristiansen, Flemming Ove Olsen  
Outlet: 8th International Conference on Photonic Technologies LANE 2014
- Paper C: Joining of multiple sheets in a butt-joint configuration using single pass laser welding with multiple spots  
Authors: Klaus Schütt Hansen, Flemming Ove Olsen, Morten Kristiansen, Ole Madsen  
Outlet: Journal of Laser Applications (Published, 3<sup>rd</sup> June 2015)
- Paper D: Inline repair of blowouts during laser welding  
Authors: Klaus Schütt Hansen, Flemming Ove Olsen, Morten Kristiansen, Ole Madsen  
Outlet: Welding in the world (abstract accepted, changes prior to acceptance is required)
- Paper E: Multispot laser welding to improve process stability  
Authors: Klaus Schütt Hansen, Flemming Ove Olsen, Morten Kristiansen, Ole Madsen  
Outlet: World of Photonics Congress - Lasers in Manufacturing , 2015 (published, June 2015)

This dissertation has been submitted for assessment in partial fulfilment of the PhD degree. The dissertation is based on the submitted or published scientific papers which are listed above. Parts of the papers are used directly or indirectly in the extended summary of the dissertation. As part of the assessment, co-author statements have been made available to the assessment committee and are also available at the Faculty. The dissertation is not in its present form acceptable for open publication, but only in limited and closed circulation as copyright may not be ensured for all papers.

# TABLE OF CONTENTS

|   |           |
|---|-----------|
| Nomenclature .....  | 8         |
| Abbreviations and symbols .....   | 8         |
| Terminology .....   | 9         |
| <b>Chapter 1. Introduction.....</b>   | <b>11</b> |
| 1.1. Background .....   | 11        |
| 1.2. Historical background .....  | 11        |
| 1.2.1. Industrial background.....   | 12        |
| 1.3. Problem domain .....   | 15        |
| 1.4. Dissertation structure .....   | 16        |
| <b>Chapter 2. State-of-the-art .....</b>                                      | <b>18</b> |
| 2.1. Fiber laser technology .....   | 18        |
| 2.2. Laser welding technology .....   | 22        |
| 2.2.1. Light coupling and plasma in laser welding.....                        | 24        |
| 2.2.2. Effects of improved brightness .....                                   | 25        |
| 2.2.3. Techniques to improve laser welding.....                               | 27        |
| 2.2.4. Tools for analysing laser welding .....                                | 28        |
| 2.3. Beam shaping technology .....  | 29        |
| 2.3.1. Manufacturing techniques for DOE's .....                               | 35        |
| 2.4. Multi beam laser welding.....  | 37        |
| 2.5. Modelling of laser welding .....   | 43        |
| <b>Chapter 3. Problem formulation .....</b>                                   | <b>45</b> |
| 3.1. Hypothesis.....  | 45        |
| 3.2. Research objectives.....   | 46        |
| 3.3. Approach.....  | 47        |
| 3.4. Advisory group.....  | 47        |
| <b>Chapter 4. Equipment, construction, beam patterns and experiments.....</b> | <b>49</b> |
| 4.1. Experimental setup at IPU.....   | 49        |
| 4.1.1. Flexible beam shaping unit at IPU .....                                | 51        |
| 4.2. Experimental setup at AAU .....  | 52        |
| 4.2.1. Integration into commercial laser heads.....                           | 52        |
| 4.2.2. Thermal load .....   | 55        |
| 4.2.3. DOE rotator.....   | 56        |

|   |           |
|---|-----------|
| 4.3. Summary of Paper A: Design of measurement equipment for high power laser beam shapes .....   | 58        |
| 4.3.1. Objectives .....   | 58        |
| 4.3.2. Results .....  | 59        |
| 4.3.3. Analysing of thermal drift .....   | 61        |
| 4.3.4. Further work .....   | 61        |
| 4.4. Test of DOE's .....  | 61        |
| 4.4.1. Measurement definitions and terminology .....  | 63        |
| 4.4.2. Gray scale etched DOE's .....  | 66        |
| 4.4.3. Multilevel etched DOE .....  | 67        |
| 4.4.4. Diamond turned DOE .....   | 69        |
| 4.4.5. Flexible beam shaping unit .....   | 73        |
| 4.4.6. Discussion and comparison of performance .....   | 73        |
| 4.4.7. Discussion .....   | 75        |
| 4.5. High speed photographing .....   | 77        |
| 4.5.1. Introduction .....   | 77        |
| 4.5.2. Setup .....  | 78        |
| 4.5.3. Experiments .....  | 79        |
| 4.5.4. Results .....  | 80        |
| 4.5.5. Suggestions for improvements .....   | 81        |
| 4.5.6. Conclusion .....   | 82        |
| <b>Chapter 5. Examples of multispot fiber laser welding .....</b>   | <b>83</b> |
| 5.1. Summary of Paper B: Beam shaping to control of weldpool size in width and depth .....  | 83        |
| 5.1.1. Objectives .....   | 84        |
| 5.1.2. Results .....  | 84        |
| 5.1.3. Conclusion .....   | 88        |
| 5.1.4. Further work .....   | 88        |
| 5.2. Summary of Paper C: Joining of multiple sheets in a butt-joint configuration using single pass laser welding with multiple spots ..... | 88        |
| 5.2.1. Objectives .....   | 88        |
| 5.2.2. Results .....  | 89        |
| 5.2.3. Conclusion .....   | 94        |
| 5.2.4. Further work .....   | 95        |
| 5.3. Summary of Paper D: Inline repair of blowouts during laser welding .....   | 96        |
| 5.3.1. Objectives .....   | 96        |

|   |            |
|---|------------|
| 5.3.2. Results .....  | 97         |
| 5.3.3. Conclusion .....   | 99         |
| 5.3.4. Further work .....   | 100        |
| 5.4. Summary of Paper E: Multispot laser welding to improve process stability   | 100        |
| <b>Chapter 6. Discussion &amp; future work .....</b>  | <b>102</b> |
| 6.1. Effect of spot power/intensity .....   | 102        |
| 6.2. Implementation possibilities .....   | 103        |
| 6.3. Possible welding cases for this technology .....   | 104        |
| <b>Chapter 7. Conclusion .....</b>  | <b>105</b> |
| <b>Literature list.....</b>   | <b>109</b> |
| <b>Appendices.....</b>  | <b>119</b> |
| <b>Appendix A: Design of measurement equipment for high power laser beam shapes .....</b>   | <b>1</b>   |
| <b>Appendix B: Beam shaping to control of weldpool size in width and depth .....</b>  | <b>17</b>  |
| <b>Appendix C: Joining of multiple sheets in a butt-joint configuration using single pass laser welding with multiple spots .....</b> | <b>34</b>  |
| <b>Appendix D: Inline repair of blowouts during laser welding .....</b>   | <b>52</b>  |
| <b>Appendix E: Multispot laser welding to improve process stability .....</b>   | <b>71</b>  |



# TABLE OF FIGURES

|  |    |
|--|----|
| Figure 1 Terminology for a standard modified laser head used for welding with lasers with fiber transmission.....  | 10 |
| Figure 2 The overall objective of this project is to investigate the new possibilities which arise through a combination of beam shaping technology, single mode fiber laser technology and laser welding technology.....  | 16 |
| Figure 3 Principle of resonator in a fiber laser. a) Produces a multimode beam, as the emission of photons is based on a spontaneous emission in the active fiber. b) Produces a single mode signal, as the active fiber amplifies the signal from the master oscillator (seed laser). Reprint from [116]..... | 19 |
| Figure 4 Principle structure of amplification in a single mode fiber laser [9].....  | 20 |
| Figure 5 Sketch showing the principle in keyhole welding. Constructed from [35].   | 23 |
| Figure 6 Laser welding process. Vertical fixed input parameters. Horizontal input variables, and process output parameters. ....   | 24 |
| Figure 7 a) Illustration of a beam consisting of plane waves going through a duplet lens and being focused. Reprint from Wikimedia [72]. b) Sketch of a plane wave going through a DOE. Here the plane waves are being reshaped. The reshaped waves then pass the focussing lens. ....                         | 30 |
| Figure 8 Top row: Energy distributions from a) DOE beam shaper, b) DOE beam diffuser and c) DOE beam splitter. Bottom row corresponding transmission phase/DOE pattern for the transformation. ....  | 34 |
| Figure 9 Cross section of a DOE. Example of shadow effect on the outgoing reflection of the laser beam for a reflective DOE. Dimension is out of scale, ratio between depth and width $\gg 1$ . ....   | 35 |
| Figure 10 Binary mask $2^N$ fabrication process for DOE's. Rework from [81]. ....  | 36 |
| Figure 11 Example of two suggested energy distributions to be used in the project.   | 46 |
| Figure 12 Initial optical setup at IPU. Left: Photo from the optical bench.. Right: Principal beam path for the setup. Note the many mirrors and the hereby large alignment task. ....   | 50 |
| Figure 13 principle construction of flexible beam shaping processing at IPU.....   | 51 |
| Figure 14 Left: Photo of SLM with white cover plate together with rest of necessary optics. Right: Components and construction around lens and camera solution in the IPU setup.....   | 52 |
| Figure 15 Left) HighYAG laser head mounted with 780 mm focus lens. Middle) Optoskand laser head with 300 mm focus lens. Both shown with principle beam propagation and in same scale. Right: DOE drawer in detail.....   | 54 |

|   |    |
|---|----|
| Figure 16 HighYAG laserhead mounted in robot cell. The robot is only used as fixture, as the movements in this project where performed using the XY stage. ....   | 55 |
| Figure 17 DOE rotator with some of the protective housing removed. Arm with DOE shown in “open position”. a) CAD image. b) Photo. ....  | 57 |
| Figure 18 The constructed CCD camera based assembly with attenuation, beam dumps and protective cover. Rework from “paper A: Design of measurement equipment for high power beam shapes” [100]. a) The full setup with beam dump in bottom. b) Zoom on the region with camera and attenuation. See appendix A for full details of beam path. ....   | 59 |
| Figure 19 a) Profile with 1.3 kW. b) Profile recorded with 60 W. Both with 780 mm focal length $\Delta Z = 3$ mm between each plane. ....   | 60 |
| Figure 20 Design and naming of different parts in the pattern. ....   | 62 |
| Figure 21 Optoskand laser head with DOE drawer, and the terminology used. Principle beam path is shown to the left. ....  | 63 |
| Figure 22 Spot pattern with designed, simulated and measured energy distributions. In the measured data is shown examples of three apertures for evaluation. Numbers are rounded values, and sum in the two first rows yield 101%. Rework of data from paper C: Joining of multiple sheets in a butt-joint configuration using single pass laser welding with multiple spots” [101]. ....   | 64 |
| Figure 23 Top left) Example of transmission phase in grayscale values. Top right) Transmission phase calibrated with Bottom left) calibration curve. Bottom right) Calibrated transmission with control patterns in the corners. ....   | 67 |
| Figure 24 Fabrication process and resulting surface geometry. (nTFS is the position of the tool in the material). a) Scheme for the machining process for DOE's. b) Schematic structure in the feed direction and imprint of the diamond tool shape. c) Section of the surface of the DOE. d) Detailed view of the same part of the surface. The highlighted area corresponds to one single cutting depth value in the control signal of the nFTS (the highlighted area corresponds to one pixel). The maximum height difference displayed equals 700nm. Reprinted from Dankwart et.al [76]. .... | 70 |
| Figure 25 Design and model of pattern together with the four tested methods for beam shaping. a) Design. b) Modelled performance. c) Best result achieved from several attempts of grey scale etching with same design. d) Multilevel etched DOE. e) Diamond turned DOE. f) Flexible beam shaping unit. ....  | 74 |
| Figure 26 Setup for high speed photographing. Top) Principle. Bottom) Actual setup. ....  | 79 |
| Figure 27 Welding with the seven spot DOE. Details of spot pattern are given in the paper “Beam shaping to control of weldpool size in width and depth”, Hansen et.al. [110]. ....  | 80 |
| Figure 28 Sequence of images in a sideview. Welding is perfomed with the seven spot DOE. Timedistance between each frame is 80 $\mu$ s. ....  | 81 |

|   |    |
|---|----|
| Figure 29 Principle of placing multiple laser spots on a row for controlling weldpool geometry. Sketched on a joint containing four sheets. “a” indicates spot distance. .  | 84 |
| Figure 30 a) Simulated intensity and intensity profile with DOE “as designed. b) Cross section of the phase transmission “as designed”. c) Simulated intensity and intensity profile for a DOE which is etched to 80%. d) Cross section of phase transmission at 80% and grey scale view of the phase transmission. All arrows in the figure shows where the respectively intensity/phase profiles are taken. ....                                      | 85 |
| Figure 31 Measured energy profile from three spot DOE.....  | 85 |
| Figure 32 Measured energy profile from seven spot DOE.....  | 86 |
| Figure 33 Cross sections of welds with 139 $\mu$ m spot performed: a) with three spot DOE, 800 W, 50 mm/s, b) with seven spot DOE, 50 mm/s, 1500 W. Spot patterns shown above with same scale as cross sections. ....   | 87 |
| Figure 34 Relation between power, penetration depth and focus spot size for the individual beams in the pattern for stainless steel and three spot DOE.....   | 87 |
| Figure 35 Surface of a typical weld for performed with a three spot pattern in stainless steel.....   | 87 |
| Figure 36 Top row) Measured spot pattern using an intensity sensitive CCD camera. Bottom row) The resulting cross-sections for different spot distances performed as bead on sheet, all with focus placed on top of the sheet. (F0). Power is set to an average of 200 W per spot. All figures have the same scale. ....  | 90 |
| Figure 37 Top row) Measured spot pattern using an intensity sensitive CCD camera. Differences in intensity between images are due to different power settings in the laser as the number of spots are increased. Bottom row) The resulting cross-sections for different spot distances performed as bead on sheet, all with focus placed on top of the sheet. (F0). Power is set to an average of 200 W per spot. All figures have the same scale. .... | 90 |
| Figure 38 Dimensions of welds shown in figure 37.....   | 91 |
| Figure 39 Cross-sections for different laser power performed as bead on sheet, all with focus placed on top of the sheet. (F0). Distances are a = 300 $\mu$ m in all cases. Powers are average power per spot in the pattern. The applied pattern is the same as the one shown for the three spot patterns with a = 300 $\mu$ m spacing in figure 36. All figures have the same scale. ....   | 91 |
| Figure 40 Dimensions of welds shown in figure 39.....   | 91 |
| Figure 41 Decreasing travel speed, three spots, constant power at total 600W, focus F0 and spot spacing at a = 300 $\mu$ m. The applied pattern is the same as in figure 5 with a = 300 $\mu$ m spacing. ....   | 92 |
| Figure 42 Dimensions of welds shown in figure 41.....   | 92 |
| Figure 43 Three spots pattern with a spot distance of a = 300 $\mu$ m and 200 W average power per spot.....   | 92 |

|   |    |
|---|----|
| Figure 44 Multiple butt joining with alignment errors and positioning tolerances: a) for the configuration shown in figure 46, b) for the configuration shown in figure 45. ....                            | 93 |
| Figure 45 Cross sections from increased gaps and bridging by a five spot pattern, on two sheets in a butt joint configuration. ....   | 93 |
| Figure 46 Double butt joints with increasing height of centre sheets. All welds are performed with four or five spots and similar parameters. Initial geometry is outlined. ....                            | 94 |
| Figure 47 Principle for applying a second row of spots. ....  | 96 |
| Figure 48 Spot pattern and definitions for experiments to determine power ratios. Individual spots are $\varnothing 85 \mu\text{m}$ . ....  | 97 |
| Figure 49 The power ratios for equal depth of fusion for varied distances between main spots and trailing spot for one power level. Performed with $a = 300 \mu\text{m}$ . ....                             | 97 |
| Figure 50 Graph of distance and required power to penetrate weld pool for different power. ....   | 98 |
| Figure 51 a) Two spot pattern. b) Weld with two spot pattern. c) Four spot pattern. d) Weld with four spot pattern. Both crosssections taken are at the location, where the zinc powder was deposited. .... | 99 |

## Nomenclature

### Abbreviations and symbols

| Symbol                    | Unit                   | Description   |
|---------------------------|------------------------|---|
| $\alpha$                  | $K^{-1}$               | Linear expansion coefficient  |
| $a$                       | mm                     | Spot distance perpendicular to welding direction  |
| $A$                       | $mm^2$                 | Area  |
| $b$                       | mm                     | Spot distance from main spots to trailing spots in a spot pattern with multiple row of spots        |
| <b>BPP</b>                | mm mrad                | Beam Parameter Product  |
| <b>Brightness</b>         | $kW/(mm^2 \text{ sr})$ | Intensity related to focusability   |
| $c$                       |                        | Spot distance perpendicular to welding direction for trailing spots                                 |
| $c_p$                     | mm                     | Heat capacity   |
| $d_{1-3}$                 | mm                     | Distance tolerances in butt joint configuration with multiple sheets                                |
| $D_0$                     | mm                     | Collimated beam diameter  |
| $D_{\min}$                | mm                     | Focused beam diameter   |
| $d_{\max}$                | mm                     | Maximum etching depth   |
| <b>DOE</b>                |                        | Diffractive Optical Element   |
| $dn$                      |                        | (delta n) Change in refractive index  |
| $dT$                      |                        | (delta T) Change in temperature   |
| $E$                       | [Count value]          | Energy. Refers to pixel value measured using a CCD camera. This is proportional to local intensity. |
| $E_{\text{meas}}$         | [Count value]          | Energy measured in a given area using a CCD camera This is proportional to local intensity.         |
| $E_{\text{total}}$        | [Count value]          | Total energy measured in a spot pattern using a CCD camera This is proportional to local intensity. |
| $\eta$                    |                        | Efficiency  |
| $\eta_{\text{energy}}$    | %                      | Energy efficiency of total energy in a spot pattern   |
| $\eta_{\text{transform}}$ | %                      | Transformation efficiency for a spot pattern  |
| $\eta_{\text{electric}}$  | %                      | Transformation efficiency from electric energy to emitted light from a laser resonator              |
| $F$                       | mm                     | Focus position relative to work piece. Negative indicates a focus inside the workpiece              |
| $F_{\text{col}}$          | mm                     | Focal length of collimation lens  |
| $F_{\text{foc}}$          | mm                     | Focal length of focusing lens   |
| $h_{1-3}$                 | mm                     | Height tolerances in butt joint configuration with multiple sheets                                  |
| $i$                       |                        | Counter in sum function   |
| $I$                       | $kW/mm^2$              | Intensity   |
| $\lambda$                 | mm                     | Wavelength  |
| $\lambda$                 | $W/(m \text{ K})$      | Thermal conductivity  |

| Symbol                    | Unit | Description   |
|---------------------------|------|---|
| $M^2$                     |      | Beam quality factor. Is always $\geq 1$ . 1 Corresponds to a perfect Gaussian energy distribution with a perfect plane wavefront in the focal region. |
| $N$                       |      | Number of etching steps/masks in multilevel etching   |
| $n$                       |      | Refractive index  |
| $n_{\text{mat}}$          |      | Refractive index of a material  |
| $n_{\text{air}}$          |      | Refractive index of air (1.03)  |
| $n_{\text{fused silica}}$ |      | Refractive index of fused silica (1.45)   |
| $P$                       | kW   | Laser power   |
| $P_i$                     | kW   | Laser power for spot $i$  |
| $P_{\text{max}}$          | kW   | Max laser power   |
| $R$                       | %    | Reflectance   |
| $\tau_i$                  | %/cm | Internal transmittance  |
| $v$                       | mm/s | Travel speed  |

### Terminology

Figure 1 shows some of the basic terms and definitions used throughout the report.

The term *beam* refers to a laser beam from a laser resonator. This beam can be inside a fiber, be diverging, converging, focused etc.

The term *spot* refers to a part of the energy from a laser beam, which is focused to a limited area. In general spots are clearly separated in the focus region, and it is easy to distinguish a limited area which each spot is covering. A *spot* can also be the full part of a laser beam when no pattern is applied. *Spots* always refer to *energy* from *laser beam(s)* which is either in its focus or in the close distance from its focus position.

In the report the two terms single mode fiber laser and high brightness are used several times. A single mode fiber laser with more than 100 W of power is by the author considered to classify as a “high brightness laser”. Further it is possible to produce single mode fiber lasers with different doping materials. In this report “single mode fiber laser” always refers to an Ytterbium doped fiber laser with a wavelength of 1075 nm.

Especially in state-of-the-art there is a distinction between single mode fiber laser and high brightness lasers, as other laser sources than a single mode fiber laser can be considered. Brightness is defined in section “2.2.2 Effects of improved brightness”

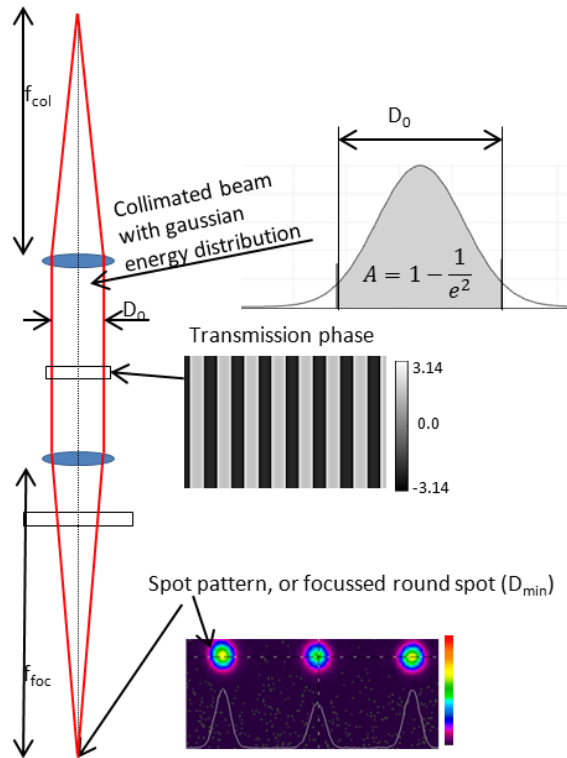


Figure 1 Terminology for a standard modified laser head used for welding with lasers with fiber transmission.

# CHAPTER 1. INTRODUCTION

## 1.1. BACKGROUND

Chapter 1 contains a short historical introduction to the laser and development of lasers. The introduction ends with the development of the modern fiber laser, which is used in this project. Also a short industrial and historical background for laser welding is presented.

The two historical sections form the background for the problem domain for the project. The problem domain presents the technologies and ideas investigated in the project.

## 1.2. HISTORICAL BACKGROUND

Many of the basic principles of the laser were developed in the 1950's and the first laser was built in 1960. Since then many different types of lasers have been developed [1]. New lasers with other wavelengths, higher power, better beam quality and lower costs have given rise to new possibilities in almost every context of science and production.

In 1963, the first experiments with laser welding were performed, by W.N. Platte and J.R. Smith, using a pulsed ruby laser. Four years later, Arthur Sullivan performed the first oxygen assisted laser cutting using a CO<sub>2</sub> laser [2]. From then on the laser has been a competitor to other techniques within welding and other mechanical processes.

The first lasers only gave low power, but this quickly changed as new lasers with higher power were developed, and the term "high power laser" has continuously referred to lasers with increasingly higher power and increased brightness.

Throughout the years many different welding methods have been developed. These are generally divided into two groups: fusion welding and solid state welding. Laser welding belongs to the fusion welding group. In this group most methods deliver the energy required for fusion at the surface of the parts. Therefore, in order to perform deep welds, these methods rely on heat conductivity, and they often require multiple passes whenever dimensions are increased. Only a few welding methods provide the option of delivering the energy deep within the material. Laser welding is one of the methods allowing for deep penetration welding, also known as laser keyhole welding [3].



In the beginning, laser macro welding was primarily performed using CO<sub>2</sub> lasers. Later this shifted towards Nd:YAG lasers being used for welding and CO<sub>2</sub> lasers for cutting. The Nd:YAG laser then changed further from being lamp pumped to being diode pumped. In 1990 the fiber laser entered the market, in the beginning only with a few watts. It was originally used in the telecommunication industry, but it was quickly discovered, that the power could be scaled and therefore might be useful in the material processing industry. Since its introduction in 1990, the power has increased with a factor of ten every fifth year, reaching 100 kW in 2014 [4], [5].

The disc laser was developed by Trumpf GmbH as a competitive technology and was also marketed as a fiber laser, although the active gain medium is not in a fiber, it is on a thin disc. However, the light from the laser is fiber guided from the resonator to the process head [6].

Direct diode lasers for the welding of metals are also marketed by several companies. The advantage of the diode laser is that the diode light produced is directly transmitted to the process zone without the extra lasing step which is involved in diode pumped Nd:YAG lasers, fiber lasers or discs lasers. This results in a cheaper product with higher electric-optical efficiency. The beam quality is also lower, as the beam consists of a relative large area of diode lasers. In 2009 TeraDiode announced a new diode laser concept in which multiple diodes with slightly different wavelengths were combined. This resulted in a higher beam quality while maintaining the high power [7], [8].

Industry has always demanded lasers with higher power, better beam quality and lower price. With the introduction of the fiber laser to the laser material processing market at least the two first demands were met. The scalability of the fiber laser has provided the possibility to produce up to at least 100 kW of laser power for a multimode laser and at least up to 20 kW of laser power for a single mode laser [9] [5].

The fiber laser and disc laser have turned out to be almost maintenance free with promised lifetimes of 20.000 hours or more. Moreover, they have an electric to optical efficiency higher than any other industrial laser. Furthermore, they have excellent beam quality which can be fiber guided to the work zone. All these advantages combined have helped these lasers getting into the market [5].

This project will use the knowledge and experiences of laser welding of metals gained throughout the years.

### **1.2.1. INDUSTRIAL BACKGROUND**

Today the fiber/disc laser continues to take market shares from the CO<sub>2</sub> laser; hence the solid state lasers for materials processing are the preferred laser source in many

processing systems. This development is expected to continue for several more years [10].

Many industries have taken advantage of the laser's ability to make deep and narrow welds with little energy input and minimal material damage. Especially the automotive industry has implemented laser welding. It began in 1981 when British Leyland started welding sheets with different thickness. From then on the automotive industry has played a large role in developing the laser welding industry [2]. An example is Volvo. As early as 2008, Volvo had more than 17 different laser welds with a total length of more than 10 meter in the XC60, and Volvo claims still to be able to make even more design and technical improvements by adding further laser welds [12], [13]. VW has also has a long history of using laser welding. The Golf V had more than 70 meter of laser welds, and VW had more than 150 Nd:YAG lasers installed already in 2005. Hybrid welding has also been exploited by VW [14]. Today almost all car manufacturers use laser welding in several steps when assembling the bodies of cars [15], [13].

The laser has given designers the option of performing overlap welds which used to be limited to either explosion welding or resistance welding. For obvious reasons, explosion welding is difficult to utilize along an assembly line, and is therefore a niche welding procedure.

Today, there are still only three known methods for producing keyhole welding in steel; plasma welding, laser beam welding and electron beam welding. These are the only methods which can deliver enough energy and focus this energy to areas, which are small enough to give the intensity required for keyhole welding. Plasma welding has a low maximum power and limited focus ability, which narrows its usefulness. In electron and laser beam processes the spot, at which the energy is focused, is much smaller and the intensity much higher than in plasma welding. Therefore, these processes produce much narrower and deeper keyholes.

However, the electron beam requires for the process to be performed in a vacuum chamber. But with high power laser welding there is no need for vacuum for the process to run: it is possible to do laser keyhole welding in a normal atmosphere. The possibility of doing keyhole welding in a normal atmosphere or with a protective inert gas present quickly gave the laser its own niche. This niche is continuously growing in the market with a long list of joining and welding technologies used for assembly in the industry.

Resistance spot welding has been the preferred joining method for the automotive industry. Resistance spot welding requires for the overlap to be at least the same size as the electrodes and for the electrodes to be able to access the joint from both sides. The laser is more flexible when it comes to access to the weld. It only requires a few tenths of space for an overlap, a line of sight from the lens and a good clamping.

The demand for clamping is of particular importance when doing laser overlap welding. If the gap between the two sheets is too large, there will be no joint. Therefore, in practical implementation, an advanced fixture and clamping system is often a prerequisite for the parts to be welded together. Further a precise positioning of the spot from the laser beam according to the joint is also important, as the spot is smaller than the sheet thickness in most cases.

When welding butt joints, a gap is often present. If this gap is too large it becomes difficult to produce stable laser welds, since it poses the risk that the focussed beam will pass through the gap. If the spot is increased, the intensity drops; and it often does so to a level on which the keyhole depth either drops significantly or the welding changes from a keyhole welding to a surface conduction weld instead.

Researchers have sought solutions for this problem. One example is a system with a scanning mirror which allows for the spot to be moved from side to side to allow for an advanced joining of multiple sheets in one butt joining which also allows for increased tolerances [16]. This method has also been successful in reducing the cooling rate in the welding of duplex stainless steel [17].

Today, most new laser welding systems use a fiber/disc laser. However, the multimode version of the lasers is mainly being installed in macro processing systems. There are two major reasons for this: the multimode laser is cheaper than the single mode, and the focussed spot from a multimode laser is *small enough* for many purposes, but not *too small*. In many cases, the smaller spot from a similar single mode fiber laser will present problems as the cut kerf in laser cutting will be too small for the cutting gas to eject the melt [11], and since a small gap often is present during laser welding, there is a risk that the beam will pass through the sheets or that the weld becomes too narrow in an overlap welding, in which a certain cross section often is desired.

The above statements are true for macro material processing. Depending on the final demands, the situation is slightly different for micro processing. Here pulsed single mode fiber lasers have found niches in stent cutting, stencils, shaping and welding of micro components, jewellery, battery packs, etc.

### 1.3. PROBLEM DOMAIN

Laser welding is a widespread technology, and in the last years single mode lasers providing high brightness laser beams has become commercially available. This has given even smaller spots and higher intensities. In some laser processes the spots becomes *too small*. But in many welding processes the spot produced by a multimode fiber laser is sufficient for a given laser welding task.

This means that the spots produced from beams from single mode lasers has an *excess of quality*, and that the spots produced from such a laser often is too small.

This project aims to utilize these small spots to give new options within the field of laser welding. The basic idea is to use multiple spots close to each other, and in this way have a common interaction in the process area. The hypothesis is that this will result in new welding options.

Hence the overall purpose is to investigate:

High intensity multispot laser welding and if it can provide the industry with a range of new welding options.

To do this a beam shaping technique to control the laser beam and the energy distribution into spots is needed.

This PhD will take up the thread and explore multispot fiber laser welding. To use multi spot fiber laser welding technology in practical production the first basic knowledge has to be formed. This project starts on the basis on limited existing knowledge on multi spot laser welding, which is to be elaborated further in the following chapter. Previous work often has used multiple laser sources to produce multiple spots. This work is instead focussed on reshaping a single beam into multiple spots. And where the individual spots until now has been quite large due to limited laser power it is now possible to produce spots which is more than a full order smaller in diameter than those from older laser sources.

Figure 2 shows a graphical layout of the technologies which are combined in the project.

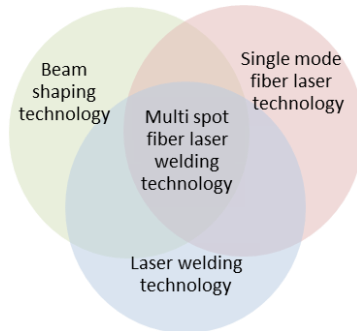


*Figure 2 The overall objective of this project is to investigate the new possibilities which arise through a combination of beam shaping technology, single mode fiber laser technology and laser welding technology.*

Experience about the effect of combining these technologies is limited, hence focus is therefore on establishing a basic knowledge base. In particular focus will be on the following three tasks:

- How to establish multiple spots in a line and use these for laser welding
- To generate general design rules for welding with spot patterns
- Increase the process tolerances for gaps and misalignments and also reduce the needs for cleaning

The tests are mainly performed in laboratory settings, but the PhD-project will have focus on how to take the results from laboratory into industrial implementations.

The project is performed in cooperation with IPU and Aalborg University, Department of Mechanical and Manufacturing Engineering.

## 1.4. DISSERTATION STRUCTURE

This dissertation is written as a summary report of five papers. The project focus has been on providing basic knowledge about the problem domain and on exploring, which requirements needs to be fulfilled to take the technique from laboratory to industrial implementation.

Chapter 1 contains a general introduction to the research area for the project.

Chapter 2 contains state-of-the-art for the technology areas being combined in the project; fiber laser and single mode fiber laser technology, laser welding technology, beam shaping technology and multi beam laser welding technology. In this chapter work performed with multiple laser sources, beam splitting and beam shaping is included. Further a short overview of the problems and challenges for modelling of laser welding is included.

Chapter 3 presents the problem formulation and hypothesis for the project. Six Project related Research Questions (PRQ's) are asked. Throughout the dissertation PRQ's refer to Project related Research Questions, where RQ's (Research Questions) refers to Research Questions asked in each of the first four papers (paper A to D).

Chapter 4 presents the experimental setup including design of measurement equipment to experiments with high speed photographing. Further it presents the first paper:

Paper A: "Design of measurement equipment for high power laser beam shapes". This paper describes the demands and considerations for construction of a CCD based beam analysing system, which can measure and quantify spot patterns with energy less than a watt to 3 kW of laser power.

Chapter 5 present a summary of the results from a number of welding experiments. The chapter refers to the papers:

Paper B: "Beam shaping to control of weldpool size in width and depth". This paper presents some of the first achieved results with multispot laser welding in the project. The experiments are performed using poor performing DOE's. The work and results are expanded and repeated with a more stable beam shaping procedure in paper C.

Paper C: "Joining of multiple sheets in a butt-joint configuration using single pass laser welding with multiple spots". This paper describes a systematic work where parameters for welding with multiple spots on a row perpendicular to the welding direction is examined.

Paper D: "Inline repair of blowouts during laser welding". This paper describes how a secondary spot in line with the primary spot(s) penetrates into the weld pool. Further the technique is examined to see if it can be used for inline repair welding of blowouts in laser welding by introducing provoked blowouts in a butt joint configuration with zinc-powder.

Paper E: "Multispot laser welding to improve process stability". This paper is a summary of paper C and D highlighting some of the achieved results in the project. In this paper no additional research questions are asked.

Chapter 6 summarizes on the work performed and the achieved results in the project and includes a general discussion of these.

Chapter 7 completes the project with a conclusion about the whole project.

The five papers are reprinted in the appendices.

## CHAPTER 2. STATE-OF-THE-ART

The purpose of this project is to investigate the state-of-the-art of the technologies; single mode fiber laser technology, laser welding technology and beam shaping technology, and how they may be combined in the best possible way to find new possibilities within the field of laser welding.

First state-of-the-art for these three technologies will be presented. This leads to a description of how this project will use the three technologies combined; *multispot fiber laser welding*, and why. Finally a presentation of the state-of-the-art for *multi beam laser welding*.

A short section about modelling of the laser welding process, and why, this is still a complicated task, is also included and used to explain why there in this project work has been focus on empirical study rather than simulations and models.

### 2.1. FIBER LASER TECHNOLOGY

All lasers, including fiber lasers, works in the same way: an atom or molecule is excited – brought out of its preferred energy state – and when the atom returns to its preferred energy state, it does so by passing specific energy levels. When it goes from a higher to lower energy level, it emits a photon with a specific wavelength. It's important that the laser resonator is built so that it causes the photons to be emitted in the same direction and in the same phase. The photons emitted from energy levels, which is not producing the desired wavelength, is absorbed, and the heat is transported away. [22]

Excitation of molecules or atoms in the laser resonator may take place in many ways, for example with a high voltage field, light, a chemical reaction or semiconductor technology.

The quality of a beam from any laser may be characterised and quantified by its beam quality factor, referred to as  $M^2$ . This number expresses the chaos in the wavefront of the beam. The lower the beam quality factor is, the less chaos exists in the wavefront and the better is the quality of the beam. For any beam  $M^2$  cannot be lower than 1. If a beam has a beam quality factor of 1, the energy distribution in a cross section of the beam is a perfect Gaussian distribution, and the wavefront is perfectly plane in the focal plane, and thereby the beam contains only one mode, hence it is a “single mode beam”, in the fundamental mode ( $TEM_{00}$ ) [114].

A multimode fiber laser uses a series of laser diodes as energy pump from which light is lead into an active fiber through a pump coupler/beam combiner. From here it excites electrons in the doping material (Ytterbium) and brings them to a higher

energy state. The end of the active fiber contains Bragg gratings allowing for the wavelength of the fiber laser beam to pass through while the wavelength from the pump lasers is retained. The basic principle is sketched in figure 3. [9], [5], [18].

For a single mode fiber laser the principle is a little different, instead of the pump light being led into a large active fiber as in the multimode laser, the light is led into a double clad fiber. The active part of the fiber is placed in the center of the double clad fiber, as sketched in figure 4. The inner core in the double clad fiber is “triggered” with a seed laser signal from a low power single mode laser (a master oscillator). This is amplified through the fiber by the excited electrons in the doping material, which then return to their neutral energy state. The basic principle is sketched in figure 3b. [9], [5], [18].

To produce laser power in the kilowatt range, a large number of pump diodes are used. [9], [5], [18].

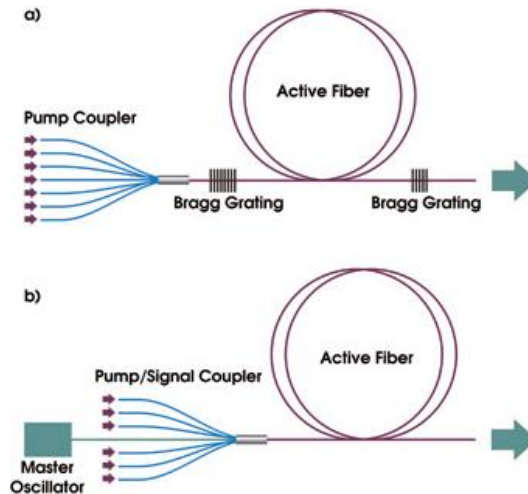


Figure 3 Principle of resonator in a fiber laser. a) Produces a multimode beam, as the emission of photons is based on a spontaneous emission in the active fiber. b) Produces a single mode signal, as the active fiber amplifies the signal from the master oscillator (seed laser). Reprint from [116].

The single mode (SM) fiber laser does not contain any beam combiners after the double clad pump fiber. Instead the delivery fiber is spliced, fused or welded to the core of the double clad fiber after the end grating. A schematic of the principle is shown in figure 4. [9].



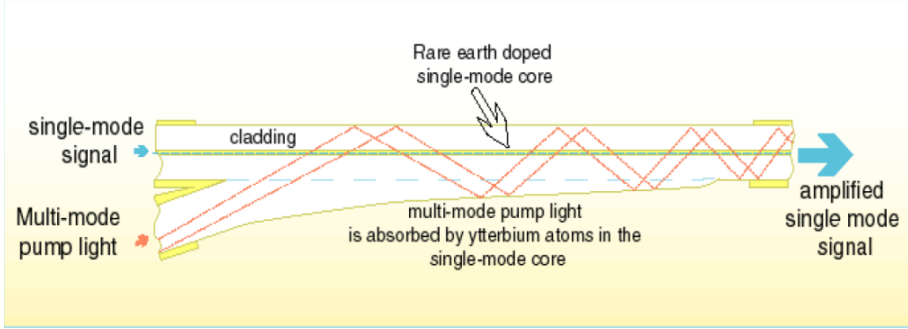


Figure 4 Principle structure of amplification in a single mode fiber laser [9].

Tests have found that, compared to the CO<sub>2</sub> laser, the fiber laser creates higher demands for cleanliness, quality of optics and handling and cleaning of the external optics. Even when the external optics is completely clean, it may still be subject to some focus shift at high power [18], [20], [21].

In recent years, high power single mode fiber lasers with nearly perfect beam quality have developed significantly in terms of power and price; and today continuous wave (CW) power up to 20 kW is available with an  $M^2 < 1.3$  [9].

The single mode fiber laser offers new options within the field of high intensity (*intensity* is here used as the power in the laser beam divided with the diameter of the beam); these laser beams may be focused to spots which are only one tenth of the diameter of focus spots used with traditional high power lasers (both CO<sub>2</sub>- and Nd:YAG-lasers), and still offers same amount of power [22]. This is possible due to the fact that some of the best CO<sub>2</sub> lasers have a beam quality factor close to 1, but the wavelength is 10.6  $\mu\text{m}$ . Some of the best Nd:YAG lasers have a beam quality factor of 10, and the wavelength is 1.064  $\mu\text{m}$ . Equation 1 [22] gives that the minimum spot diameter achievable with both laser types from a similar aperture and focusing lens is identical.

$$D_{min} = \frac{4M^2 f_{foc} \lambda}{\pi D_0} \quad (1)$$

$D_{min}$  is the minimum spot diameter,  $M^2$  is the beam quality factor,  $f_{foc}$  is the focal length,  $\lambda$  is the wavelength of the laser beam and  $D_0$  is the diameter of the collimated beam which passes the focusing lens.

The single mode fiber laser is offering both a short wavelength at 1.07  $\mu\text{m}$  and a low beam quality factor, which is close to 1.0 [23]. Hereby the achievable minimum spot diameter becomes 10 times smaller than that of both the CO<sub>2</sub> laser and the Nd:YAG laser (again under the assumption of similar aperture and focus lens). Hereby the

intensity becomes a factor of 100 (or more) higher than any other laser commercially available on the market.

Table 1 shows data and minimum beam diameter and intensity calculated for six different lasers, all commercially available. The calculations are all based on similar power, focal length and collimated beam diameter. The intensity from a single mode fiber laser is 40 times higher than for the MM fiber, which is the closest competitor regarding intensity.

|                                      |                    | CO <sub>2</sub><br>(slab)<br>[0261] | Nd:YAG<br>(diode pumped)<br>[25] | Disc<br>[24] | MM<br>fiber<br>[25] | Direct<br>Diode<br>[26] | SM<br>fiber<br>[23] |
|--------------------------------------|--------------------|-------------------------------------|----------------------------------|--------------|---------------------|-------------------------|---------------------|
| Power, P                             | kW                 |                                     |                                  | 1            |                     |                         |                     |
| Focal length, $f_{\text{foc}}$       | mm                 |                                     |                                  | 200          |                     |                         |                     |
| Collimated beam<br>diameter, $D_0$   | mm                 |                                     |                                  | 12           |                     |                         |                     |
| Wavelength, $\lambda$                | $\mu\text{m}$      | 10.6                                | 1.064                            | 1.030        | 1.070               | 0.970                   | 1.076               |
| Beam quality, $M^2$                  |                    | 1,05                                | 35.4                             | 24.4         | 7.3                 | 13.0                    | 1.1                 |
| Beam parameter<br>product, BPP       | mm<br>mrad         | 3,5                                 | 12                               | 8            | 2.5                 | 4.0                     | 0.39                |
| $\emptyset$ -focus, $D_{\text{min}}$ | $\mu\text{m}$      | 236                                 | 800                              | 534          | 167                 | 267                     | 26                  |
| I (@P=1 kW)                          | kW/mm <sup>2</sup> | 23                                  | 2                                | 4            | 46                  | 18                      | 1879                |
| Efficiency, $\eta_{\text{electric}}$ | %                  | Unknown<br>(typ 6-12)               | 1-4                              | 20-40        | 25-40               | 40                      | 32                  |
| Max-power, $P_{\text{max}}$          | kW                 | 8                                   | 1                                | 16           | 4                   | 4                       | 3                   |

*Table 1 Data and calculated minimum diameters and intensities in focus for six different commercial available lasers. For the calculation of  $D_{\text{min}}$  and the intensity of the power, the collimated beam diameter ( $D_0$ ) and the focus lens ( $f_{\text{foc}}$ ) distance have been set to identical value for all six lasers. The maximum power available for each laser is also given.*

The beam quality factor is often used in comparing laser sources with similar wavelength; however, as shown above, the achievable minimum spot diameter is also affected by the wavelength. Therefore, the term Beam Parameter Product (BPP) is used. It describes the focus ability and can be used to compare the quality from any laser beam independently of the lasers wavelength. The relationship is given in equation 2 [22]. The lower BPP, the better focus ability a laser has. A typical single mode fiber laser at 1 kW will have  $\text{BPP} = 0.36 - 0.4 \text{ mm mrad}$  [23], [27]. From table 1 it can be seen that even though CO<sub>2</sub> lasers are available with a  $M^2 = 1.05$  the BPP and hereby also minimum spot size is much higher than for the single mode fiber laser with same  $M^2$ .

$$\text{BPP} = \frac{M^2 \lambda}{\pi} \quad (2)$$

Laser keyhole welding needs certain intensity in order to form the keyhole. From the above it can be seen that single mode fiber laser can produce intensities similar to those produced from other lasers with much less power and in a smaller area.

### **Summary of fiber laser technology**

The single mode fiber laser can be focused to spot sizes smaller than for any other laser source available with comparable power. The laser is available with power in the kilowatt range, and hereby offers significantly higher intensities than any other laser source available with comparable power.

The single mode fiber laser is a fully developed industrial product, and is commercially available.

## **2.2. LASER WELDING TECHNOLOGY**

Laser welding is a globally used technology known for its precise welding using very little heat input [28], [29], [30], [31]. In the following section, as well as in section “2.4 *Multi beam laser welding*” only applications and examples with sheet thickness’ up to 5 mm is included.

Laser welding has been studied extensive by several research groups throughout many years, which has led to many tools and strategies. Yet the process is complicated and not yet fully understood. The main reasons for this are the many physical events and properties, which interacts with each other, often with extreme gradients and at temperatures, where material properties are not well known.

The basic principle is, that a beam of electromagnetic radiation (laser light) is focussed towards components which should be welded together. Some of the light is reflected, and the rest is absorbed. The absorption of light starts a process which heats the surface of the materials. If the intensity is high enough, the temperature is increased so that the materials melt. This can lead to a surface conduction welding, where the energy is absorbed only at the surface of the materials.

If the intensity is high enough, the liquid material will begin to vaporize. This will cause a pressure on the melt, which will form a hole into the liquid. If the intensity is even higher, some of the vaporized material will absorb additional energy, and the temperature will be high enough for the material to ignite into plasma. This plasma forms a plume, which can absorb the incoming light to various degrees [35].

Figure 5 shows the main principle and details in keyhole welding in the Rosenthal regime [35] (Rosenthal regime is defined as keyhole welding with travel speed < 83 mm/s. The name also refers to Rosenthal’s line heat source analytic model for heat distribution in a plate, since this model suits well for low travel speeds, and can be used to produce simple models of laser keyhole welding [35]). Only basic melt flow

is sketched, as melt flow during laser welding is complicated to describe, because many physical phenomenon interacts [35], [36].

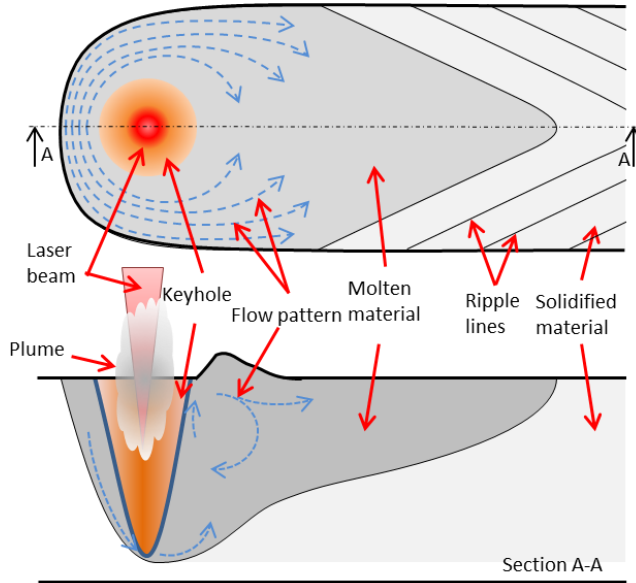


Figure 5 Sketch showing the principle in keyhole welding. Constructed from [35].

Melt flow during welding has been studied extensively by means of in-situ X-ray photography and high speed imaging. Depending on the regime in which the welding is performed, studies have shown that different phenomena occur, like spatters, flow fields or humps. The regimes are mainly classified according to welding speed, but also intensity and power have an influence [47], [48].

The melt flow in and around the keyhole has a large influence on the resulting weld, and many quality aspects like surface roughness, pores, welding depth, undercut and spatters can be found to be a result of specific details of the melt flow and absorption of the laser light. Figure 6 shows a process diagram of a laser welding system with some of the adjustable input parameters, where the outcome is a weld defined by some of its geometry and weld quality parameters.

The term weld quality can cover many aspects of a weld, and many parameters from the finished weld can be said to influence on the final *weld quality*. In connection to this the quality will also depend on the final use of the weld. In some cases it is the penetration depth which is most important, in others it is the surface roughness or other parameters. Therefore the final measure for quality is to be decided from the list of parameters above and evaluated to each case.

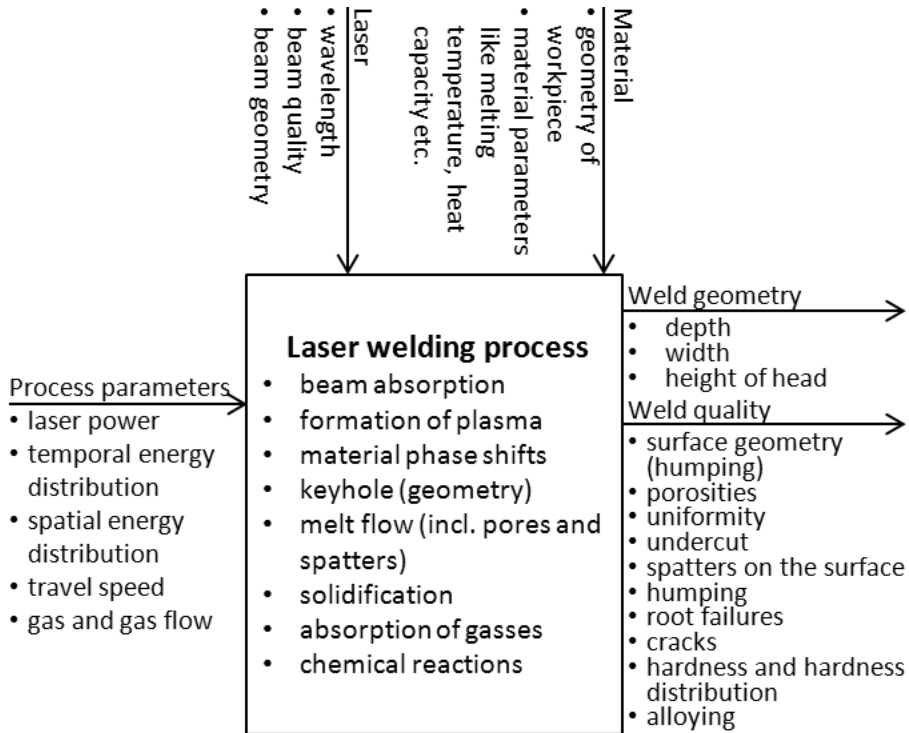


Figure 6 Laser welding process. Vertical fixed input parameters. Horizontal input variables, and process output parameters.

### 2.2.1. LIGHT COUPLING AND PLASMA IN LASER WELDING

An important detail in figure 5 is the plume in and above the keyhole. This plume interacts with the incident laser beam, and if the intensity is high enough plasma is formed in some part of the plume. The formation of plasma induces disturbances in the incoming beam. These can result in absorbing all light, so that no light will enter into the keyhole. This will result in a keyhole collapse, thus no penetration into the material and no new vapours are formed. After a short period the plasma will disappear, and the process can restart when the beam again start to heat the material. This collapse is another failure in laser welding, which often is avoided by proper use of shielding gas and tuning of welding parameters [35].

In the field of laser cutting the CO<sub>2</sub> laser has been dominant. This has also changed in the recent years towards cutting with fiber and disc lasers. Some of the same phenomena as in laser welding appear in laser cutting with fiber and disc lasers. Fiber and disc laser have, with their shorter wavelength than that of the CO<sub>2</sub> laser, demonstrated cutting speeds of steel much higher than those of CO<sub>2</sub> lasers with equivalent power in thin sheets. When cutting steel thicker than 5 mm, the cut

quality (cut quality is covering the surface geometry, angles of the cut to the surface and if there is any craters) is much lower [37]. This has led to additional examinations and discussions on how the energy in the material is transferred from light to heat, and on what happens when some of the material is transformed to a plasma plume. So far it is known that the plasma plume interacts with the incident beam and the melt, but it is not yet fully understood how. In laser welding the same discussion is relevant, since the keyhole is formed by metals which are being evaporated to gas and expanding, and when the metal gas interacts with the incident beam some of it transforms into plasma. The whole process and its energy balances are equally complicated as in laser cutting and not yet fully understood [38], [39], [40], [41].

### 2.2.2. EFFECTS OF IMPROVED BRIGHTNESS

The development of fiber and disc lasers has offered new options in the laser welding industry since good beam quality combined with low wavelength and high power can produce very deep and narrow keyhole weld seams similar to those which could previously only be produced using electron beam (EB) welding. Several researchers and companies have demonstrated this [32], [33], [30], [34].

The new high brightness laser beams with small spots causes the beam to be absorbed in a smaller area; and combined with the higher intensity, it leads to narrower and deeper keyholes than offered by any other high power laser source in macro processing (with equivalent power). Details are shown in table 1. Therefore this presents opportunities for new processing techniques in the field of welding and other laser material applications.

Some of the findings are:

- Smaller spots results in increased stability of keyholes giving a stable welding depth [29]. It is known that a weld with a smoother surface and more stable depth can be achieved if the keyhole is steady without fluctuations [35]
- Higher welding speeds with same power when keyhole size is decreased [28]
- More narrow welds with less heat input compared to all other fusion welding processes [33], [29], [28] (except electron beam welding)
- “Micro applications” ranging from the engraving of jewellery to micro welding [42]
- Laser hole drilling with even smaller holes and higher aspect ratios than traditional hole drilling using lasers [43]
- Ablation cutting: the process works by ablating small amounts of material at a time. Instead of making a kerf, in which the molten metal is ejected, the metal is vaporized and blown away. Since the process only penetrates some tenth of a millimetre, multiple passes are often necessary [44]

- The vaporisation occurring in both laser hole drilling and ablation cutting is similar to what is going on in the keyhole in laser keyhole welding, where the evaporation pressure is the driving force for forming the keyhole

In addition to the benefits, there are also some drawbacks. Some of the challenges of the new high brightness lasers for welding are:

- That the weld becomes too narrow and that it is difficult to widen the melt pool in some macro applications. This would be necessary, for instance, if the gap tolerances of the parts to be joined were larger than the spot diameter
- Too high cooling rates which leads to undesirable grain structures and grain compositions in and around the weld [45]
- Increased risk of rough surfaces or humping beads [46], [47]

Further some researchers claims there is a maximum brightness/intensity, from where the laser beam no longer penetrates deeper into the material, but on contrary reduces the penetration when it is increased further. Results and conclusions differ between various researchers and are discussed further in the following.

Verhaeghe et al. [64] have performed studies, where different lasers, optics and intensities have been used. From this Verhaeghe et al. [64] claim there is an optimum of brightness for laser welding in steel. Brightness is defined in equation 3, where P is laser power.

$$\text{Brightness} = \frac{\text{intensity}}{\text{solid angle}} = \frac{P f_{\text{foc}}}{\pi^2 D_0^2 D_{\text{min}}^2} \quad (3)$$

Verhaeghe et al. [64] show that the depth of penetration drops, when the brightness is above 3.200 kW/(mm<sup>2</sup> sr) (sr = steradians), and in some cases it is actually reduced [64].

Weberpals et al. [29] have performed studies applying different divergence angles (lenses), laser powers and beam qualities to a laser process. They conclude that the stronger the focusing power and the higher the actual power, the deeper and narrower is the resulting weld [29]. Weberpals et al. [29] do not find the same maximum brightness as Verhaeghe et al. Weberpals performs his analysis without calculating brightness. Instead he uses divergence angles and spot diameters.

To compare the two studies, brightness can be calculated from the data given by Weberpals et al. [29]. This makes it possible to compare the data from Weberpals et al. [29] with the findings from Verhaeghe et al. The two findings do not support each other, as Weberpals is getting increased depth of fusion up till 195.000 kW/(mm<sup>2</sup> sr), which is nearly two decades more than the optimum/maximum

stipulated by Verhaeghe et al. [64]. None of the two studies discuss the gas coverage in depth, nor tries to optimize it. This can also have a significant influence on the differing results [35].

The contradiction in the two findings might originate from the fact that Weberpals and Verhaeghe et al. [64] are experimenting with different beam diameters: Verhaeghe et al. [64] is examining from 300 to 600  $\mu\text{m}$ , while Weberpals et al. [29] is experimenting uses spot diameters from 50 to 300  $\mu\text{m}$ .

### 2.2.3. TECHNIQUES TO IMPROVE LASER WELDING

As shown laser welding can potentially be improved by using high brightness laser spots. However a lot of research and development is performed in order to improve laser welding

Examples of work for improving laser welding in specific cases are:

- High frequent scanning of the spot in the focus area to widen the keyhole and control the melt flow around it [17]
- Conducting the laser weld in a vacuum, thus avoiding any influence from surrounding gasses on the melt pool [57]
- Electromagnetic control of the weld pool – an electromagnetic field is applied for stabilising the melt. This should increase the quality of the final weld and decrease the amount of spatters [58], [59]
- Hybrid welding with other fusion processes; mainly Gas Metal Arc Welding (GMAW). The laser beam makes the deep penetration, and the GMAW process adds filler wire and extra energy to the weld, thus filling up any gaps in the weld [60]
- Humps are reduced by using helium as shielding gas compared to using other gasses [28]
- Pulse shaping, which can apply short pulses with high peak powers, is found to stabilise keyholes and suppress plasma formation [45], [65]
- Superposition of a diode laser to a pulsed Nd:YAG laser has proven to improve the weldability of aluminium [66]
- Surface tension stabilised laser welding (donut laser welding) can be used to reduce the amount of spatters or fully avoid them [67]
- Twin spot welding can be used to utilise multiple laser sources or to widen the process zone transverse or perpendicular [68]
- Micro scanning of beam: By doing a high speed micro scanning of the beam in the process area the keyhole is extended. This may cause longer cooling times, wider welds and change the dynamic behaviour of the weld pool. In this way it is possible to affect the cross section of the weld [17], [69], [70]



In industrial implementations of laser welding there exist examples of closed loop systems where sensors monitoring welding process online gives feedback to adjust specific weld parameters accordingly while the process is running:

Some examples are:

- In line process monitoring and analysing of reflected light from the process [61], [53]
- In line process monitoring applying a second low power laser. Depending on setup, an analysis of the reflected light may produce different information: on keyhole geometry, welding depth and gap width among others [62]

Most of the techniques listed change the energy distribution and energy coupling in the welding zone. Hereby the melt flow around the laser spot is influenced, and specific phenomena like humping, spatters and pore formation is enhanced or suppressed. Some of the methods include multiple laser sources and thus they make any installation expensive or difficult to implement in an industrial production. Some of the combinations and laser types can be built together in a single unit, and the beams can be combined in the processing head. This will lower the complexity and make it easier to implement in an industrial setup. Examples of such constructions are given in the section “2.4 Multi beam laser welding” If any of these setups turns out to improve laser welding significantly, a new market most likely will arise, and the area will receive increased competition, thus most likely lowering the prices.

## 2.2.4. TOOLS FOR ANALYSING LASER WELDING

Today several research groups work on developing analysing tools for laser welding in general. In their work, they utilise many different approaches.

Some of the more advanced tools are:

- On-line x-ray photography of the keyhole: this technique can show the *geometry of the keyhole* which has a tendency to bend backwards compared to the welding direction. The melt flow may partially be seen on the x-ray photographs by adding small pellets of metals with higher densities, and increased melting temperature. X-ray photography can also be used for analysis of the formation of *porosities* and how the keyhole shape influences on this formation [48]
- High speed photographing: this may provide information about the formation of *spatters*, *melt flow on the surface*, *waves in the fluid* and how the melt *solidifies*. Illumination might render this difficult as there is often a strong light in the reflexes from the processing laser beam and in the black body spectrum of the process which disturbs the images taken [49], [50], [51], [52]

- Online analysis of signals from different sensors coupled to the process: ranging from measuring the *depth of keyhole* over the determination of the amount of *spatter* to the analysis of *plasma* plume parameters and optical characteristics from the process [53], [32]
- Computer modelling of parts of the process: such as laser beam *absorption in the keyhole*, *plasma formation & interaction* and *melt flow* [54], [55], [1], [39], [56]

### Summary of laser welding technology

Laser welding of metals is a complicated process, where energy coupling and balances are not fully understood. The process is however widely used in industry, and it has found several niches and implementations, where it is performing better than other welding processes and hereby justifies the higher installation costs than more traditional fusion welding technologies like TIG or MIG/MAG welding has.

Laser welding has shown a great potential in production, and it is used extensively in various industries. Several tools and special setups have been developed to further improve laser welding in different niches.

The extremely high intensities which can be achieved with the new lasers could raise new problems within laser welding with single mode fiber lasers. However so far only an optimum for maximal brightness has been identified to be a potential problem.

## 2.3. BEAM SHAPING TECHNOLOGY

By shaping a laser beam the energy distribution changes transformed. The transformation is performed to give one or more specific effects in the process zone, e.g. multiple beams or a more uniform energy distribution.

On example of how this can be performed is shown in figure 7 which shows a sketch of how light propagates through a duplet lens and a DOE. As it will be described in this section several other methods for beam shaping exists.

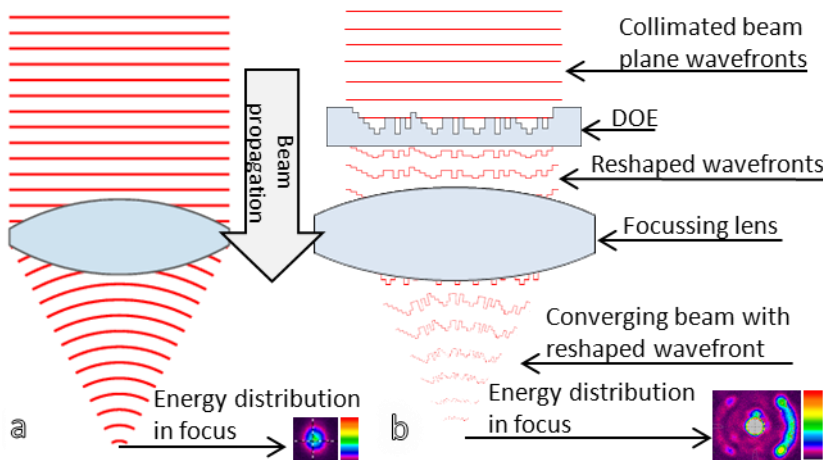


Figure 7 a) Illustration of a beam consisting of plane waves going through a duplet lens and being focused. Reprint from Wikimedia [72]. b) Sketch of a plane wave going through a DOE. Here the plane waves are being reshaped. The reshaped waves then pass the focussing lens.

Light, including laser light, can be regarded as either photons or electromagnetic waves. Physicists use both, since, in some cases, light is best characterised as photons, which can be traced as rays. In other cases, light is best characterised as waves, which require a different approach when the whole electric field is considered instead of just single rays [71].

In order to calculate the propagation of laser beams through optical components such as lenses, beam splitters, polarisers and DOE's (Diffractive Optical Elements), the best approach is to regard the beam as an electromagnetic wave and then recalculate the wavefront through the optical component. From the recalculated wavefront it is possible to reconstruct parameters of the beam such as diameter, beam quality, divergence factor (or convergence), angle, etc.

A focussing lens changes the wavefront of an incident beam by slowing the speed of the light in a controlled manner, during which the centre is slowed the most and the edges less. This effect is obtained by using a material for the lens with a higher refractive index than air and a surface with a convex curvature.

Scientists have developed many different ways for reshaping a beam. As described above, (almost) all of these work by changing the wavefront of the electromagnetic waves. The methods for reshaping laser beams and changing the energy distribution in the focal plane can be divided into seven sub groups.

- Multiple lasers – multiple optics: each laser has its own processing head, which brings the focused spots close to each other in the desired spot pattern. This is a quite expensive solution, and the whole system will be quite bulky with multiple optical heads. An advantage is the possibility to

control the power in each spot/laser individually. Examples of such are listed in the section “2.4 Multi beam laser welding”.

Instead of having multiple lasers with their own optical head, the fibers can be combined into a single cable, but still in their own fiber. In this way the final spot pattern becomes a replica of the fiber positions in the plane, where the beams exit the fibers. The method is costly, as multiple lasers are required. Advantages are the possibility to control the power in each spot individually, and also the solution only need a single optical processing head. The most severe disadvantage is that after production, the geometry fiber bundle/spot pattern cannot be changed, only scaled, according to the choice of optical components [112]

- Beam splitting and realigning of beams: A laser beam is split multiple times and arranged so that an almost parallel set of beams propagates towards the lens and is focussed in the same plane. This allows for a manual construction of various patterns and geometries by rearranging the positions from which the beams are sent towards the lens. Making the beams almost parallel, will often require a rather large setup and lead to some aberrations in the focal plane [73], [74]
- Beam splitting by use of a prism in the optical head of the system. The component split the collimated laser beam and produces a set of twin spots. The construction is quite robust and is commercially available. This splitter/prism could be repeated multiple times in the laser head making it possible to split the beam into more than two spots (depending on which technology, there is used for splitting the beam). Unfortunately current commercial available systems only allow for two spots, and the splitting ratio is fixed [113]
- Microlens arrays: One example of microlens arrays is the commercial product Pi-shapers from AdlOptica GmbH [77]. It transfers a Gaussian profile to a top-hat. This is primarily used when a uniform energy distribution is needed, for example during welding of polymers and in engraving [77], [78], [79]
- Diffractive Optical Elements (DOE's): Works by reshaping the wavefront of the laser light typical in small “pixels”. The delay is caused by structures in a substrate with different refractive index than the surroundings. This group can cover many different subtypes of construction of small surface geometries, which may vary in distance and height. If the DOE has a fixed spacing between each pixel, the height of each pixel may be varied. If it only contains two discrete steps, it is said to be a binary DOE, and the distance between each top has to be changed instead. Various methods, in which both distance and height are changed, exist together with DOE's, where each pixel is connected and continual [80], [81]
- Gratings: This is a form of DOE in which the size of the geometries is of wavelength or sub wavelength size. They work almost as DOE's, except that interference in the element is of great importance. To calculate the effect of these geometries on a laser beam, it is often necessary to employ

more rigorous calculation methods than those used for the calculation of transmission through lenses, DOE's and microlens arrays [81]. Gratings are used as mirrors inside the fiber laser, and beam splitters are used on the active fiber.

Typical gratings offers very little loss in the transformation, and is used as repeated structures like saw-toots, micro pyramids and other simple shapes. Due to the smaller feature size in gratings more precise production equipment is needed than for DOE's [5]

- Free form surfaces: This group may cover all other groups of optical components, since the surface of the components could be of any shape from spherical to micro geometries as in gratings. However, it is included here in order to sum up any shape not belonging to any of the predefined groups. An example could be the use of a spherical convex lens in which two spherical caps are removed. In this way the lens produces two extra beams, which are trailing the main beam. The purpose of this work is to even out the edges between the weld head and the surface of the base material [75]. This type of reshaping often involves micromachining with ultra-precise machines. The production of these elements requires materials consisting of micro grains [76]

Lastly a technology that is not strictly a beam shaping technology, as the beam is scanned at high speed while it still maintains its original energy distribution. It is included here due to the effects which arise, when the scan speed increases and the scanned area is kept small enough:

- High speed scanning of laser beams for welding: If the speed is high enough, the beam can be moved, and then the keyhole is not having enough time for collapsing. Instead the keyhole is experiencing the scanned beam as a larger beam or a beam pattern. In this case the intensity distribution should be seen as the mean intensity of the spot being scanned in one scan cycle. The method often leads to altered flow patterns and increased turbulence in the melt pool. The advantage of using this method is that it allows for an easy change of scan strategy and thereby energy distribution in the scan zone. This allows for adapting the scan pattern during welding if changes occur in the gap which is to be welded [17], [69], [70]

When designing DOE's, different shaping strategies may be used, all of which create different types of results:

- DOE beam shapers are associated to free form lenses. The wavefront is changed in are "more continuous way". Enough to shift some of the energy in the focal plane to other positions. Beam shapers are great for simple shapes like ovals, donuts, increased spot size and arbitrary placed beams. The element must be carefully aligned to the incoming beam. If correct design is carried out, it is possible to achieve high transformation efficiencies [81], [82]

- DOE diffusers can produce almost any shape imaginable. It is great for images, logos and other complex graphics. The disadvantage is that the final pattern contains speckles. The more complex pattern, the higher resolution is needed. Transformation efficiency is often low, but this depends on the complexity [81], [82]
- DOE beam splitters produce copies of the spot in focus. Patterns of the original beam can be made in arbitrary patterns, and they can be placed with different distances between each other. It is also possible to skip some of the spots in the pattern and control the relative energy in each spot. Placing the beams in a fixed grid may increase efficiency. In this way the transmission pattern is simplified and can be placed in a repeated pattern which will often yield a higher efficiency [81], [82]  
If the transmission pattern is a repetitive pattern, it becomes insensitive to alignment in the collimated beam. The size of the repeated part of the transmission depends on the spacing in the focal plane. A final pattern contains some shadow spots, which are placed in the same grid as the rest of the spots, however with less intensity. In general, the method has good transformation efficiency [81], [82]

In figure 8 is shown examples of energy distributions for a DOE beam shaper, a DOE beam diffuser and a DOE beam splitter. As seen they all create different patterns. Also the phase transmissions are significantly different. The transmission for the beam shaper has soft curves and large uniform areas. Beam diffusers appear more “randomly” and pixelated with many details and sharp steps. The phase transmission for the beam splitter is quite simple as the spots lay on a line, so that the phase transmission becomes two dimensional, and therefore is repeated multiple times. If e.g. multiple spots in a beam splitter design is moved closer to each other, so that the spots are merged, and forms an oval shape instead, the DOE ends up being more like a beam shaper than a beam splitter. If many details are introduced to the design, the DOE ends up being more like a diffuser, and will contain speckles like shown in figure 8b.

Energy distributions in figure 8 for beam shaper and beam splitter are measured. The higher colour on the scale on figure 8c the higher intensity. The center in figure 8a is grey, as intensity is higher than the maximum intensity in the colour bar. In figure 8b is seen the result from a simulated performance. The intensity is quite even, the greener, the higher intensity. The speckles with no intensity (energy) are due to interference in the incoming beam.

The phase transmissions in the bottom row in figure 8 is phase changes from  $-\pi$  to  $\pi$ . Colour bar is shown in figure 8c.  $2\pi$  correspond to a full phase change for a given wavelength ( $\lambda$ ). To produce this phase change in reality equation 4 can be used to calculate required etching/machining depths in an optical material.

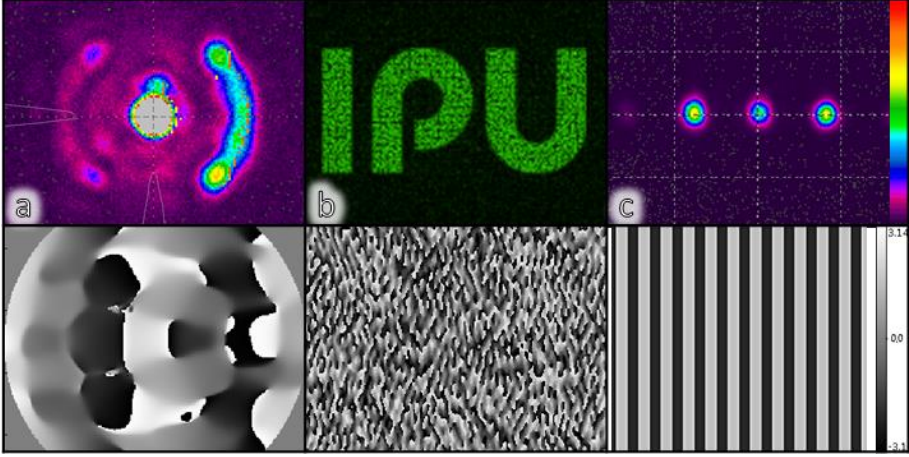


Figure 8 Top row: Energy distributions from a) DOE beam shaper, b) DOE beam diffuser and c) DOE beam splitter. Bottom row corresponding transmission phase/DOE pattern for the transformation.

All three strategies can be manufactured as either reflective or transmissive, depending on the material used in the manufacturing process. A more comprehensive review on techniques for beam shaping can be found in “Paper A: Design of measurement equipment for high power laser beam shapes”.

If a transmissive diffractive setup is used, the required depth of structures in a DOE can be calculated from equation 4 [81].

$$d_{max} = \frac{(2^N - 1)\lambda}{2^N(n_{mat} - n_{air})} \quad (4)$$

$d_{max}$  is the required depth,  $2^N$  is the number of discrete steps having been selected,  $N$  is the number of etching steps and hereby also the number of masks required,  $n_{mat}$  is the refractive index of the material, and  $n_{air}$  is the refractive index of air (or the material which surround the structure), which is approximately 1,01 at room temperature. If the DOE is manufactured in fused silica, the required maximum depth becomes  $2,43 \mu\text{m}$  for a fiber laser with  $\lambda = 1,075 \mu\text{m}$ ,  $N = 8$  and  $n_{fused\ silica} = 1.45$ , and hereby  $2^N = 256$  steps. Machining depths in micro meter with height details in the nano-meter scale requires special considerations and special equipment, and is further described in the following.

If a reflective solution is used instead, the required depth will be half the wavelength of the beam. The halving of the wavelength is due to light being delayed both on the way in and out of the reflective structure.

In a reflective structure, the angle of incidence starts influencing the performance of the DOE if the angle of incidence becomes too high. If this is the case the structures

will then cast a shadow on some of the details. The problem is sketched in figure 9. As long as the angle of incidence is limited and the pixel depth is relatively small compared to the pixel size, the problem is negligible. Further the lights travel distance in the structure will be increased with  $1/\cos(\text{angle})$ . Unless the angle is unknown, this may be compensated for in the design phase.

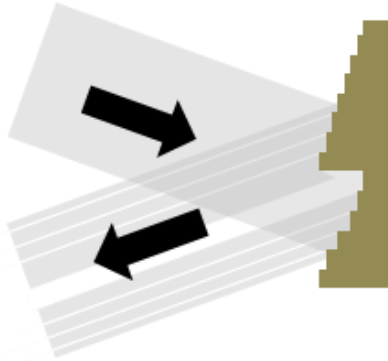


Figure 9 Cross section of a DOE. Example of shadow effect on the outgoing reflection of the laser beam for a reflective DOE. Dimension is out of scale, ratio between depth and width  $\gg 1$ .

### 2.3.1. MANUFACTURING TECHNIQUES FOR DOE'S

The following presents a list of processes, which can be used to produce DOE's. The processes, which involve etching or are programmable chip, all originate from the micro electronic industry, and they all use the same machines and processes as those used for producing microchips. The other processes are more classical mechanical processes, which has been improved and scaled to micro manufacturing.

A basic list of the processes is:

- **Machining/polishing:** This is the primary production method for lenses, but it can also be used to produce free form surfaces with new high precision machines [76], [75], [83]
- **Diamond turning:** This is a process which has many similarities with a classic turning operation on a lathe. The main axis is rotating with a low speed while a tool is moved into the surface in order to remove chips in a controlled manner. The tool can be controlled in a fast and precise way which allows for making non rotational symmetric machining. The resolution of each discrete level may only be down to a few microns when using this technique. The method is used for manufacturing prototypes; however, it is quite slow when used in a serial production. As regards fiber lasers one of the preferred materials is zinc sulphide (ZnS), which has excellent machining properties. Zinc sulphide has a high refractive index, which means only small machining depths is required according to equation (4) [83], [80], [75]



- Multilevel etching:** The basic principle of multilevel etching is as follows: a blank wafer of optical material, often fused silica, is coated with a photoresist, which is then exposed by means of a binary mask. The element with the photoresist is then developed and etched. In this way the photoresist is only present on areas, which are not exposed to the light through the binary mask. The sample with the resist pattern is then set through a reactive ion etch. This employs uniaxial material removal where the photoresist is not protecting the surface. The etching depth is controlled by the length and intensity of the exposure. Finally, the protecting layer of resist is removed.

The method can be repeated  $n$  times. This gives  $2^n$  steps in the final DOE, providing that the etching depth of each step is controlled.

The principle is sketched in figure 10 [84], [81].

This process has many different varieties where some of the process steps is changed.
- Grayscale etching:** This method uses the same principle as multilevel etching. However, instead of using multiple layers, the exposure of each pixel is controlled. This affects the removal by the subsequent etching process. The exposure can be controlled in different ways ranging from micro holes to semi developing of the photoresist by using grayscale masks [85], [86], [87]
- Programmable reflective chips:** These are often Liquid Crystals on Silicon (LCoS) which work by changing the tilt of elliptic micro crystals; in this way the length which the light needs to travel is changed. The disadvantage of this method is that the chips usually only work with one polarization of the light and only with power up to a few watts [88]

Figure 10 shows the main principle in the multilevel etching of DOE's. Several sub-steps, including the spin coating of photoresist, are not shown, but the basic principle of how to produce  $2^N$  steps by  $N$  loops is shown. In the figure two loops are shown. First loop is step 1-4. Second loop is step 5-8. This gives  $N = 2$ , and a total of  $2^N = 2^2 = 4$  steps. If additional levels is needed an additional loop is introduced, increasing  $N$  to 3 and number of steps to  $2^3 = 8$ .

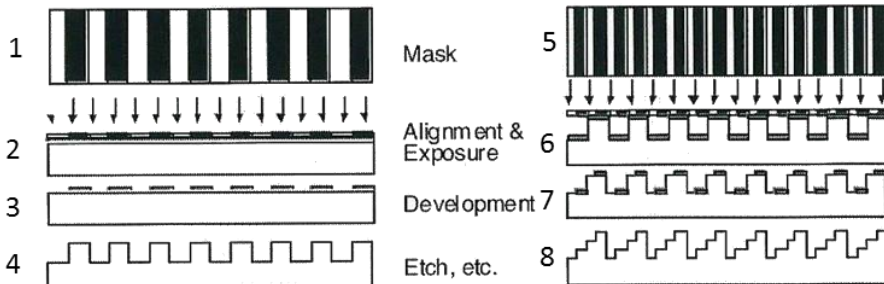


Figure 10 Binary mask  $2^N$  fabrication process for DOE's. Rework from [81].

Apart from the shape of any optical element, the surface coating of the element is of great importance for the overall performance. For diffractive elements such as DOE's, and lenses, an antireflection coating is often applied to reduce unwanted reflections from the surfaces. Fused silica has a reflection of approximately 4% for a polished uncoated surface which is exposed to randomly polarized light. This means, that using a standard lens or DOE would lead to a loss of 8% per element (for two sides), if it is left uncoated. Furthermore, the optical reflection will lead to internal reflections within the element. Therefore, optical elements for high power lasers are always treated with an AR-coating. These may be applied using various sputter techniques such as PVD, and they consist of several layers of metallic alloys in the nanometre range [81].

The technique used for AR-coating can also be used for designing reflective coatings, which reflect nearly 100% of any given wavelength. A reflective coating applied to an element of fused silica for 1075 nm fiber laser wavelength will often appear transparent to the human eye. Numerous different surface coatings exist and there are several ways to which these can be applied, ranging from various Physical Vapour Deposition (PVD) processes to ion beam sputtering. [81]

Several techniques are available for calculating and manufacturing DOE's. The calculation is often performed using Inverse Fourier Transformation – IFTA [71], [89]. Once the phase change is known, this should be transferred to a physical DOE. Figure 7 shows how a DOE can be inserted into a collimated beam, and how the plane waves are changed into more bulgy waves after passing the DOE. The challenge is to calculate the shape of the waves in order to get the desired pattern in the focus region.

#### **Summary of beam shaping technology**

It is possible to perform beam shaping in many different ways ranging from multiple lasers to special optical components. DOE's appear to be a very powerful cost effective tool for shaping of high power laser beams. Although there exist other ways of efficient beam shaping like gratings, DOE's offers structures much larger than those in gratings and a beam shaping quality which is sufficient.

## **2.4. MULTI BEAM LASER WELDING**

The following section is an extended version of state of the art from paper 3 D *Inline repair welding of blowouts during laser welding* in appendix D.

Laser welding with multiple spots has been known in many years and has found some specific niches. Lasers have also found application areas in hybrid processes, in which the ability to dose energy precisely in both time and space have found several applications in many other process areas, like grinding and milling [1].

Especially hybrid solutions with lasers and traditional fusion welding processes like Gas Metal Arc Welding (GMAW) have shown significant benefits [60].

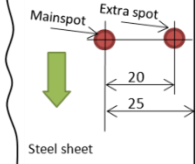
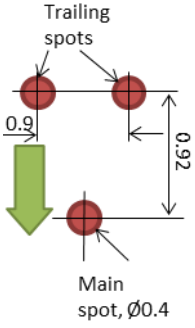
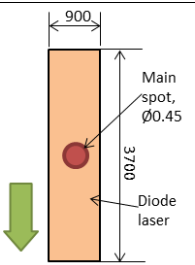
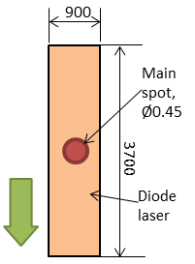
Examples of previous work in which a laser has been combined with other laser sources, or where the beam has been reshaped (data and results are summarised in table 2):

- It has been shown, that a centreline solidification crack can be avoided in situations, in which it normally occurs by using an extra laser spot placed to the side of the main spot to reduce the uneven cooling of the weld, and hereby the crack susceptibility is reduced [90]
- Reduction of hot cracking in welding of austenitic stainless steel has been sought achieved by splitting the laser beam into a main spot and using two trailing side spots to reduce the cooling rate. It is concluded that the penetration drops, and no improvements in quality (same susceptibility to hot cracking) is observed. The work was performed using a multimode lamp pumped Nd:YAG laser with limited power and a relative poor quality diffractive optical element [91]. The lack of power and the relative high beam parameter product from lamp pumped Nd:YAG lasers are most likely the explanation for the lack of success
- Two 3 kW lasers inline can be used to increase welding depth in aluminium. Deeper penetration, higher welding speeds and lower surface roughness is achieved [92]
- Superimposing multiple laser welding processes has also been performed in various versions. E.g. using a Nd:YAG laser to do a keyhole welding and an extra diode laser to perform a surface conduction welding in the same weldpool. It is concluded that the total process is more than a superposition of the two processes, and a better weld quality is achieved in the entire weld seam [94]
- A double spot optics on a CO<sub>2</sub> laser can perform inline cleaning of the weld. The purpose of the first spot is to remove dirt and oxides before the second spot makes the actual weld. In this way a cleaning step can be skipped in many cases and the process stability is improved [93]
- A M-shaped profile produced by a DOE in the beam path on a multimode laser to widen the melt pool in a surface conduction weld. It is claimed that the technology can be used to affect the microstructure in the resulting weld [95]
- A diamond turned element can be used to produce two trailing spots, which is smoothening the toe on the surface at the edge of the weld. The weld toe (the angle of the weld face relative to the untouched surface) is reduced from 125 degrees to 163 degrees [75]
- There has been other experiments with multispot welding, primarily with twin spots, from various laser sources; mainly Nd:YAG and CO<sub>2</sub> lasers. These produce twin spots in different ways, like prisms, dichroitic mirrors and multiple laser heads

Results from the experiments range from increase of gap tolerance in butt-joining, less porosities in welding of aluminium and stainless steels,

degassing in welding of zinc-coated steel and welding of dissimilar materials to reduce intermetallic phases [68]

In table 2 in the column showing spot patterns, figures from the original work is preferred. Where none is present, a figure has been produced from the description in the work. Various terms are used for the different parts of spot patterns. The term *main spot* typical refers to the part with the most energy/the highest intensity. The term *trailing spot(s)* refers to spots after the main spot, typical with less energy and lower intensity.

| Application (material / geometry)   | Result  | Laser(s)  | Beam shaping by   | Beam / spot geometry (all numbers in mm)   |
|---|---|---|---|--|
| Avoiding centreline solidification crack in aluminium (AA6056, 2 mm thick) close to a free edge (distance: 25 mm)   | Crack susceptibility is reduced   | Laser#1: 3 kW Nd:YAG.<br>Laser#2: 750 W, type not specified   | Two lasers + two set of optics [90]   |    |
| Attempt to reduce hot cracking in welding of austenitic stainless steel (SS2002) by splitting the laser beam into a main spot and using two trailing side spots to reduce the cooling rate. | Reduced penetration depth and no improvement in quality (same susceptibility to hot cracking as welds performed with normal optics) | One 1 kW pulsed Nd:YAG laser from Rofin Sinar with NA 0.2 and 600 $\mu\text{m}$ fiber (used at 500 W with various pulse energy) | Splitting of main beam by use of diffractive optics (kinoform/DOE) [91]   |    |
| Increase welding depth in aluminium, EN AW6060, butt joint, 2 mm thickness  | Deeper penetration, smoother surface, less pores, no longitudinal crack   | 2 x 3 kW  | Two lasers + two set of optics [92]   |   |
| Improved welding quality in aluminium (same lasers as above row, different optical setup and different authors)   | Better weld quality in entire weld seam (reduction of pores, smoother surface, reduction of undercut)                               | Nd:YAG laser to do a keyhole welding and an extra diode laser   | Two lasers, combined with a dichroitic mirror to a coaxial welding head tilted 18° back from the welding direction [94] |  |

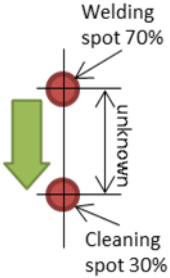
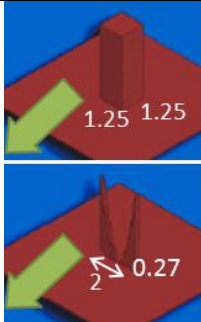
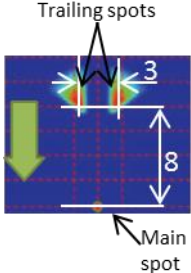
| Application<br>(material /<br>geometry)   | Result  | Laser(s)                                       | Beam shaping by  | Beam / spot<br>geometry (all<br>numbers in mm)                                       |
|---|---|--|--|--|
| Inline cleaning of the weld seam. The purpose of the first spot is to remove dirt and oxides before the second spot makes the actual weld. In this way a cleaning step can be skipped in many cases and the process stability is improved (both AA5056 and steel) | Significant reduction of porosities, much smoother surface  | CO <sub>2</sub>                                | Parabolic beam dispersion and two ellipsoid focussing mirrors [93] |    |
| Widen the melt pool in a surface conduction weld on 1 mm mild steel and 1 mm 316L stainless steel   | The M-shape is concluded to give the best results. The depth of fusion is controlled and the result is an even depth of fusion through the entire width / cross section. Keyhole welding is avoided | 1 kW CO <sub>2</sub> laser                     | Reflective DHOE (Diffractive Holographic Optical Element) [95]     |   |
| Smoothering of weld toe on the surface at the edge of the weld (weld toe angle: the angle of the weld face relative to the untouched surface)   | Reduction of weld toe angle from 125 to 163 degrees   | 10 kW multimode fiber laser used at 5 and 7 kW | Diamond turned element in ZnS [75]                                 |  |

Table 2 Data and results from multi beam laser welding. Green arrow indicates welding direction.

The above list is covering nearly all cases found in the literature study of multibeam and multispot welding of metals. In the light of this the list is remarkably short.

Despite the above list, welding with multiple beams, multiple spots or beam shaping has so far only found limited use in laser welding of metals. One of the main reasons for this is the need of several costly laser resonators. However, beam shaping has been used on several occasions in a mid-power range in laser plastic welding and laser ablation/marketing processes [96]. In laser welding of plastic beam shaping has shown significant improvements: less porosity and sharper weld borders. In ablation cutting sharper details are created by applying beam shaping which leads to a more precise control of the final geometry.

Welding of polymers differs significantly from welding of metals. During the former, a very narrow temperature gap is present from the melting temperature until it starts to decompose into more basic molecules. Furthermore, the material properties of polymers differ significantly from metals. The most significant differences are the heat transfer coefficient, viscosity and melting temperature. The heat transfer coefficient is often in the range of 0.1-0.4 W/(m K) compared to 16 and 43 W/(m K) for steel and stainless steel. The viscosity is highly temperature dependent, but it is much higher for all temperatures of polymers than for those of steel. The melting temperature for most polymers is also much lower, often in the range of 100-250 °C.

Therefore keyhole welding is not possible in polymer welding, and often the high intensities from the laser cannot be utilised. For this reason, most polymer welding is performed with cheaper diode lasers, where the beam quality and thereby the minimum focus spot is much larger than those of, for instance, fiber lasers.

The energy distribution of the laser welding of metals is often some variant of a Gaussian distribution in which the highest intensities are found in the middle. A more uniform distribution is preferred for polymer welding during which low temperatures and only little heat conduction occurs. Therefore, different systems have been developed for reshaping a Gaussian laser beam into various shapes, ranging from top hats over rectangular beams to M-shaped energy distributions [97], [96].

#### **Summary of multi beam laser welding**

Several examples of multi beam and multispot laser welding has been identified, each addressing different problems and challenges within laser welding.

No examples of beam shaping of high brightness laser sources for macro material processing have been identified, thus no existing knowledge exists. Only examples are the use of multiple laser sources or simple beam splitting prisms, typical with intensities which are much lower than those achievable with single mode fiber lasers.

## 2.5. MODELLING OF LASER WELDING

For most laser processes, producing a computer simulation of the process is a complicated job, and laser welding is no exception. Many physical properties and events must be taken into account, and numerous mathematical problems will be clear to anyone, who tries to implement an algorithm for predicting the process. First of all, a model of the laser beam is needed. This is quite simple, since the beams from single mode fiber lasers can be considered as Gaussian beams [22]. Then information about how the beams interact with the material is needed. This interaction is influenced by wavelength, polarisation, angle of incidence, temperature and material properties which determine the amount of light being absorbed or reflected.

As described in section “2.2 *Laser welding technology*” following happens for metallic materials; when the beam interacts in any given point: heating, melting, vaporisation and transition to plasma depending on the intensity and energy which the material is absorbing. The production of metal vapours produces a pressure that interacts with the molten material. If the energy is high enough, a keyhole is formed. In this keyhole multiple reflections occur. Some of the formed metal vapours will be ignited into plasma resulting in an even more complicated absorption. The waviness of the surface complicates the whole process even further since it changes the angle of incidence and thereby the absorptivity of the laser beam [39], [98].

Besides this complicated energy coupling, a complicated material flow exists. The melt flow is driven by several phenomena. Some of these are pressure gradients around the keyhole, high temperature gradients which lead to Marangoni convection, natural buoyancy from differences in density, surface tension forces and gravitational forces. The surrounding gas of the melt pool also influences laser welding, as it affects the ionization, surface tensions and directly interacts with the melt pool [39], [40].

All these factors are known to be part of laser welding and are described in literature. However, most of the material properties for extreme temperatures in the keyhole are unknown. Several attempts have been made to make simplifications to practical implementations [39].

Simplified models of various complexities may be found. These provide tips and indications on different details of the laser keyhole welding process. Some of the simplest examples are models that estimate temperature gradients at some distance from the keyhole. Newer and more complicated models are based on various forms of finite element modelling which deals with the different physical phenomena numerically. To a certain degree, these methods suffer from a limited knowledge of the material properties under the extreme temperatures and gradients, such as those present in laser keyhole welding [39].



Researchers have attempted to produce models of multibeam welding. In one case they developed a model of a stationary dual-beam laser welding in order to calculate the transient heat transfer and fluid flow in the weld pool and to study weld pool dynamics during the dual-beam laser welding process [99]. Although some agreement with the final weld shapes is found, significant work still needs to be performed on such models.

### **Summary of modelling of laser welding**

Modelling of laser welding is shown to be a complicated process, where several physical phenomena interact with each other, while extreme temperature gradients exist. Especially the temperature gradients, light coupling and unknown material properties at these temperatures are a problem for realistic models.

Still, no commercial software dedicated to model laser keyhole welding exists. Thus, implementing any useful model, would be a large and time consuming project, which would take several years. For this reason this project has focussed on a more practical approach instead.

### **Summary of state-of-the-art**

State-of-the-art for single mode fiber laser technology, laser welding and beam shaping technology has shown that it should be possible to produce spot patterns for welding by applying beam shaping technology to fiber lasers. Further it has been found that only limited examinations of multi laser beam welding has been performed. None of the identified experiments with multi laser beam welding has been performed with the intensities possible by applying a single mode fiber laser.

This means there is an almost new research field within high power laser material processing with beam shapes.

Several challenges and quality issues in laser welding has been shown. All ready other researches has shown that some of these challenges can be solved by use of multiple lasers/spots/beam shapes. By applying the new high brightness beams from e.g. high power single mode lasers it has been demonstrated that even smaller spots can be produced.

The above findings in state-of-art form the basis for the problem formulation in next chapter.

## CHAPTER 3. PROBLEM FORMULATION

Chapter 3 builds on the knowledge obtained in the two previous chapters. It has been concluded, that the lack of examples of macro material processing with high brightness lasers with multiple spots in state-of-the-art shows that multi spot fiber laser welding is a new approach. It has also been shown, that the new technology has a great potential for improving laser welding technologies.

This dissertation is based on the concept that in general, spot patterns can be designed to deal with specific quality challenges in laser welding. Further it is claimed that improved quality and tolerances can be achieved compared to the same weld produced with only a single round spot.

These spot patterns are achieved by shaping high quality laser beams into an application specific pattern wherein each spot forms its own keyhole. This can be understood quite widely, as laser welding has many aspects. Therefore a hypothesis is presented so that this dissertation only will focus on a narrow part of the field: reshaping of beams into multiple spots. In this dissertation the details which is to be examined is presented along with specific research objectives and research questions.

### 3.1. HYPOTHESIS

The appearance of high power single mode fiber laser, with good beam quality, allows for making very intensive spots. These high intensive spots make it possible to produce more narrow welds using less energy than in traditional laser welding [29]. By reshaping the wavefront of the beams it becomes possible to produce almost any pattern or shape from a laser beam [81].

The hypothesis is that the excessive intensity produced by a high brightness single mode fiber laser can be used for reshaping a beam into multiple spots in the same interaction zone. This should then result in new welding options in which the energy distribution is designed for the specific application.

In this project the following (key) elements should be investigated:

1. It should be possible to control the geometry of the final weld in both width and depth, e.g. by placing a row of beams transverse to the welding direction
2. By placing beams in multiple rows of various distances, it should become possible to gain more advanced control of the melt pool

3. Spot patterns should make it possible to affect the melt flow and by doing so open up for new possibilities such as welding materials with different material properties

The use of multiple spots in the interaction zone has been described in section “2.4 *Multi beam laser welding*”, and in this sense is not new. However, previous work has often used lasers with a low beam quality or has been using multiple lasers and has therefore often been limited to two or three systems. In this work a new approach is investigated. The spots are produced by reshaping the energy distribution of *one* laser beam with DOE's. This allows for placing multiple beams in a pattern. In this way, the technique is not limited to any specific number of spots, but paves the way for new design options for energy distribution in laser welding.

By reshaping the beam, new options within many laser procession fields will present itself. In this project multi spot welding of metallic materials with sheet thickness up to 2 mm is examined using a single mode fiber laser. As regards the reshaping technique, a multimode fiber laser might have been chosen; however, this would have limited the level of details in the pattern, since the focussed multimode spot is several times larger than the focused spot from a single mode laser (see table 1 for further details). It would also have resulted in rather coarse patterns, where it would be difficult to take advantage of the effects and new design options. In figure 11 two examples of spot patterns are shown.

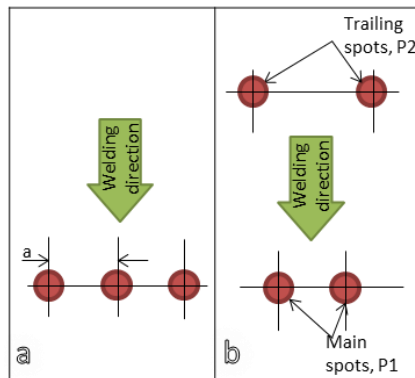


Figure 11 Example of two suggested energy distributions to be used in the project.

The three listed key elements above including the investigation of state-of-the-art in this project have led to the formulation of the projects research objectives and research questions.

### 3.2. RESEARCH OBJECTIVES

In this project the following objectives will be examined:

Project Research Questions (PRQ's):

1. How can single mode fiber laser beams efficiently be shaped into specific patterns?
2. How are spot patterns characterised and measured?
3. How can design rules be established for a suitable spot pattern meeting the demands of a specific application?
4. To what extent can multispot welding give better weld qualities than today's state-of-the-art laser welding?

The following questions, which are of more industrial relevance, will also be addressed:

5. How is multispot welding technology integrated into the existing production setup?
6. Can beam shaping of single mode fiber laser beams expand the market for laser welding?

### **3.3. APPROACH**

The empirical approach chosen for this dissertation focuses on implementation, design of patterns, realisation and characterisation of beam patterns and real industrial cases. The use of this approach does not rely on computer models and simulation of the process. Instead, a database of practical results and knowledge is established. This serves as basic input for the design of beam patterns.

This approach has been chosen instead of a more analytic approach based on e.g. computer models due to the complexity of simulations of laser welding. Also a basic knowledge database of results from welding with a single spot can be established with a workload which is reasonable to perform within a PhD project with weld geometry and quality as function of various input parameters, and is therefore a useful tool when working with implementation and realisation of laser processes

Furthermore, different ways of changing the beam into spot patterns are examined along with methods for the analysis of patterns and beam propagation. Focus is primarily on using DOE's. DOE's offer the required flexibility to produce spot patterns with spots, which has a high beam quality, and hereby also depth of field. There exist other ways of more efficient beam shaping techniques like gratings. However DOE's with structures much larger than those in gratings offers a beam shaping quality which is considered good enough for spot patterns to be produced in this project.

### **3.4. ADVISORY GROUP**

As part of the project a group of industry representatives from Grundfos and Danfoss is established.

Both Grundfos and Danfoss are market leading, world-renowned companies within each of their fields. Grundfos designs and manufactures pumps of almost any variation, and Danfoss designs and produces valves and other control equipment for almost any application within the regulation of thermal flow.

The group's task is to provide input for the ideas and solutions generated throughout the process to be put into practice and implemented in industry. Furthermore, the group provides cases based on the current challenges of their productions.

The group has provided several ideas and suggestions for the cases of the project:

- Control of weld geometry
- Robust welding (zinc/pollution)
- Control of cooling rate when welding duplex steel
- Butt joining of ultra-thin sheets
- Control of the mixing of metals
- Uneven heating of materials with different thermal properties
- Humping beads: how can this phenomenon be suppressed/avoided

### **Summary of problem formulation**

A hypothesis has been presented along with a choice of how spot patterns will be produced during the project. From the hypothesis there is an implicit choice of the use of high power single mode fiber lasers. Further evaluation of spot patterns have received its own research question, as it is considered to be important to have a well-defined way of characterising and describing transformation of laser beams into spots.

The problem formulation, hypothesis, research objectives and the monitoring group all has a focus on empirical study and demonstration of the technology along with routes of how to implement multi spot laser welding into an industrial production.

Two cases from the advisory group has been selected for further examination. It is *control of the weld geometry* and *robust welding (zinc/pollution)*.

Regarding control of weld geometry one of the main thing this can be used for is welding of multiple parts in a butt joint configuration with lower tolerance sensitivity to gaps and misalignment. The final weld should be comparable with state-of-the-art welds performed on similar geometries. Work and result of this is presented in "*paper B: Beam shaping to control of weldpool size in width and depth*" and "*paper C: Joining of multiple sheets in a butt-joint configuration using single pass laser welding with multiple spots*".

In the case with robust welding the aim is to make a process which is more robust than the single laser spot process being used today. The final weld seam should have the same or improved quality properties. Results from work with improved weld stability are presented in "*paper D: Inline repair of blowouts during laser welding*".

# CHAPTER 4. EQUIPMENT, CONSTRUCTION, BEAM PATTERNS AND EXPERIMENTS

In chapter 4 the experimental setup will be presented together with results of experiments with laser beam welding.

The sections “4.1 *Experimental setup at IPU*” and “4.2 *Experimental setup at AAU*” presents the experimental setups developed at IPU and AAU. The section “4.2 *Experimental setup at AAU*” also contains a description of the parts developed in this project making it possible to insert DOE’s into laser heads at AAU. The laser heads that were used are close to the ones used by industry. The section is thus answering Research Question 5 (PRQ 5) about how multi beam welding technology (beam shaping) can be integrated into an existing production setup.

The section “4.3 *Summary of Paper A: Design of measurement equipment for high power laser beam shapes*” addresses PRQ2 about how spot patterns are characterized and measured.

In section “4.4 *Test of DOE’s*” more tests and results are given in which spot patterns generated by different DOE’s are tested and evaluated. The section addresses PRQ1 and presents suggestions to how laser beams efficiently can be shaped into specific patterns.

The section “4.5 *High speed photographing*” presents experiments and some limited results in which a high speed camera has been used to try to get information about the melt flow when introducing multiple keyholes in the same melt pool. The purpose was to obtain information which could be summarised in design rules and used for answering PRQ 3.

Many of the problems and challenges are similar to challenges in the research project Robocut. [117] Robocut is a “Højteknologifondsprojekt” financed by Højteknologifonden with several Danish partners, including IPU and Aalborg University. The project aims at improving laser cutting using beam shaping. Some of the problems and challenges are therefore addressed in a joint cooperation between this Ph.D.-project and Robocut.

## 4.1. EXPERIMENTAL SETUP AT IPU

IPU had at the start of this Ph.D.-project a test bench with two single mode fiber lasers (100 W and 400 W). The test bench was made so that a beam from one laser

could be split multiple times and arranged so that a nearly parallel set of beams propagated towards the lens and was focused in the same plane. This allowed for manually construction of various patterns and geometries by rearranging the positions from where the beams were sent towards the lens [73].

The advantage of this setup was

- each beam was a replica of the original beam from the laser, only with less power. There was therefore no reduction in beam quality (polarization of the individual beams where not examined)
- the beams could be placed and thereby superimposed in many different beam patterns
- no scattered light

The major disadvantages in this setup

- alignment of beams, which required a lot of work
- the relative power in each beam could only be chosen in fixed steps, and only by rearranging beam splitters and mirrors
- a very long beam distance was needed to allow for arrangements of the beam and make them propagate nearly parallel towards the lens

In figure 12 the principal beam path and a photo from the setup is shown [73]. Photo is taken from right to left in the middle of the principle beam path.

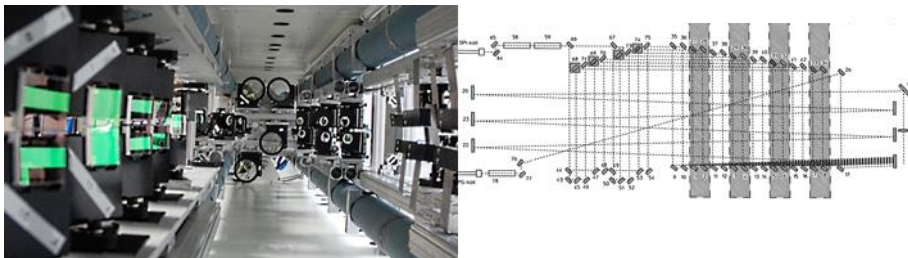


Figure 12 Initial optical setup at IPU. Left: Photo from the optical bench.. Right: Principal beam path for the setup. Note the many mirrors and the hereby large alignment task.

The laboratory at IPU was upgraded with a 1 kW single mode fiber laser from IPG Photonics, and it was decided to change the way of reshaping the beam by switching to a programmable reflective DOE-technology and implement this as a flexible beam shaping unit into the setup.

Advantages of this include

- Nearly full freedom in design of wavefront, and thereby pattern and intensity
- Test of designs without waiting for supplier
- Low cost for each design

## Disadvantages

- The individual beams in the focus have their wavefront reshaped. Thus they have a higher  $M^2$  value and less depth of focus
- Limited resolution and size of programmable DOE, whereby large patterns became difficult to produce
- Not possible to test designs with more than 1 kW which was installed at IPU, as the flexible beam shaping unit installation is fixed
- Short processing time

#### 4.1.1. FLEXIBLE BEAM SHAPING UNIT AT IPU

The flexible beam shaping unit was designed and built in cooperation with the Robocut project. It was designed for cutting applications, but it works for laser welding as well, as long as a welding gas nozzle is applied.

The setup is built around an optical component called: Liquid Crystal on Silicon – Spatial Light Modulator (LCoS – SLM). The principle can be seen in figure 13. The SLM has a resolution of  $20 \times 20 \mu\text{m}$  and  $600 \times 792$  pixels with 189 phase levels in each pixel. The integration of the SLM, optics, lens and camera are shown in figure 14.

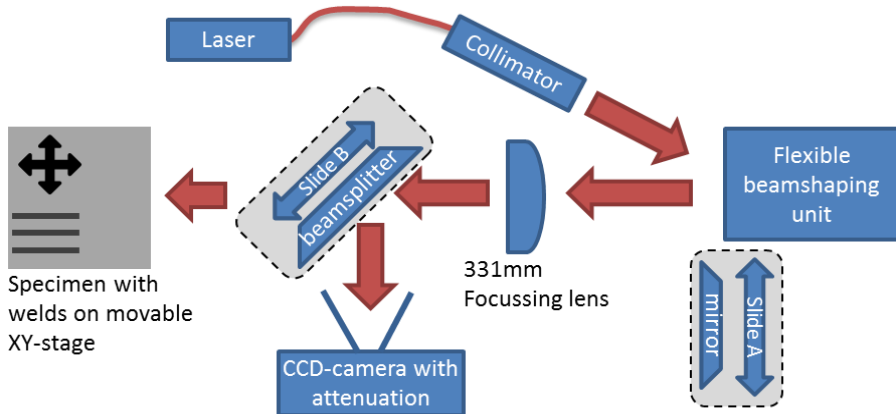


Figure 13 principle construction of flexible beam shaping processing at IPU.



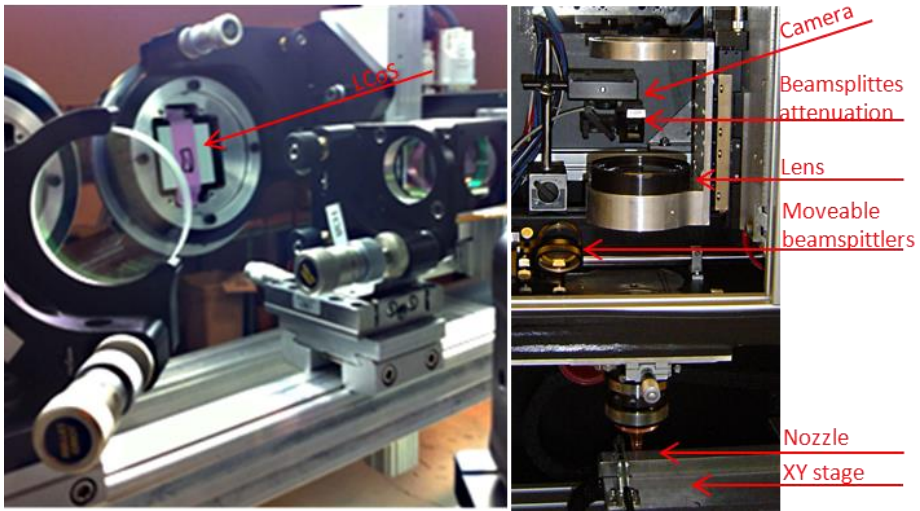


Figure 14 Left: Photo of SLM with white cover plate together with rest of necessary optics. Right: Components and construction around lens and camera solution in the IPU setup.

Most of the tested designs and welds performed with the flexible beam shaping unit can be seen in paper C “Joining of multiple sheets in a butt-joint configuration” [101] and paper D “Inline repair of blowouts during laser welding” [108].

The flexible beam shaping unit is not yet suited for production use. Any industrial implementation will therefore have to rely on a physical DOE, which must be rotated in the beam path.

## 4.2. EXPERIMENTAL SETUP AT AAU

At Aalborg University a 3 kW single mode fiber laser was available. Due to the higher power a different strategy regarding beam shaping was chosen. A transmissive DOE in fused silica was introduced in the beam path in the laser head.

Two laser heads, both with two different focusing modules, was present at AAU. Head 1 from HighYAG GmbH consisted of a 780 mm and a 460 mm focusing lens. Head 2 from Optoskand AB consisted of a 300 mm and a 200 mm focusing lens. Both laser heads had a 200 mm collimation lens.

### 4.2.1. INTEGRATION INTO COMMERCIAL LASER HEADS

There exist several principles by which a spot pattern can be produced. Most of them are described in section “2.3 Beam shaping technology”.

An industrial implementation is easiest made, if as much existing technology and equipment can be reused. To apply a DOE in a modified industrial laser head seems to be the simplest way to apply a spot pattern in an industrial setup.

To insert DOE's in any of the two laser heads at AAU it was necessary with a flexible system where the DOE

- can be exchanged
- aligns to the center of the beam path
- can be cooled

The HighYAG head was delivered with a drawer, in which the DOE could be placed. A similar drawer was designed and implemented to the Optoskand head. The drawer itself only had a hole in the center of it, which aligned with the beam path.

The DOE was mounted in a set of brass rings which was clamped to the drawer to give a thermal contact, which could lead away the absorbed energy. The drawer again had thermal contact to the drawer house, which for the HighYAG head was water cooled.

The Optoskand system is not equipped with water cooling, which did not give any problems in the experiments, since it wasn't necessary to run experiments under continuous conditions, but only in short time. The brass rings aligned the DOE sufficiently, and made it possible to change the DOE.

In figure 15 is shown CAD images of the two laser heads with the drawers and the brass rings that remove the heat. Figure 16 shows a photo from the robot cell at AAU with the HighYAG head mounted. The delivery fiber is above the photo, and the laser is placed outside the cabinet.

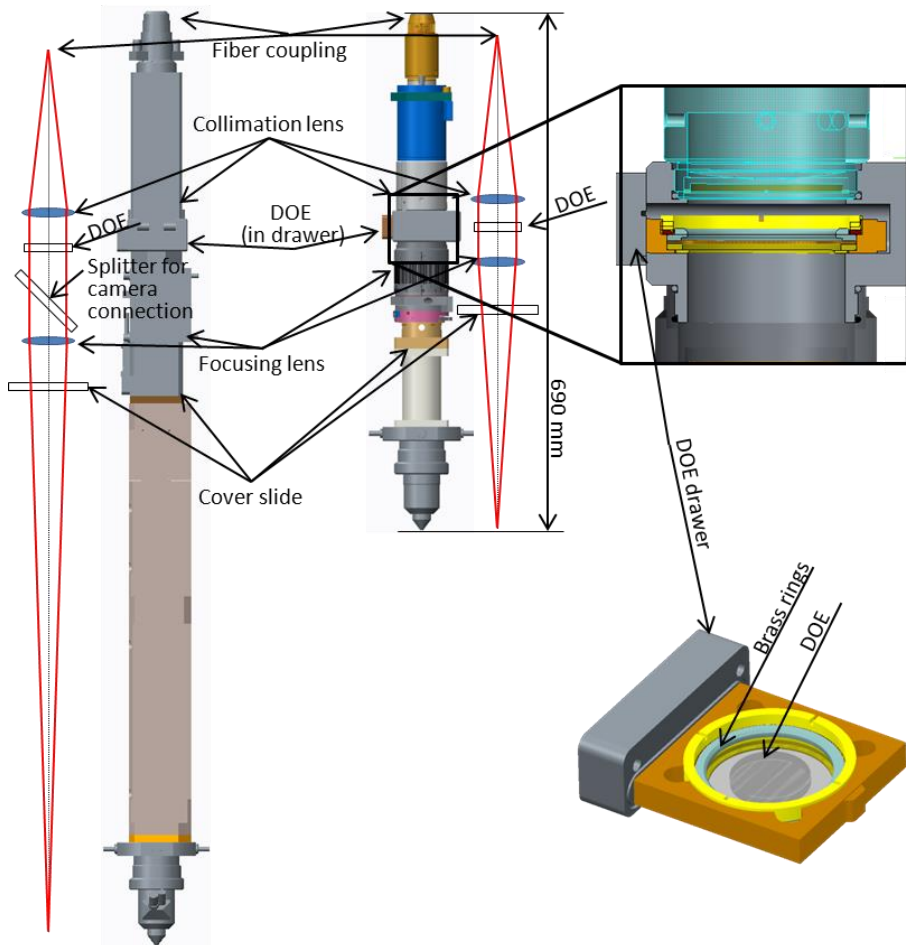


Figure 15 Left) HighYAG laser head mounted with 780 mm focus lens. Middle) Optoskand laser head with 300 mm focus lens. Both shown with principle beam propagation and in same scale. Right: DOE drawer in detail.

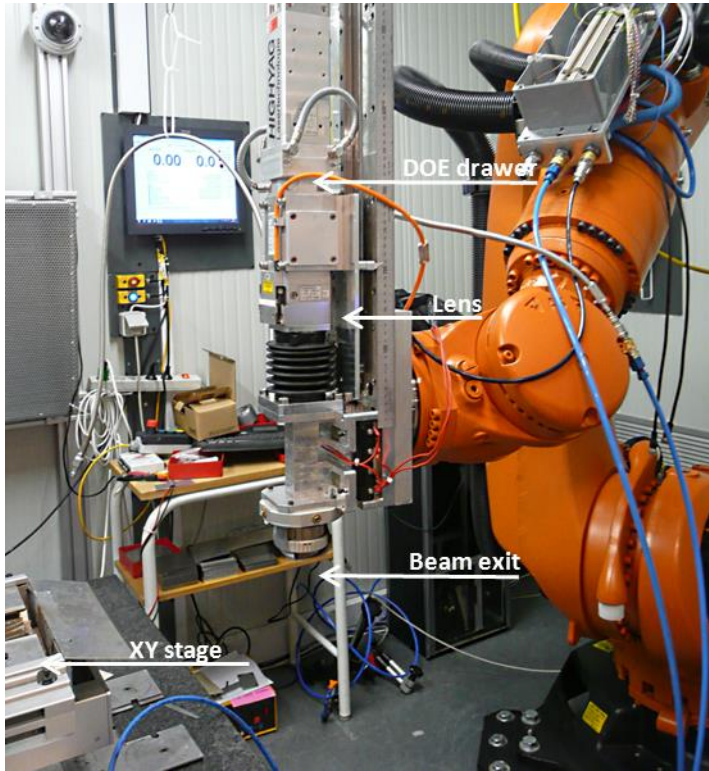


Figure 16 HighYAG laserhead mounted in robot cell. The robot is only used as fixture, as the movements in this project where performed using the XY stage.

#### 4.2.2. THERMAL LOAD

In order to design mounts and elements for continuous use in industrial setup, it is necessary to take thermal load and design of cooling into more serious consideration.

Two things affect how a piece of optic performs; its refractive index and its shape. They are both affected by the temperature, which means an element's performance is altered by the temperature in following ways:

- Overall the refractive index can change according to temperature
- The refractive index becomes a gradient across the element as consequence of uneven temperature distribution, thus the element becomes a GRIN element (GRadient INdex element)
- Change in form of the element due to expansion as temperature increases in the whole element

- Change in form as a gradient as a consequence of uneven temperature distribution

When an optical component is exposed to radiation from a laser beam (or any other source of electromagnetic radiation) it will either: reflect it, transmit it, absorb it or a combination. Most optics for fiber lasers are transmissive. Even though most of the light is transmitted a little of the light is absorbed and leading to increased temperature in the component.

On transmissive optics it is often only possible to cool on the outer part of the optics. This leads to a temperature gradient across the optics. Further the intensity profile from the collimated laser beam is Gaussian distributed. This also leads to a larger amount of energy absorbed in the center of the optics than further out.

The design of mount, cooling and the optical materials thermal properties do therefore have an important influence on the performance and any changes caused from thermal load.

#### 4.2.3. DOE ROTATOR

Since the drawers are stationary, it is only possible to perform experiments in one direction, as the pattern cannot be rotated. The cooling of the DOE is also limited in both heads. For many industrial implementations a straight welding is insufficient, and in many cases inadequate. A more flexible unit was therefore developed.

To rotate the beam pattern it is necessary to rotate the transmission phase produced by the beam shaping unit. In the case upon which the whole beam shaping unit is a DOE, the DOE must be rotated in the collimated beam.

The DOE is basically a round disc. The disc will absorb and reflect some of the energy. It will therefore heat up and lead to thermal drift. It is therefore necessary with cooling of the DOE. The amount of absorbed and reflected absorbed light depends on the material by which the DOE is made of and if the DOE has an anti-reflection coating. Even small amount of absorbed energy will lead to significant absorbed energy as the DOE will be exposed with up to 3 kW of laser power.

IPU has developed such a unit. The author of this dissertation has participated with specs and input to the design process. The unit is developed as part of the Robocut project, which also uses beam shaping, but for improving laser cutting instead of laser welding. The developed unit can be used for rotating a DOE – regardless of the process, it is used in.

Basic functional requirements for the unit were:

- Heat transportation: It is important to establish good thermal contact in order to cool the DOE. A cooling capacity of minimum 30 W was set corresponding to cooling of up to 1 % of maximum power under continuous load
- Flexibility in rotation: It should be possible to rotate the DOE with an arbitrary number of revolutions
- Homing: The orientation should be known – also after loss of power
- Rotation: Angle of the DOE should be known within 0.2 degree
- Dynamic performance: Positioning tolerances was set to allow for up to 0.5 degree of dynamic misalignment
- Flexibility: It should be possible to change the DOE with minimum disassembly
- Pollution: It should be provide protection against dirt and impurities to enter the beam path. As smoke is developed during many thermal processes, the head should be sealed, when it is closed
- Rotation speed: The rotation was set to maximum 20 rounds per second
- Future development: There ought to be a space for mounting additional sensors for scattered light, which can be used to detect if performance of a DOE changes, since it could be an indication of failure

The developed unit is shown in figure 17. It is ready to be mounted on the Optoskand head. The flanges can be exchanged, so it can be mounted on the HighYAG head instead.

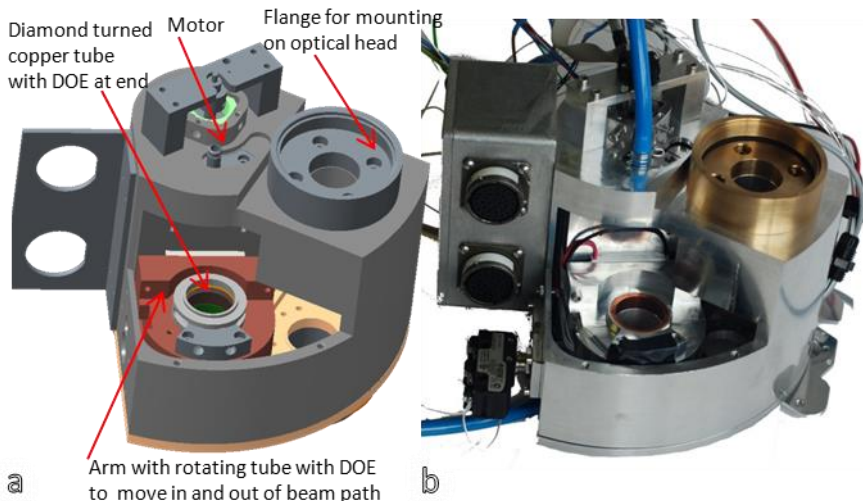


Figure 17 DOE rotator with some of the protective housing removed. Arm with DOE shown in “open position”. a) CAD image. b) Photo.

The basic functional requirements for the DOE rotator is met by

- mounting the DOE on a diamond turned surface at the end of a copper tube, so the heat can be transported efficiently away. To remove the heat from the copper tube, the whole rotating part is mounted with very little distance to a stationary outer tube. This small distance optimizes the heat transport, as there only is a limited amount of isolating air. On the stationary part is mounted a water cooled peltier element to cool the outer tube. The tube is mounted in a pair of precision bearings, which again is set on an arm which can swing out of the beam path and allow for changing the DOE.
- The tube is rotated by a tooth belt drive to a brushless DC servo motor with an encoder to detect its position.
- In the unit there is mounted a homing diode to detect zero position after power off.
- The whole unit is sealed with O-rings and gaskets in all outer lids and openings.
- Further switches to detect if unit is open are mounted for safety so the motor cannot run and laser is off while changing DOE's.

### **4.3. SUMMARY OF PAPER A: DESIGN OF MEASUREMENT EQUIPMENT FOR HIGH POWER LASER BEAM SHAPES**

To evaluate the beam patterns produced by DOE's, a beam analysing system was designed. The objective of this system is to measure and quantify the energy distribution of any energy distribution in and around the focal position. Demands for this system are: a high dynamic range, flexibility, ability to withstand high power and a high resolution. These issues are discussed and dealt with in the paper presented at NoLamp14. The full paper is reprinted in appendix A.

The following is a short summary of the paper and also includes information about improvement since the paper was written.

#### **4.3.1. Objectives**

##### Hypothesis:

High power beam shapes can be measured and characterized using a commercial laser beam measurement system by applying proper attenuation.

This raises the following research questions:

##### Research questions (RQ's):

1. Which system is best for characterizing details in complicated beam patterns, where the beam can be down to a diameter of 20  $\mu\text{m}$ ?
2. How much attenuation is needed in front of the sensor?

3. How can attenuation be adjusted?
4. How to visualize, interpret and compare measured data with expected data from the design process.

### 4.3.2. RESULTS

First an analysis of the requirements for the analysis system where listed. These included dynamic range, scan area, signal to noise ratio etc. Full list of requirements are given in paper in appendix A.

A solution based on a commercial CCD camera with measurement software and attenuation was found to fulfil the requirements listed. Thus RQ 1 is answered with the statement that CCD camera is the best solution to characterize complicated beam patterns with a sufficient resolution.

In order not to damage the sensitive CCD chip attenuation is needed. It was chosen to use beam splitters for the first steps of reducing the intensity. After the beam splitters exchangeable ND-filters where installed. In appendix A calculation of required attenuation for each focus lens and power level is calculated. The whole range of required attenuation is further shown to be covered by the chosen ND-filters. The required attenuation is installed in a way which allows for adjustments (exchange of ND-filters). Thus RQ 2 and 3 is answered.

RQ 4 which deals with visualization and evaluation of measurement data is answered by the use of the commercial available software where the measurement data can be compared with the design using a spreadsheet, and proper evaluation. Examples of measurement and calculations of such is shown in section “4.4.6 Discussion and comparison of performance”. Figure 18 shows the final assembly mounted in a frame with beam splitters and ND-filters. A more detailed beam path can be found in the paper in appendix A.

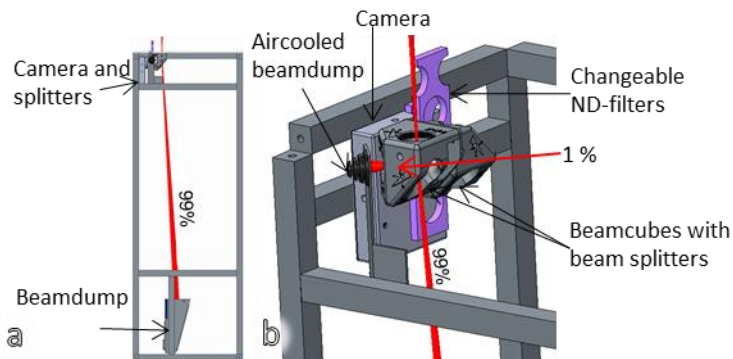


Figure 18 The constructed CCD camera based assembly with attenuation, beam dumps and protective cover. Rework from “paper A: Design of measurement equipment for high power



beam shapes" [100]. a) The full setup with beam dump in bottom. b) Zoom on the region with camera and attenuation. See appendix A for full details of beam path.

The paper presents all the technical aspects of the design and development. The most important, from the author's point of view, is, however the flexibility the camera system possesses to produce profiles (caustics) in the laser's full power range and its possibility to evaluate spot patterns.

Figure 19 shows example of a profile produced from measurement of a recorded laser beam through focus for two different power levels. Figure 22 and 25 in the next sections shows examples of spot patterns recorded with the camera and comparisons of those to the design of the spot patterns.

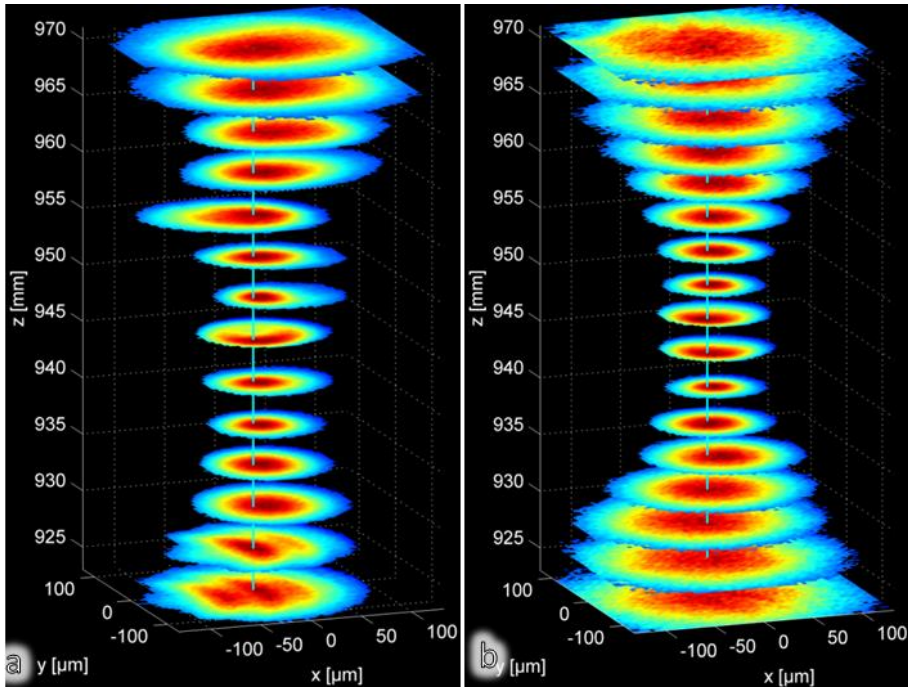


Figure 19 a) Profile with 1.3 kW. b) Profile recorded with 60 W. Both with 780 mm focal length  $\Delta Z = 3$  mm between each plane.

The evaluation of spot patterns has later been used to examine how different DOE's perform compared to their calculated performance. This has turned out to be an indispensable tool in the process of development and evaluation of spot patterns and alignment of these.

The method to evaluate the energy distribution in subareas of a given design one by one has turned out to be a robust way, and it is easy to implement in daily work. An aperture is placed around each spot, and this is compared to the total measured

energy in the focal plane. In this process it is necessary with careful calibration and subtraction of background noise. In figure 19 there is only one “sub-area”, as it is used to evaluate the beam propagation through focus for two power levels.

The method is discussed further in section “4.4.1 Measurement definitions”, where four different ways of making the required phase transformation are tested and evaluated.

### 4.3.3. ANALYSING OF THERMAL DRIFT

The measurement system has been implemented and tested further. This has shown that thermal drift from different parts in the optics also can be evaluated. The test is performed by recording data at highest possible framerate, 40 Hz, from a raw focused beam. Only little thermal drift was found in such a test using IPU's setup with 1 kW of laser power and a similar camera construction. (No images from this is presented, as they only show a single round laser spot with no change to it through an chosen amount of time). It is therefore concluded, that the attenuation in front of the camera only causes little to none thermal drift. Therefore, any additional drift can be expected to originate from whatever additional component which is added to the system or an existing component which has become dirty and thereby starts to heat up from the absorbed energy.

If strict cleanliness is kept and the beam is alignment through the system, it can be used for analysis of thermal drift from a DOE.

### 4.3.4. FURTHER WORK

The system can be improved by changing the position of the first beam splitter in the beam cubes in the assembly shown in figure 18. This should be placed so the optical load is minimised, i.e. as close to the focusing lens as possible.

## 4.4. TEST OF DOE'S

In order to have success with implementation of beam shaping of beams from single mode laser sources for macro material processing, it is necessary to be able to produce spot patterns under conditions which resembles those in industry.

In the project different ways to produce a spot pattern has been evaluated. Focus has been on DOE's, where several designs have been tested and evaluated.

The results are presented in the following, together with discussion of the findings and suggestions on how measurement definitions could be performed to be in closest possible link to ISO-standards and still practical to perform.

Some of the produced and tested DOE designs have been made for the Robocut project and therefore for cutting, but results in evaluation of energy distributions are just as valid as if they were designed for welding.

Tests has been performed with four different DOE's:

- Grey scale DOE's on fused silica with 190 steps and 100x100  $\mu\text{m}$  pixels
- Multilevel etched DOE in fused silica with  $N = 3$ ,  $2^N = 8$  steps with 25x25  $\mu\text{m}$  pixels
- Diamond turned DOE with 256 steps in zinc sulphide (ZnS) and 100x100  $\mu\text{m}$  pixels
- Flexible beam shaping unit at IPU with 189 steps and 20x20  $\mu\text{m}$  pixels

In order to compare the four methods, one of the Robocut designs were used – see figure 20: The Robocut design contains a strong centre beam (A) with a half-moon shaped trailing barrier (C) in which the edges of the barrier (B1, B2) are more intense. Around the center spot is an area with low intensity light spread out in a circle (D). The design is therefore split up into five parts for evaluation as shown in figure 20.

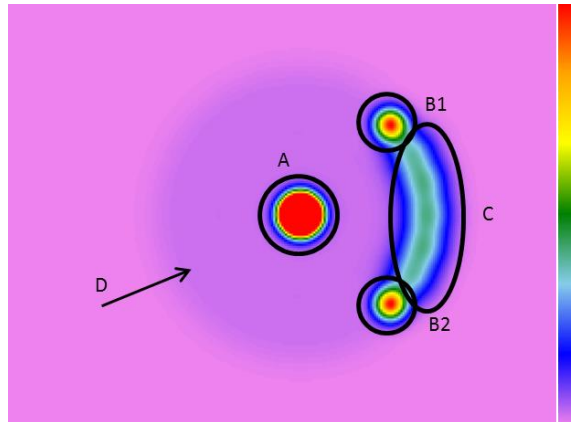


Figure 20 Design and naming of different parts in the pattern.

In the next sections terminology for different designs and definitions referring to different parts of the development work is used. Results from each production method are summarized and discussed in section 4.4.6 *Discussion and comparison of performance*.

#### 4.4.1. MEASUREMENT DEFINITIONS AND TERMINOLOGY

Figure 21 shows the principle rays in the Optoskand laser head together with a CAD image of the head. To the right are shown examples and definitions of collimated beam diameter, transmission phase and spot pattern.

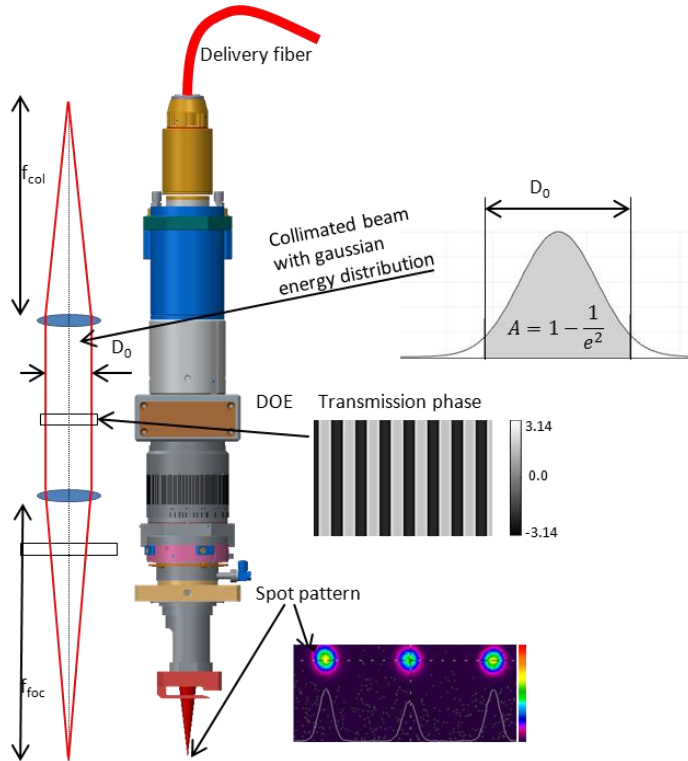


Figure 21 Optoskand laser head with DOE drawer, and the terminology used. Principle beam path is shown to the left.

Figure 22 shows the examples of a designed spot pattern, a simulated spot pattern, and a measured spot pattern.

In the project, the commercial available software VirtualLab™ from LightTrans GmbH is used to calculate the beam propagation. The same software is used to calculate the transmission phase, which corresponds to the pattern which should be produced in the DOE. Calculation of transmission phases is performed using Inverse Fourier Transformation Algorithm (IFTA) integrated into VirtualLab™.

The algorithm is a self-learning algorithm where the result from each sub-steps is fed back as starting guess for next step in the calculation. The algorithm is divided into four optimization loops where first an optimized energy distribution is sought.

Second the result is optimized to get best signal to noise ratio. Third the pattern is optimized for quantification into pixels of finite size. Fourth step is optimization of the signal to noise ratio for the quantized transmission. [82] The last two steps are for optimizing for production, as most manufacturing processes works in discrete pixels.

The designed spot pattern shows how the designer would like the pattern to be without considering any constraints and limits in the reshaping. This pattern is used as input for the IFTA. The IFTA returns a phase transmission with the given constrains (pixel size, numbers of pixels and number of levels in the design) for a given input beam diameter,  $D_0$ , and wavelength,  $\lambda$ .

The “simulated spot pattern” is the calculated pattern for a given phase, considering the number of levels, number of pixels, pixel size and collimated beam diameter. It results in an ideal model of the DOE, which does not take any misalignment, production tolerances or beam quality factors into account.

The measured spot pattern is the spot pattern produced by the actual laser beam, using the actual DOE. It is measured with a CCD camera, as presented in section 4.3 in the paper “Design of measurement equipment for high power laser beam shapes” [100]. The diameters of the spots in figure 22 are  $\varnothing 85 \mu\text{m}$  using an aperture/sub-area on each beam with a size of  $\varnothing 180 \mu\text{m}$  (marked with circles and “A1”, “A2” and “A3”). The percentages are amount of energy in each sub-area.

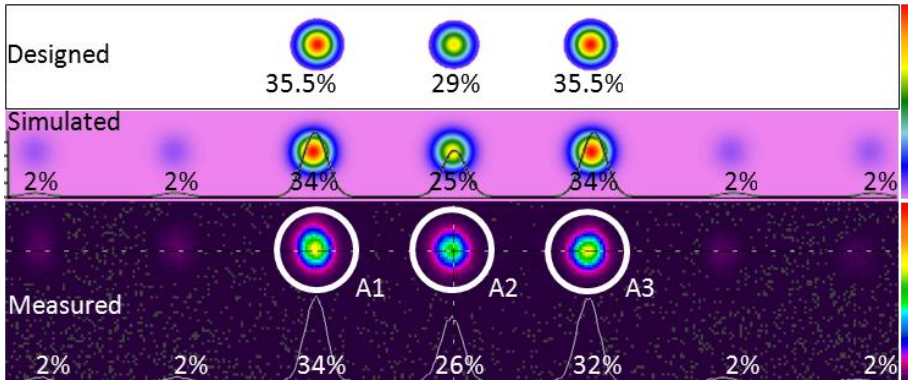


Figure 22 Spot pattern with designed, simulated and measured energy distributions. In the measured data is shown examples of three apertures for evaluation. Numbers are rounded values, and sum in the two first rows yield 101%. Rework of data from paper C: Joining of multiple sheets in a butt-joint configuration using single pass laser welding with multiple spots” [101].

From the images in figure 22 it is clear that the simulated performance differs from the original design. Further “shadow spots” are seen to both sides of the designed spot pattern. The measured performance differs again from both the simulated performance and the designed pattern.

ISO 13694:2000 “Optics and optical instruments — Lasers and laser-related equipment — Test methods for laser beam power (energy) density distribution” [8] can be used for evaluation of any energy distribution. It builds upon statistical methods for evaluation of the energy distribution to determine maximum deviation, goodness of fit etc. The principle in the method is quite simple to implement in an algorithm, in which each pixel is compared to the designed pixel or to the theoretical distribution.

In this work the method is considered too general and too complicated to implement if minor deviations is allowed without being considered as an error. E.g. a change in spot spacing of 10  $\mu\text{m}$  could maybe be insignificant for the final result, but the evaluation of performance of a DOE producing 10  $\mu\text{m}$  spot spacing would be poor. To overcome this the basic ideas in ISO 13694 have been simplified, so instead of evaluating all measured pixels, the evaluation is based on comparing the amount of energy in a given area with the designed energy in that area. Errors in distances between spot centres and other geometric errors are evaluated manually, as small errors are considered to be without significance as long as they are known.

Two numbers have been found to be of importance, when evaluating the efficiency of a DOE. Energy efficiency  $\eta_{\text{energy}}$  and transformation efficiency  $\eta_{\text{transform}}$ .  $\eta_{\text{energy}}$  tells how much of the input energy which is distributed in any of the given apertures (e.g. A1, A2 or A3 on figure 22).  $\eta_{\text{transform}}$  tells how well the produced spot pattern corresponds with the designed spot pattern, taking energy balance between the different spots into account. The two efficiencies can be calculated from equation 5 and 6.

$$\eta_{\text{energy}} = \sum_{i=1}^n \frac{E_{\text{meas},i}}{E_{\text{total}}} \quad (5)$$

$$\eta_{\text{transform}} = 1 - \sum_{i=1}^n |E_{\text{meas},i} - E_{\text{design},i}| \quad (6)$$

$E_{\text{meas},i}$  is the energy in the sub-area number  $i$ , and  $E_{\text{total}}$  is the total energy measured in the process zone from the laser beam.  $E_{\text{design},i}$  is the amount of energy that area “ $i$ ” was designed to contain.  $n$  is the total number of sub-areas.

Both efficiencies are of importance.  $\eta_{\text{energy}}$  would yield 100% if a single round spot was focused in any of the three spots in figure 22., thus  $\eta_{\text{energy}}$  would not tell anything about if the energy goes into the correct spots or not.  $\eta_{\text{energy}}$  is however telling how much of the energy which goes in the produced pattern, and hereby indirectly how much energy which is outside the pattern in e.g. shadow spots.

The capability of the different DOE's is evaluated by the transformation efficiencies, as well as their visual performance. The term visual performance is difficult to quantify. It will be discussed further in section 4.4.6 "*Discussion and comparison of performance*".

#### 4.4.2. GRAY SCALE ETCHED DOE'S

Grey scale etched DOE's were produced by Laser optical Engineering (LOE) in England.

The manufacturing process used by LOE was a semi-development of photoresist on substrate: A fused silica disc was spin coated with photoresist and then uneven exposed, so that some of the resist was more developed than other. After this the DOE was etched and – in the areas covered by semi-developed photoresist – was etched faster, dependent on the level of exposure. In this way the etching depth were varied. Unfortunately, the process is not linear and required careful calibration on the exposure and spin coating along with calibration of the etching process.

LOE had some problems to etch the desired depth. This was due to nonlinearity's in the (semi-)development of the photoresist.

Attempts by LOE to improve the quality of the outcome of the grayscale etch continued to fail. Calibration areas outside the transmittive pattern were therefore introduced. These areas were measured at IPU using an ultra-precise roughness tester with an internal linear guide. This was able to measure the etching depth. Thus it was possible to make a graph showing etched depth compared to the grayscale value used. The inverse of the function for this was then used to produce a graph (and factors to a polynomial fit), with original grey values and calibrated grey values. In this way the design was calibrated to the nonlinearity in the grey scale etching process.

In theory, the measurement of etching depth on a DOE produced with this calibration applied should yield a linear line, as the calibration curve counteracts the nonlinearities from the production process. This was however never the case. Consequently the tested grayscale DOE's all performed poor ( $\eta_{\text{transform}} = 71\%$ ) compared to a calculated performance ( $\eta_{\text{transform}} > 91\%$ ). An example of a phase pattern design and calibration curve is shown in figure 23. A total of more than 25 DOE's have been produced by LOE during 3 years, none of them performed better than  $\eta_{\text{transform}} < 80\%$ .

In the figure 25 in section "*4.4.6 Discussion and comparison of performance*" a beam pattern produced from a grey scale etched DOE is shown and compared to design parameters.

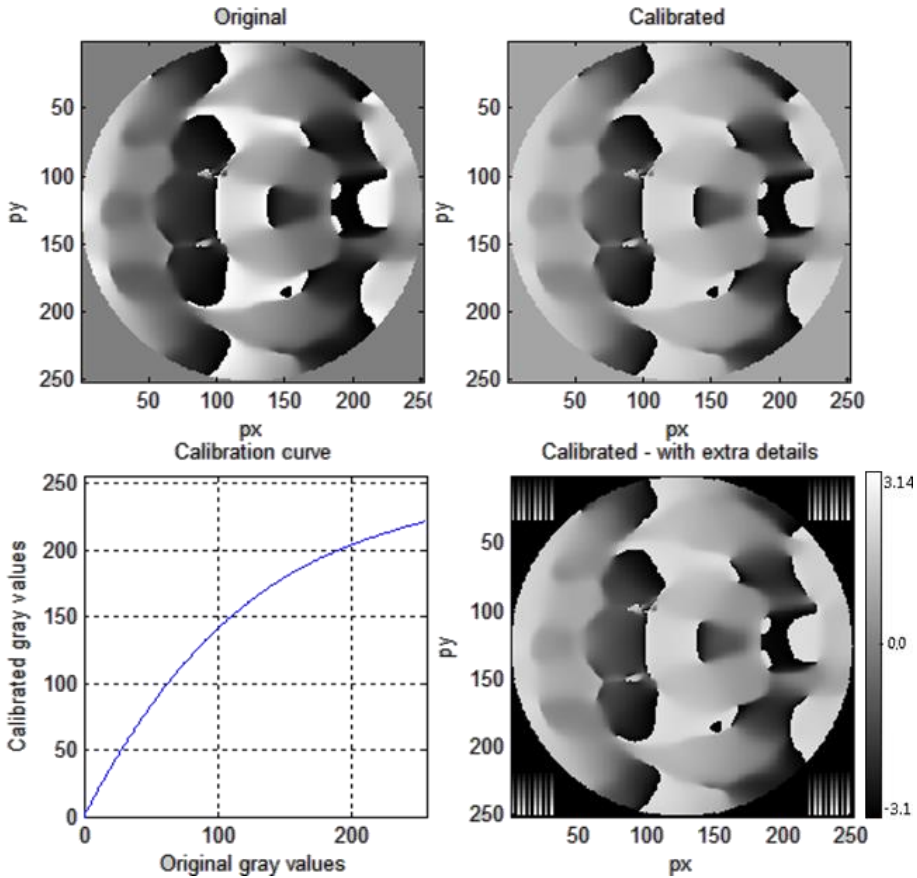


Figure 23 Top left) Example of transmission phase in grayscale values. Top right) Transmission phase calibrated with Bottom left) calibration curve. Bottom right) Calibrated transmission with control patterns in the corners.

The author believes that the many calibration steps in the manufacturing process of the grey scale DOE's along with the unlinear process results in poor performance of the grey scale etching. Other ways of performing grayscale etching exist [85], [86], [87], [102], [81]. Results using other grey scale production methods have not been evaluated in this project.

#### 4.4.3. MULTILEVEL ETCHED DOE

For multilevel etching it is necessary to apply special masks, which typical has a long delivery time, adding extra steps and time in the production chain. The masks can be reused to produce multiple DOE's with same pattern, thus lowering the cost and lead time in series production.



A multilevel etched DOE was ordered from SILIOS Technologies in France. The DOE was designed with eight levels for the Robocut project. By first thought a DOE with only eight levels was expected to perform with significantly less transformation efficiency than a grey scale etched DOE with 256 levels. A simulation presented in table 3 of performance with different number of levels had, however, revealed that the DOE would perform with a transformation efficiency close to 90%, and increasing the number of levels in the DOE from eight to 16 or even 256 would not increase the transformation efficiency by more than a few percent.

Table 3 shows calculated transformation efficiencies as function of the number of levels for three different designs tested. The efficiencies are calculated using VirtualLab™. The first design with three spots in a row is quite simple, which results in quite high transformation efficiencies. From eight levels and above the efficiency varies less than 1.5%. It is the same situation when the complexity of the pattern is increased, and the transformation efficiency only increase with up to 4.5% percent when the number of levels is doubled from eight, or even increased to 256 levels.

A multilevel DOE with eight levels is therefore concluded to be sufficient for almost any beam shaping application in which a beam splitting DOE is applied.

The DOE ordered for the Robocut project was AR-coated on both sides to minimize the reflected and absorbed light in the DOE.

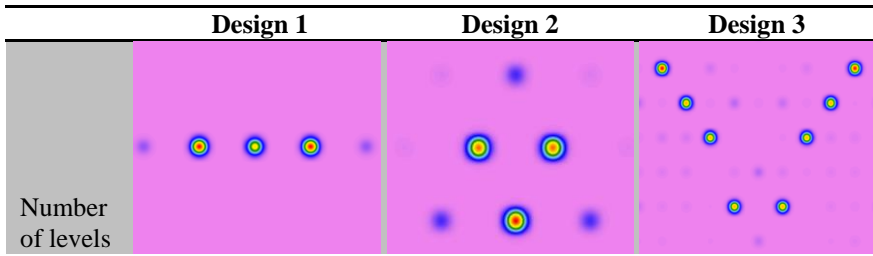
|   | Design 1 | Design 2 | Design 3 |
|---|----------|----------|----------|
|  |          |          |          |
| Number of levels  |          |          |          |
| 2   | 69.9     | 37.9     | 34.3     |
| 4   | 72.4     | 75.8     | 67.5     |
| 8   | 89.3     | 79.9     | 77.2     |
| 16  | 90.1     | 81.7     | 80.7     |
| 256   | 90.7     | 82.6     | 81.7     |

Table 3 Simulated energy distribution for 8 levels and calculated transformation efficiency,  $\eta_{transform}$  (percentages) for three different spot designs and number of discrete levels.

In figure 25 in section "4.4.6 Discussion and comparison of performance" a beam pattern produced from a multilevel etched DOE is shown and compared to design parameters.

#### 4.4.4. DIAMOND TURNED DOE

Instead of utilizing etching and other processes from the microelectronic industry it is possible to use a more traditional process like turning or milling. Due to the small pixels this needs to be very accurate compared to classic macro machining. Since designs typical are asymmetric, the turning process needs to have a tool, which can be varied during processing. Both requirements can be fulfilled by modern diamond turning lathes. The principle is shown in figure 24. The diamond tool can be moved in and out of the material (referred as nFTS-movement in the figure), thus machining the required depth from the grayscale transmission in the material.

In order to cut in a substrate, the substrate needs to be machinable with diamond tools. This is not possible in many glass materials like fused silica. It is however possible in zinc sulphide (ZnS), which is a well-known material for optical elements to CO<sub>2</sub> lasers. Zinc sulphide exists in a version called “MS” or “clear” – dependent on manufacturer – which also can be used for 1075 nm lasers and poses good machinability for diamond turning [103], [104].

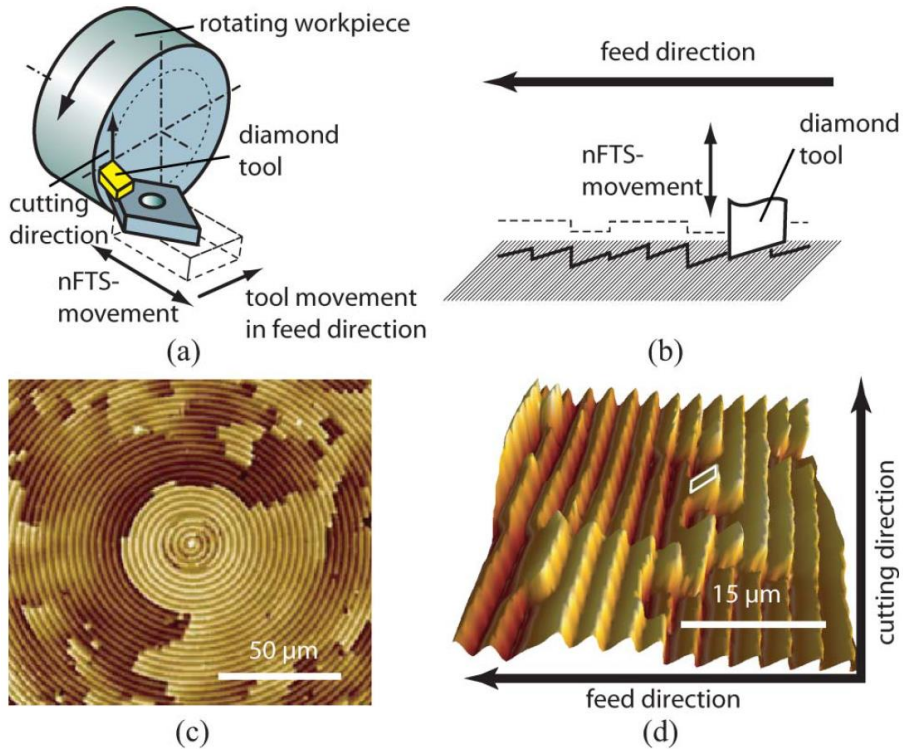


Figure 24 Fabrication process and resulting surface geometry. (nTFS is the position of the tool in the material). a) Scheme for the machining process for DOE's. b) Schematic structure in the feed direction and imprint of the diamond tool shape. c) Section of the surface of the DOE. d) Detailed view of the same part of the surface. The highlighted area corresponds to one single cutting depth value in the control signal of the nFTS (the highlighted area corresponds to one pixel). The maximum height difference displayed equals 700nm. Reprinted from Dankwart et.al [76].

In section “4.2.2 Introduction” four factors which affects an optical elements performance is listed. The two factors which refers to changes in form of the element are further influenced by how the element is fixed in its mounts, as it can affect the way the element expands.

In optical elements the effect on the optical performance are normally small from:

- Change in form due to the elements overall temperature as the whole element expands
- Gradient change in form due to temperature gradients

The change in refractive index and the gradient refractive index from temperature gradients usually affect the performance of optical elements much more.

Currently zinc sulphide is suggested as an alternative material to fused silica, not only to produce DOE's but also lenses and other optical components [105]. One of

the advantages when using zinc sulphide is its machinability. This makes it easier to produce one-of-a-kind optics and prototypes. Another advantage of using zinc sulphide instead of fused silica for DOE's (or optics in general) is its thermal conductivity, which is 20 times higher than for fused silica. However sensitivity of the refractive index and temperature change is four times higher for zinc sulphide than for fused silica. Also, the bulk absorption is about the double of fused silica. The expansion coefficient is also a factor 11 higher. Overall this means that the advantage of the increased thermal conductivity is somehow equalised when looking on the other material properties.

One major advantage of DOE's produced by diamond turning is, that it usually has the shortest delivery time of the different methods. This is caused by the shorter process chain: a blank zinc sulphide element needs just to be mounted and processed in lathe and afterwards AR-coated.

The material properties of fused silica, n-BK7 and zinc sulphide is shown in table 4. N-BK7 is included as it often is used as an alternative to fused silica.

In the figure 25 in section "*4.4.6 Discussion and comparison of performance*" a beam pattern produced from a diamond turned DOE is shown and compared to design parameters.

|                              |           |                                 | Fused silica<br>Lithosil ® | n-BK7<br>(Schott) | Zinc sulphide<br>(ZnS - clear) |
|------------------------------|-----------|---------------------------------|----------------------------|-------------------|--------------------------------|
| Surface reflection           | R         |                                 | 0.033682                   | 0.040841          | 0.15344                        |
| @1075nm (uncoated)           |           |                                 | [106]                      | [106]             | [106]                          |
| Refractive index             | n         |                                 | 1.450                      | 1.507             | 2,292                          |
| @1060 nm, 20°C               |           |                                 |                            |                   |                                |
| dn(rel)/dT                   |           | $\times 10^{-6} \text{ K}^{-1}$ | 9.4                        | 2.4               | 42                             |
| @1060 nm 20-40°C             |           |                                 |                            |                   | [105]                          |
| Internal transmittance       | $\tau_i$  | % / cm                          | 0.1                        | 0.2               | <0,2*                          |
| Heat capacity                | $c_p$     | J/g/K                           | 0,79                       | 0.858             | 0,527                          |
| Thermal conductivity         | $\lambda$ | W/m/K                           | 1.31                       | 1.114             | 27,2                           |
| Linear expansion coefficient | $\alpha$  | $\times 10^{-6} \text{ K}^{-1}$ | 0.5                        | 10                | 6.5                            |

Table 4 Material data from Schott [103] unless other is stated. \*= unit is not given in datasheet, and is therefore assumed similar to industry standard.

The fact that the surface reflection from zinc sulphide is quite high should not give problems, as this can be nearly eliminated by use of anti-reflection coatings, as well as it can for fused silica and n-BK7.

The linear expansion coefficient is 13 times higher than for fused silica so any temperature gradients will lead to larger deformations. Also the change in refractive index as result of temperature changes,  $dn(\text{rel})/dT$ , is 4.5 times higher for zinc sulphide than for fused silica. It is therefore of larger importance to have efficient cooling and an even temperature in zinc sulphide than in fused silica. The 20 times higher thermal conductivity in zinc sulphide compared to fused silica somehow accommodates for this, since the heat is being led more efficiently away in zinc sulphide, than it is in fused silica. Practical tests and evaluation to make a final conclusion is needed in order to determine which material is best for DOE's for industrial implementation.

A DOE in zinc sulphide for the Robocut project was ordered from II-VI Infrared. It was AR-coated on both sides to minimize the reflected and absorbed light at the surface of the DOE.

In figure 25 in section "4.4.6 Discussion and comparison of performance" a beam pattern produced from a zinc sulphide DOE is shown and compared to design parameters.

#### 4.4.5. FLEXIBLE BEAM SHAPING UNIT

To evaluate and compare performance from the four tested methods the Robocut design was adapted to the flexible beam shaping unit at IPU.

#### 4.4.6. DISCUSSION AND COMPARISON OF PERFORMANCE

Figure 25 shows the pattern from design including its modelled performance together with the resulting pattern from the four different beam shaping methods tested. The images are taken with several years between them, and updates and changes to the setup have occurred in this period.

The pattern is smaller, when it is produced by the flexible beam shaping unit (f). This is due to an update in the lab, where the collimator on the laser is changed, so it produces a smaller collimated beam diameter ( $D_0$ ). The transformation pattern has been resized to accommodate for this change in collimated beam diameter. The change should not affect the transformation efficiency as long as evaluation areas are scaled with the change in collimation length.

For a+b values which are red are truncated values. For c+d+e+f values which are grey are truncated values

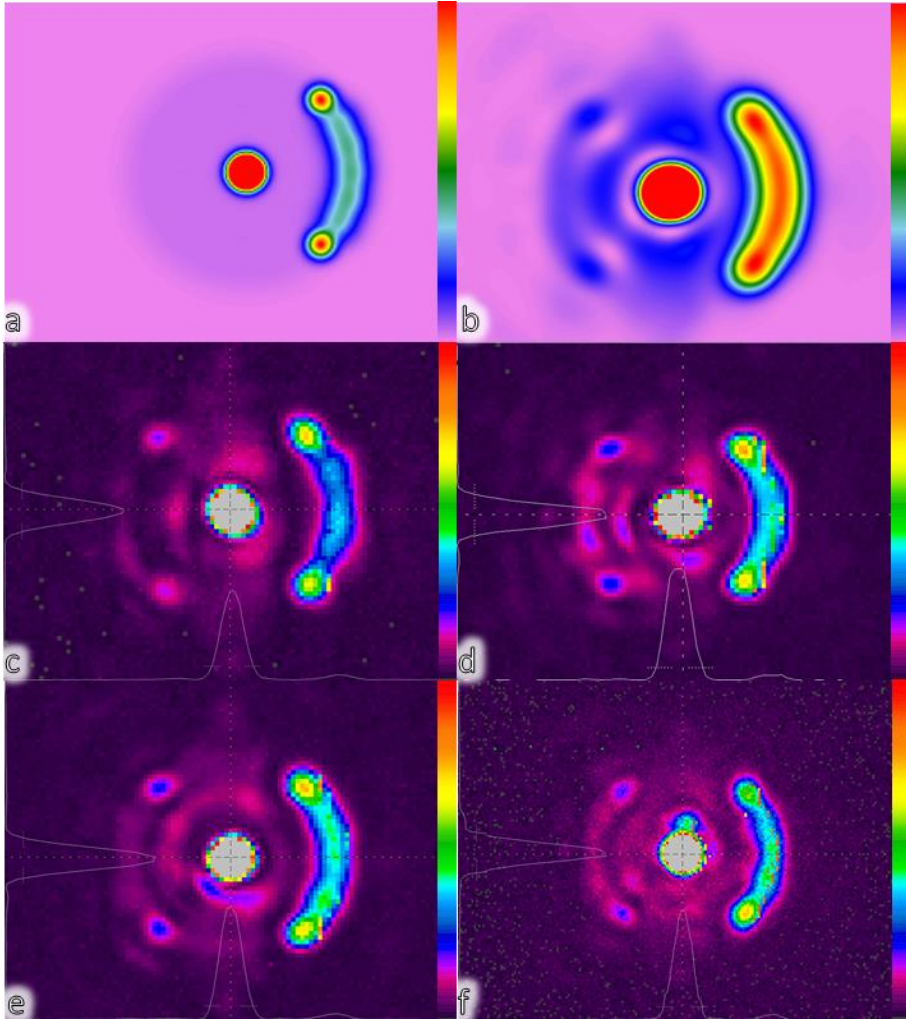


Figure 25 Design and model of pattern together with the four tested methods for beam shaping. a) Design. b) Modelled performance. c) Best result achieved from several attempts of grey scale etching with same design. d) Multilevel etched DOE. e) Diamond turned DOE. f) Flexible beam shaping unit.

Table 5 shows the measured transformation efficiency for the six patterns shown in figure 25. The designed spot pattern has per definition an efficiency of 100%.

The calculated transformation phase has been simulated in an optical model of the system.

|   |                            | A  | B1 | B2 | C  | D  | $\eta_{\text{energy}}$ | $\eta_{\text{transform}}$ |
|---|----------------------------|----|----|----|----|----|------------------------|---------------------------|
| a | Design                     | 47 | 9  | 9  | 24 | 12 | 100                    | 100                       |
| b | Modelled                   | 44 | 8  | 8  | 22 | 14 | 95                     | 91                        |
| c | Grey scale etched          | 49 | 7  | 7  | 13 | 8  | 84                     | 81                        |
| d | Multilevel etched          | 56 | 6  | 5  | 17 | 4  | 88                     | 71                        |
| e | Diamond turned             | 50 | 7  | 6  | 18 | 8  | 89                     | 83                        |
| f | Flexible beam shaping unit | 55 | 4  | 6  | 16 | 16 | 97                     | 72                        |

*Table 5 Transformation efficiencies,  $\eta_{\text{transform}}$ , and energy distributions for the different parts in the pattern for the six patterns showed in figure 25, calculated using equation 5 and 6. All numbers are percentages.*

The given numbers in table 5 have some measurement uncertainties from electrical noise in the camera system and the manual placement of apertures. The sum of measurement uncertainties is evaluated to be less than +/- 5% of the relative values.

The fact that the energy efficiency  $\eta_{\text{energy}}$  for the flexible beam shaping unit is higher than the modelled performance of the pattern can be explained by the fact that both the central spot, A, and the area around it, D, receive more energy than designed. This is happening at the cost of energy in the other defined areas, but can also originate from energy which in the simulated performance was considered as stray light.

When just looking at the images in figure 25, it is clear, that the pattern produced by the grayscale etched DOE performs significantly poorer than the others.

Especially in area D, in which the energy should be spread out in a uniform distribution, the six different methods perform significantly different. The multilevel etched DOE, the grey scale etched DOE and the diamond turned DOE are all making non uniform distributions of the energy, where the flexible beam shaping unit produces a more uniform distribution without spikes. Unfortunately, these observations are not evident in the evaluation of the transformation efficiency. Here the diamond turned DOE performs best. This is caused by the fact that the diamond turned DOE matches the energy distributions in the design best. The flexible beam shaping unit comes out with a rather poor performance, which is nearly the same as for the grayscale etched DOE.

The grayscale etched, the multilevel etched and the diamond turned DOE's have been tested at powers up to 3 kW for several minutes without breakage, and in general they are all performing well.

#### 4.4.7. DISCUSSION

Depending on the purpose of any produced design, one should be careful on how to evaluate the performance of a transformation pattern and a DOE. In the case shown in figure 25, the even distribution of energy is best performed with the flexible beam



shaping unit, but the amount of energy in the barrier is low, resulting in a poor transformation efficiency. This problem could be minimized by using the produced pattern as a feedback to the design iterations and increase the energy in the barrier beam. Hereby the result would, hopefully, be both a uniform distribution and have a high efficiency with the required energy in the barrier part of the pattern.

For spot patterns for multi laser spot welding the most important is to have a *minimum* of energy in the shadow beams, where no weld should be performed. “*Minimum*” energy is not very quantified. Preferably there were no shadow spots.

By applying DOE-beam splitters, diffractive theory says there in most designs will be energy, which cannot be delivered to the desired spots/area, thus giving either diffracted scattered light or shadow spots dependent on design. [81] Scattered light spread over a large area will rarely be a problem, as it only will lead to minimal heating of the material. The light ends in shadow spots will at a certain point cause an intensity which becomes significant, and the shadow spots will produce its own weld pool. At what level this starts has not been examined in this project, however the shadow spots have not been observed to cause any problems in the process.

In some cases the transformation efficiencies are not enough for evaluation of the performance. A visual comparison can reveal differences and local hot-spots and lack of energy in areas which are designed to have an even energy distribution. One solution is to divide the areas into subareas or use the rigorous method described in ISO13694 with comparison of each pixel.

The task was also to evaluate different technologies for production of DOE’s and their durability and ability to be implemented in an industrial environment.

The produced patterns were for the Robocut project and were designed for laser cutting, but are still valid for evaluating advantages and disadvantages. For laser welding specific patterns were produced using grayscale etching and the programmable reflective beam shaping unit. Here similar results were achieved. The production tolerances in production of a greyscale DOE were similar to those for the Robocut pattern, and a DOE with the correct etching depth was never produced for welding, so it suffered from poor performance. Spot patterns produced by the flexible beam shaping unit performed similar to the one produced with the Robocut design with high energy efficiency and transformation efficiency a little lower. Some of these spot patterns are shown in section “5.2 Summary of Paper C: Joining of multiple sheets in a butt-joint configuration using single pass laser welding with multiple spots”. As an example the spot pattern shown in figure 22 produced by the flexible beam shaping unit, has  $\eta_{\text{energy}} = 92\%$ ,  $\eta_{\text{transform}} = 84\%$ . This pattern is quite representative for many of the welding patterns which is tested.

Especially the grey scale DOE's designed and tested in the project performed different from the calculated performance.

### **Summary of test of DOE's**

Routes to determine the energy distribution and compare this to the design and simulation results has been developed and put down in guidelines.

Four different DOE's/beam shaping options, each with their own characteristics has been tested and evaluated using the found guidelines:

- The grayscale DOE gives the poorest performance, and it requires a significant amount of calibration in the production process. The delivery time is short
- The multilevel etched DOE is robust and suited for installation in a production environment with the proper protection. Delivery time is usually 4-12 weeks
- The diamond turned DOE is robust and suited for installation in a production environment with the proper protection. New designs can typically be delivered within four to eight weeks
- The flexible beam shaping unit is excellent for research and tests of large numbers of beam designs.

## **4.5. HIGH SPEED PHOTOGRAPHING**

A series of high speed recordings of laser welding with DOE were performed, the videos should give information of the flow pattern of the melt in the surface of the melt pool, and in this way give additional information on design rules and guidelines for spot patterns for multispot fiber laser welding.

### **4.5.1. INTRODUCTION**

High speed photography is a well-known tool, and it is in many ways similar to photographing with any camera. All the rules about imaging, apertures, shutter times etcetera are still valid for high speed photographing. The only difference is the speed at which each frame is captured. Where a standard camera recording for TV records with 25 frames per second, and maximum frame speed of most modern cameras is 100 frames per second, then high speed photographing is performed with up to one million frames per second. [118]

When recording small phenomena like laser welding, with e.g. focus diameters of 50  $\mu\text{m}$ , the used welding speeds are 50 mm/s. Then the beam is moved 1000 times its own diameter per second. To resolve details for such a process, it is necessary to capture several frames per moved diameter. Therefore a high speed camera with minimum 10.000 frames per second is needed together with macro optics to resolve details of the keyhole, width of weld track and solidification tail.

The maximum shutter time will maximum be the inverse of the frame rate. This assures that only a small amount of light is led to the image sensor per frame. Therefore, intense illumination is needed. This is normally handled by applying several high power lamps to the scene. In this case the scene is only approximately 1x1 mm to 5x5 mm. It is not possible to focus standard illumination down to this size. Instead, an illumination laser is used, this is synced with the camera, so each time the shutter opens, the illumination laser gives a pulse to the scene.

When performing laser welding some of the light from the process laser is reflected to the surroundings. Further, the steel is brought to high temperatures, and will therefore emit light as well (black body radiation). These effects saturate the camera and do not provide any useful information. Therefore, a band pass filter with the same center wavelength as the illumination laser is added to the optics on the high speed camera. This effectively filters away any noise in the images from the process laser and blackbody radiation while it allows the essential light from the illumination laser to pass through.

The illumination laser is allowing decreasing in the shutter time of the camera so that it is only open during the time in which the illumination laser is on. This leads to even lower influence of reflections from the process laser and black body radiation. [109], [51], [35], [50]

The setup described above is a well-known setup which makes it possible to record sequences of laser cutting, laser welding as well as other arc welding processes.

#### 4.5.2. SETUP

The used camera was a Photron SA5 mounted with an Edmund macro objective. The illumination laser was a Cavilux HF laser from Cavitax.

Movement was performed with a XY-table. The process laser was a 3 kW single mode fiber laser from IPG. Different optics was used from Optoskand AB and from HighYAG GmbH, with focal lengths,  $f_{\text{foc}}$ : 200, 300, 470 and 780 mm.

Experiments were performed with the setup shown in figure 26. All experiments were performed as bead on plate experiments, where the plate is moved, and everything else is kept steady.

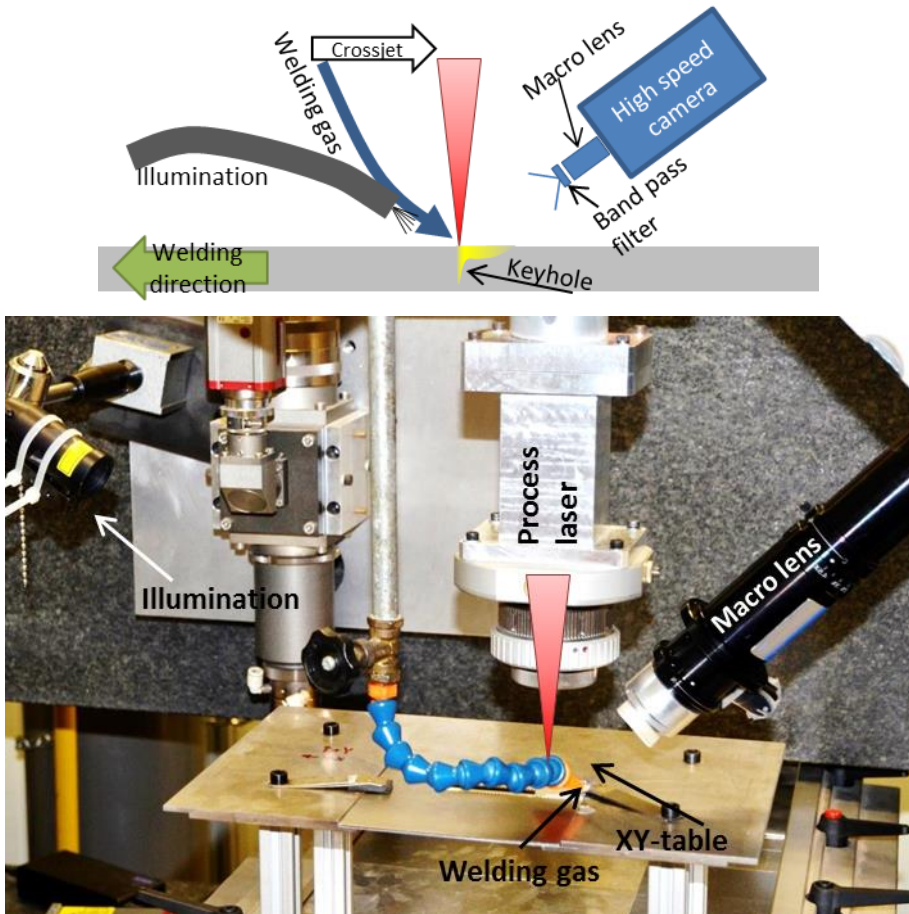


Figure 26 Setup for high speed photography. Top) Principle. Bottom) Actual setup.

#### 4.5.3. EXPERIMENTS

To gain knowledge on the melt flow on the surface in the weld pool with multiple spots a series of experiments was performed.

Experiments with different gas cover, travel speeds, focus positions and focal length were in stainless steel. Also three different DOE designs were tested by inserting grey scale etched DOE's in the collimated beam. One which produces three individual beams on a row, one with seven beams on a row and one with two rows with three beams.

Due to the high framerate and thereby large amount of recorded data, only between 0.5 and 2 seconds from each experiment were recorded. This is evaluated as

sufficient, as experiments have shown that the full depth of fusion is reached within a few millimetres when welding with 50 mm/s.

It was also tested if the contrast of the melt surface could be increased by placing wolfram powder on the top of the sheets.

#### 4.5.4. RESULTS

The achieved results from high speed recording are limited, as the melt works as a curved mirror. This gives sharp reflections from the illumination laser, and nearly no light in the areas where it is not directly reflected.

Figure 27 shows an example from a side view from welds performed with the seven spot DOE. The recording is one of the best recordings performed, and here it is still difficult to see details in the flow. It is however easy to see the individual laser spots and shadow spots.

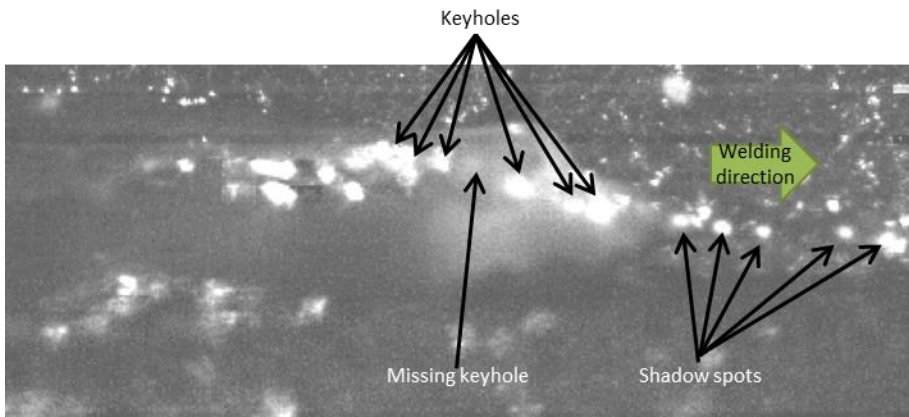


Figure 27 Welding with the seven spot DOE. Details of spot pattern are given in the paper “Beam shaping to control of weldpool size in width and depth”, Hansen et.al. [110].

In the videos which are recorded with a side view (camera perpendicular to welding direction) it is possible to observe build-up of waves which cause disturbances in the melt. A series of frames with the build-up of and propagation of such a wave can be seen in figure 28. The wave speed can also be calculated in these views and is approximately 1.5 m/s. The waves are measured from the back of the keyholes towards the solidification front. The wave speed is in the measured case 30 times higher than the welding speed.

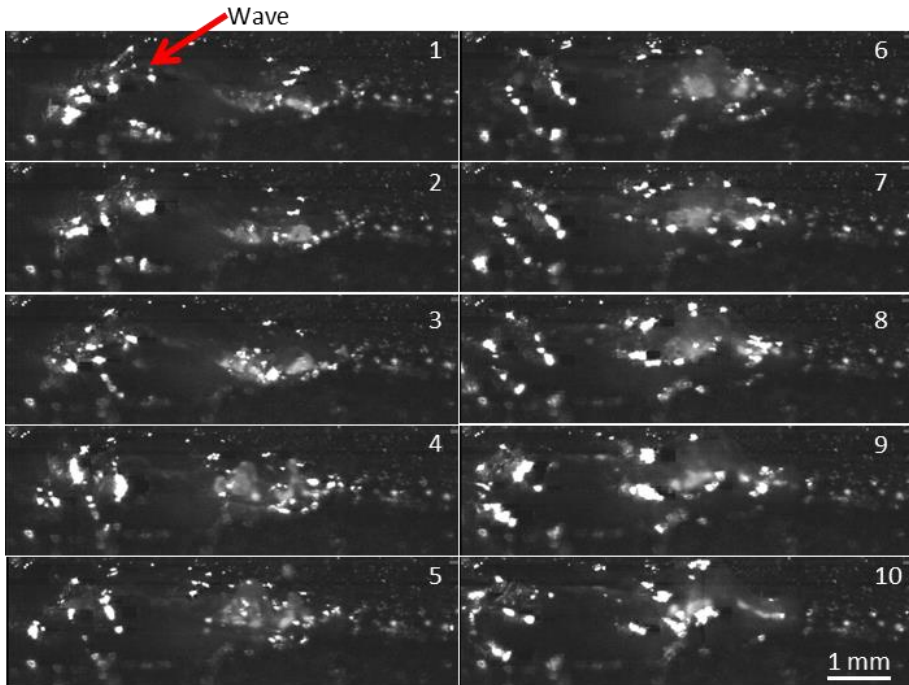


Figure 28 Sequence of images in a sideview. Welding is performed with the seven spot DOE. Timedistance between each frame is 80  $\mu$ s.

Most recordings are performed with the camera viewing angle in same direction as the welding direction. It is not possible to determine the wave speed from this – instead a side view with a calibration of distance is needed.

In the videos which are recorded with the view in same direction as the welding direction, it is only possible to see, that the melt is quite unsteady.

General observations:

- Spatters are easy to observe as objects leaving the weld pool
- The melt pool is in general highly dynamic, and the surface is irregular in the whole melt pool
- In general the flow patterns on the surface of the melt cannot be seen
- Wolfram powder placed on the top of the sheets before welding did not improve the contrast on the surface of the melt

#### 4.5.5. SUGGESTIONS FOR IMPROVEMENTS

One solution to the problem with reflections and dark areas could be to use a more diffuse illumination source. Such a product has been released by Cavilux after the

recordings were performed. This product is (instead of a single delivery fiber) splitting the light from the illumination laser into four delivery fibers, thus allowing the light to be directed to the process zone from four directions at the same time. This should make the coherent laser light more diffuse, but still focused to the small area needed, thus producing better recordings. [Mengel Engineering, Personal communication, fall 2014].

#### 4.5.6. CONCLUSION

It has not been possible to see how the mixing from the different fluid flow occurs, and how they are influenced by keyhole distance, and how trailing keyholes are affected by these flows.

In the recordings performed with a side view it is possible to determine the wave speeds in the melt. This speed is 30 times higher than the welding speed, which indicates strong movements in the liquid.

It would be possible with the present recordings to count the amount of spatters, including the speed and the direction of them, when they leave the melt pool. This is however outside the scope of this work.

##### **Summary of high speed photographing**

In general the results achieved with high speed recordings have been unsatisfactory. The tool in its present form has proven useful to see spatters and waves in the melt, as well as document the presence of multiple keyholes. It has also been possible to determine that the wave speed of waves build up behind the keyholes is approximately 30 times higher than the travel speed.

The technique still has the potential to be improved with more diffuse illumination, whereby it might be possible to improve the contrast on the molten material and from this determine surface flow lines.

## CHAPTER 5. EXAMPLES OF MULTISPOT FIBER LASER WELDING

This chapter presents the work performed with multispot fiber laser welding. The work is divided into two cases, *control of welding width and depth*, and *inline repair of blowouts*.

The results are published in four different papers, and is presented here as summaries of these papers.

- Section 5.1 “*Summary of Paper B: Beam shaping to control of weldpool size in width and depth*” presents the results of the first results from welding with spot patterns. The results are obtained using DOE’s of a poor quality and are therefore not convincing
- In section 5.2 “*Summary of Paper C: Joining of multiple sheets in a butt-joint configuration using single pass laser welding with multiple spots*” much more convincing results from welding with spot patterns is presented along with design rules for spot pattern design. It is shown how spot patterns can be used to increase tolerances and robustness in laser welding.
- Additional results are presented in section 5.3 “*Summary of Paper D: Inline repair of blowouts during laser welding*”, which are extending the design guidelines. Further, results are presented showing improvement of weld quality
- In section 5.4 *Summary of Paper E: Multispot laser welding to improve process stability*” there is a summary of the performed work with focus on the results achieved with multispot welding

### 5.1. SUMMARY OF PAPER B: BEAM SHAPING TO CONTROL OF WELDPOL SIZE IN WIDTH AND DEPTH

This section investigates, whether it is possible to control the weld pool geometry by applying multiple beams on a row.

The industrial cases supplied by the projects advisory group is about controlling the weld geometry by applying multiple spots on a row and in that way expand the weld pool. Initial tests and results are presented in the paper *Beam shaping to control of weldpool size in width and depth* published at the LANE 2014 conference. The full paper is reprinted in appendix B.



### 5.1.1. OBJECTIVES

#### Hypothesis:

It is possible to produce almost rectangular weld profiles and to control the weldpool geometry in terms of width and depth of fusion by applying multiple spots on a row perpendicular to the welding direction as sketched in figure 29.

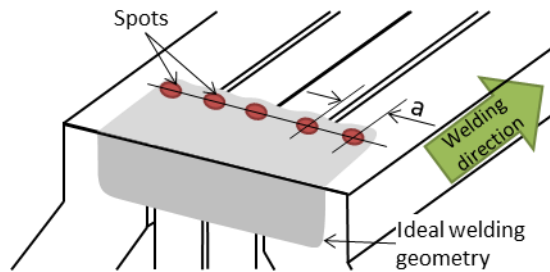


Figure 29 Principle of placing multiple laser spots on a row for controlling weldpool geometry. Sketched on a joint containing four sheets. “a” indicates spot distance.

This raised the following research questions:

#### Research questions (RQ's):

1. How can a spot pattern with multiple spots be realized and integrated into a laser welding head?
2. How deep does one spot penetrate into material as function of power?
3. How does the fusion of material from multiple keyholes interact with each other when applying multiple spots in the focus of the laser beam?

### 5.1.2. RESULTS

A theoretical study of how a beam pattern with multiple spots can be realized was performed. The study was covering DOE shapers, DOE splitters, DOE diffusers, beam splitting, multiple lasers and field mappers. Based on the investigation it was decided to do this by use of DOE splitters, as they have a good depth of field, high transformation efficiency, is insensitive to alignment and can be integrated into laser heads without too large changes in design. Further it is possible to change the spot pattern by only changing the DOE in its mount. The principle is shown in figure 21 in section “4.4.1 Measurement definitions and terminology”.

Two DOE's were designed and tested, one with three spots and one with seven spots. They were produced with grey scale etching. The manufacturing tolerances were unfortunately quite low, whereby the produced spot patterns came out quite uneven. The intensity in the middle spot in the three spot patterns was too high, and for the seven spot DOE the center spot was missing, and the rest of the spots had an

uneven intensity as well. The poor performance was due to under-etching in the production. A simulation in VirtualLab™ of an under-etched DOE design gave results similar to those measured from the actual DOE. Simulation of the three spot design can be seen in figure 30. Figure 31 and 32 shows the measured spot patterns from the two DOE's.

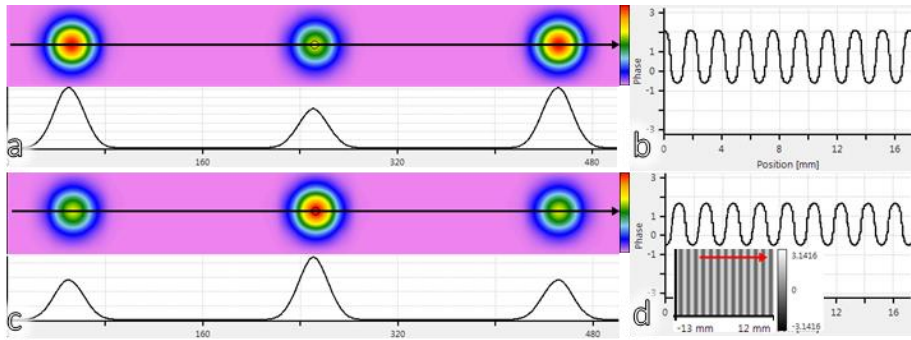


Figure 30 a) Simulated intensity and intensity profile with DOE "as designed". b) Cross section of the phase transmission "as designed". c) Simulated intensity and intensity profile for a DOE which is etched to 80%. d) Cross section of phase transmission at 80% and grey scale view of the phase transmission. All arrows in the figure shows where the respectively intensity/phase profiles are taken.

Even though the DOE's differed from the design, a series of experiments with them were performed. This gave useful information on how to handle DOE's, how to implement them in a beam path and gave the first results of the effect at using multi spots in laser welding.

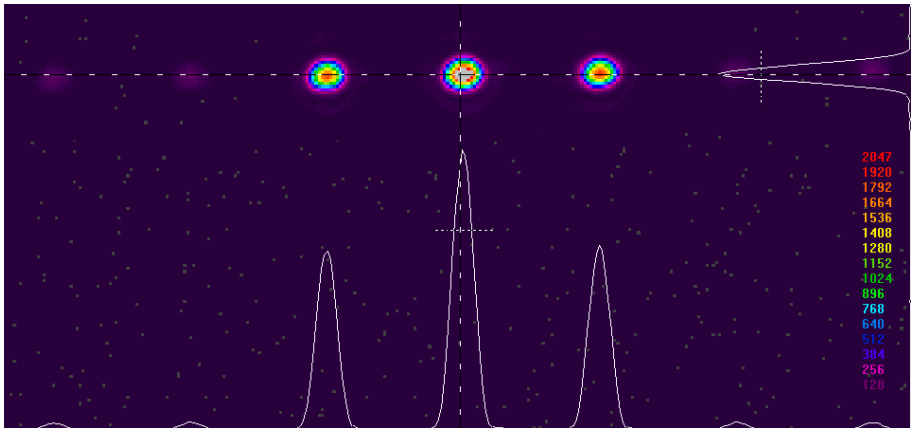


Figure 31 Measured energy profile from three spot DOE.

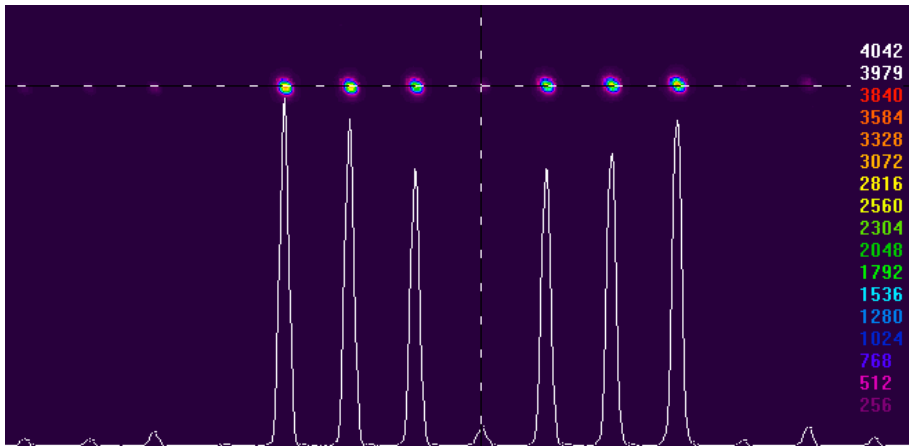


Figure 32 Measured energy profile from seven spot DOE.

Figure 33 shows cross sections of welds performed with the two DOE's. The profile of the two welds can be explained by the energy profiles produced by the two DOE's, where e.g. figure 33b shows a clear tendency to poor penetration in the centre and deepest penetration in the sides, where the intensity also is measured to be highest. The shadow spots in the patterns are not seen to produce any weld in the cross sections in figure 33.

For the three spot DOE the center spot has clearly melted deeper than the two edge spots. From the profile it is evident that the three spots must have formed individual keyholes, which are positioned with the same distance as the measured distance on the CCD camera in figure 31 and 32.

In the profile for the three spot DOE all the material between the spots is melted. The same is the case for the weld performed with the seven spot DOE, except in the center, wherein the center beam is almost missing. Here the depth of fusion is significantly less than for the six other spots. This indicates that the spots have been placed at a good distance for first test. Spots which are spaced with double distance would be too far away to produce full fusion. As there is already full fusion between each spot, no further advantage of placing the spots closer is expected.

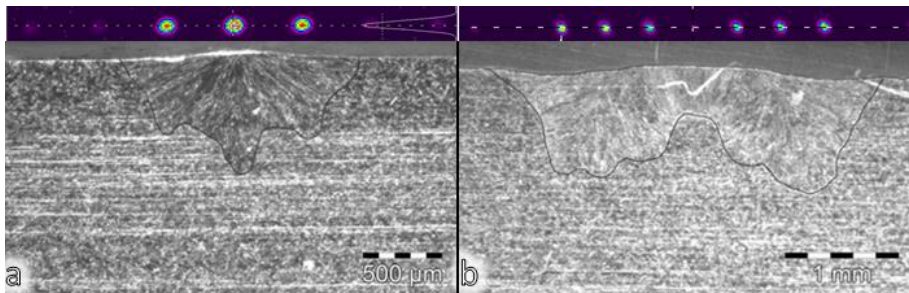


Figure 33 Cross sections of welds with 139 $\mu$ m spot performed: a) with three spot DOE, 800 W, 50 mm/s, b) with seven spot DOE, 50 mm/s, 1500 W. Spot patterns shown above with same scale as cross sections.

The relationship between power and penetration depth for various spots sizes are shown in figure 34. The three spot pattern roughly gives penetration depths which is the half of those from the same power for a single  $\varnothing 23 \mu$ m spot. The power in each spot is however only roughly 30-40% of that for the single spot as the power is distributed as shown in figure 31.

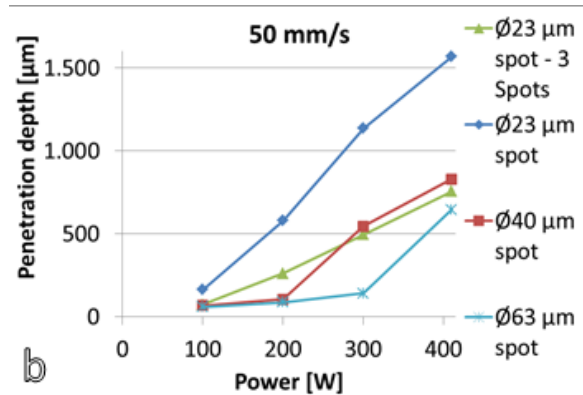


Figure 34 Relation between power, penetration depth and focus spot size for the individual beams in the pattern for stainless steel and three spot DOE.

Figure 35 shows a typical surface from a weld performed with the three spot pattern. In general it is smooth and without spatters and porosities.

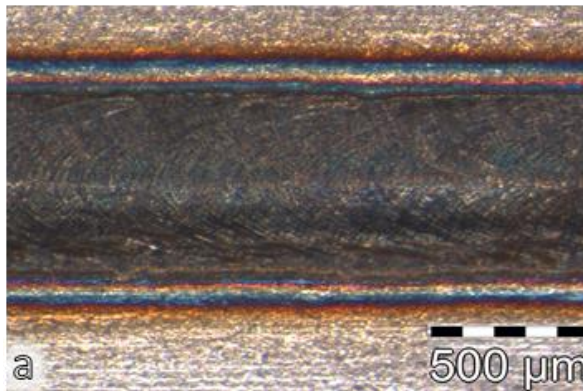


Figure 35 Surface of a typical weld for performed with a three spot pattern in stainless steel.

### 5.1.3. CONCLUSION

The use of DOE's did show it would be possible to integrate a fused silica disc etched with the phase transmission into the collimated beam in a laserhead. It also indicated that there is a possibility to control the weld width and depth through the use of multispot laser welding.

It has been demonstrated that a high power beam can be reshaped into multiple spots by applying a DOE in the collimated beam inside an industrial laser head.

The spot pattern works almost as if the impact from individual beams were superimposed. The depth of fusion and width from each spot is however increased some.

Each cross section has only been qualitative evaluated. The *quality* of the weld in terms of pores and shape of head is as seen on welds performed with only a single spot instead of a spot pattern. This indicates that laser welding with multiple spots is not to affect this in any specific direction.

### 5.1.4. FURTHER WORK

Due to the poor performing DOE's the cross sections ends up differently than expected. Only a limited amount of experiments on real parts were performed. The results posed the basis for the more extensive experiments in paper C "*Joining of multiple sheets in a butt-joint configuration using single pass laser welding with multiple spots*", where beam power, spot spacing, number of spots and focus position are examined and presented.

## 5.2. SUMMARY OF PAPER C: JOINING OF MULTIPLE SHEETS IN A BUTT-JOINT CONFIGURATION USING SINGLE PASS LASER WELDING WITH MULTIPLE SPOTS

### 5.2.1. OBJECTIVES

The results achieved in paper B "*Beam shaping to control of weldpool size in width and depth*" indicated that additional extensive examinations should be performed to analyse several other parameters, such as number of spots and spot spacing.

Robustness to tolerances for multi beam laser welding is also interesting to examine further, as real parts in production always will have some tolerances and distortions, which needs to be accommodated in the assembly process.

At IPU more extensive test options had become available by an upgrade of the laser power from a 400 W single mode fiber laser to a 1 kW single mode fiber laser. Besides this it had become possible to test several phase transmission designs by the use of IPU's flexible beam shaping unit, which produced the spot patterns with a higher quality than the tested grey scale DOE's. More details about the setup are found in section "4.1.1 Flexible beam shaping unit at IPU".

A more extensive study was therefore performed with a revised hypothesis.

#### Hypothesis:

The weldpool geometry in terms of width and depth of fusion can be controlled by applying multiple spots on a row perpendicular to the welding direction. Further, such a design will give robustness towards tolerances in the parts to be joined.

This raised the following research questions:

#### Research questions (RQ's):

1. How deep do multiple spots penetrate into the material as a function of power?
2. How does the fusion of material from multiple spots which forms individual keyholes interact with each other?
3. What is the influence of spot spacing?
4. How is the weld geometry affected by the number of spots?
5. How large a gap can a multispot pattern cover?
6. What is the effect of vertical tolerances in a butt joint configuration?

## 5.2.2. RESULTS

To answer RQ1-4 a series of bead on plate experiments were performed in which spot spacing, number of spots and power were varied. Influence of focus position and travel speed was tested as well. Parameters are shown in table 6.

| Parameter               | Interval                 | Step size        |
|-------------------------|--------------------------|------------------|
| Spot distance, a        | 150 to 400 $\mu\text{m}$ | 50 $\mu\text{m}$ |
| Number of spots         | 1-5                      | 1                |
| Focus, F                | +4 to -6 mm              | 2 mm             |
| Power (in each spot), P | 100 to 267 W             | 33 W             |
| Travel speed, v         | 20 to 100 mm/s           | 25/15 mm/s       |

Table 6 Parameters varied during experiments. Spot distance is defined on figure 29.

For a three spot design the distance, a, between each spot was varied. The results are shown in figure 36. Each spot distance design requires a different phase transmission to be calculated in VirtualLab™ and applied in bead on plate welding.

For  $a = 250 \mu\text{m}$  and  $a = 350 \mu\text{m}$  the centre beam contains less energy than the edge beams. This is also seen on the resulting cross sections. These problems originate from poor design of the phase transmissions. Experience gained later in the project has shown that the phase transmissions can be improved to give equal intensity in each spot by careful design and use of the design software VirtualLab™.

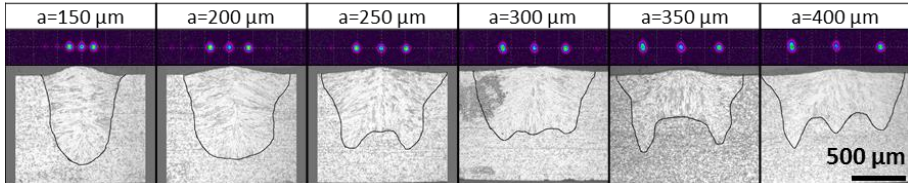


Figure 36 Top row) Measured spot pattern using an intensity sensitive CCD camera. Bottom row) The resulting cross-sections for different spot distances performed as bead on sheet, all with focus placed on top of the sheet. ( $F_0$ ). Power is set to an average of 200 W per spot. All figures have the same scale.

For  $a = 150 \mu\text{m}$  and  $a = 200 \mu\text{m}$  the individual beams cannot be seen in the cross sections. For  $a > 200 \mu\text{m}$  the results from the individual spots can be seen. For  $a = 300 \mu\text{m}$  the individual spots are visible, but the melt pool is nearly rectangular. It was therefore decided to continue with this distance for further investigation, in which  $a$  was kept constant.

For  $a < 300 \mu\text{m}$  the depth of fusion is higher than for  $a \geq 300 \mu\text{m}$  with same power applied. This means that the spots are affecting each other to give a higher depth of fusion when placed close to each other.

Figure 37 shows the cross sections from a series of experiments where the number of spots varied from one to five. As can be seen in figure 38 the width increases linearly with the number of spots, while the depth is constant. The average power in each spot was kept constant.

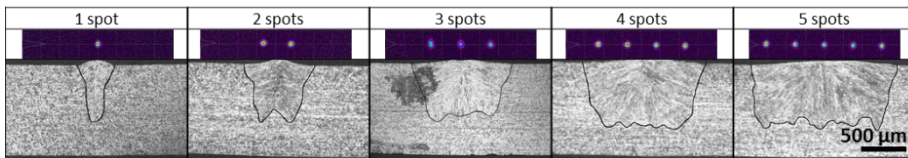


Figure 37 Top row) Measured spot pattern using an intensity sensitive CCD camera. Differences in intensity between images are due to different power settings in the laser as the number of spots are increased. Bottom row) The resulting cross-sections for different spot distances performed as bead on sheet, all with focus placed on top of the sheet. ( $F_0$ ). Power is set to an average of 200 W per spot. All figures have the same scale.

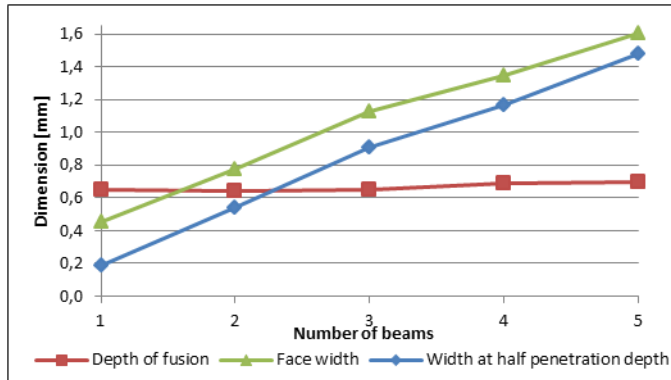


Figure 38 Dimensions of welds shown in figure 37.

Figure 39 shows a series of cross sections in which the power in each spot has been varied. Figure 40 shows that the result is a nearly linearly increasing depth of fusion as function of the applied laser power, until the depth reaches the plate thickness of 2 mm.

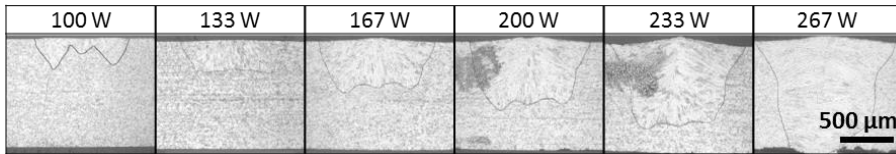


Figure 39 Cross-sections for different laser power performed as bead on sheet, all with focus placed on top of the sheet. ( $F_0$ ). Distances are  $a = 300 \mu\text{m}$  in all cases. Powers are average power per spot in the pattern. The applied pattern is the same as the one shown for the three spot patterns with  $a = 300 \mu\text{m}$  spacing in figure 36. All figures have the same scale.

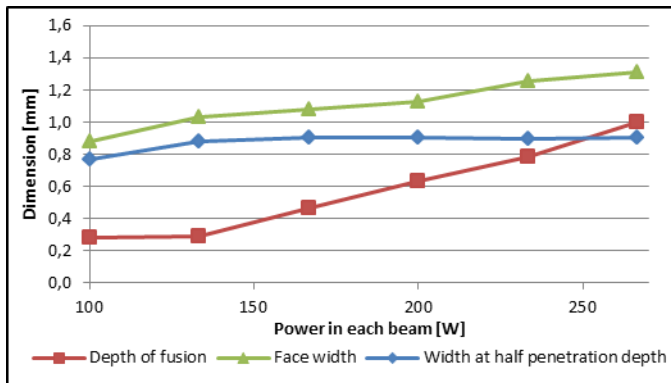


Figure 40 Dimensions of welds shown in figure 39.

When the travel speed was varied, the depth of fusion changed proportionally to the travel speed, however at higher speeds the keyholes became more distinct, and the material between each keyhole was not melted. This can be seen on figure 41 and



42. This is concluded to originate from the faster speed leaving less time for heat to be transferred from the keyholes to the surrounding material.

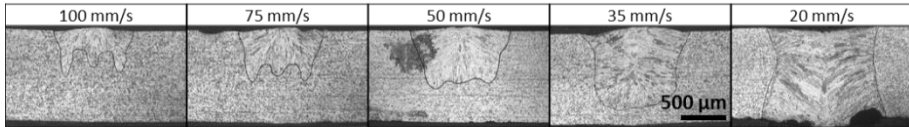


Figure 41 Decreasing travel speed, three spots, constant power at total 600W, focus F0 and spot spacing at  $a = 300 \mu\text{m}$ . The applied pattern is the same as in figure 5 with  $a = 300 \mu\text{m}$  spacing.

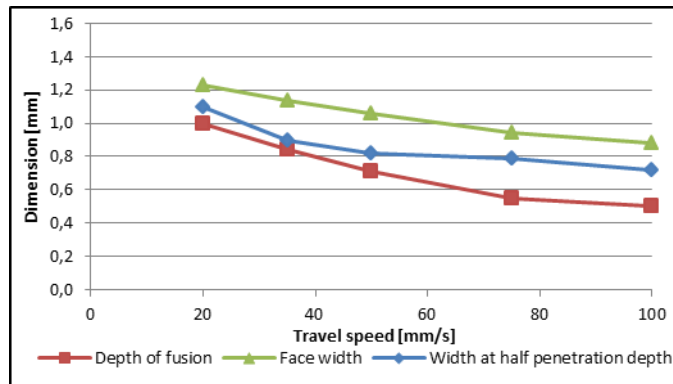


Figure 42 Dimensions of welds shown in figure 41.

The sensitivity to focus was examined. Figure 43 shows the cross sections for focus changed from  $F = +4 \text{ mm}$  to  $F = -6 \text{ mm}$ . From  $F = +2$  to  $F = -4$  the shape of the weld pool is still rectangular with nearly same depth of fusion. Outside this range the cross sections of the weld pool or the depth of fusion in the weld pool changes significantly. For comparison a spot from same beam with same laser and lens with no DOE has a single sided Rayleigh length at  $3.0 \text{ mm}$ . Welds performed with spot patterns like the ones used in this study are therefore concluded not to be especially sensitive to focus position, as the cross sections indicate that the beam pattern has same Rayleigh length as the raw beam. This allegation can be different for other spot designs and depends on how the design is realised.

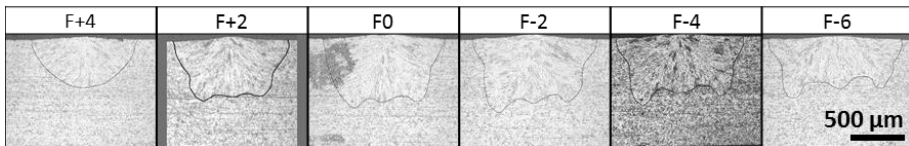


Figure 43 Three spots pattern with a spot distance of  $a = 300 \mu\text{m}$  and  $200 \text{ W}$  average power per spot.

To answer RQ5 and 6 experiments with a more complex joining geometry, with up to four parts that had to be joined simultaneously, were used. The geometry

originates from the advisory group, and is a design current industrial production from. The principle and dimensions are shown in figure 44.

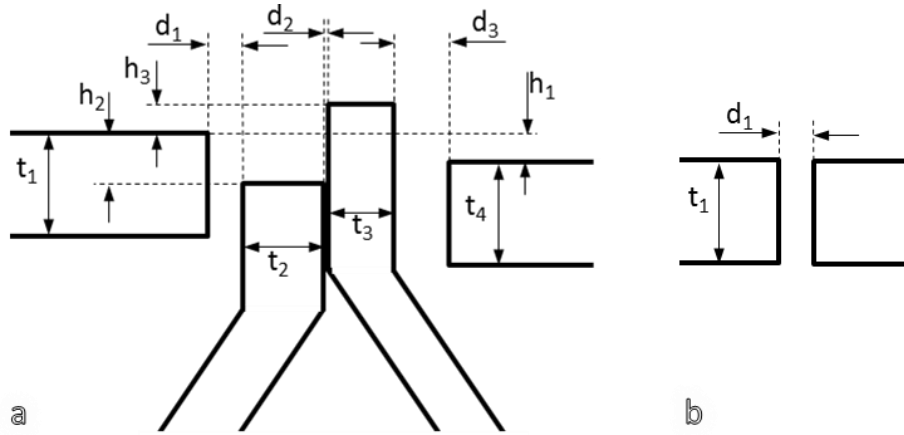


Figure 44 Multiple butt joining with alignment errors and positioning tolerances: a) for the configuration shown in figure 46, b) for the configuration shown in figure 45.

To answer RQ5 experiments with butt joint of two sheets, as sketched to the right in figure 44, were performed with a five spot pattern to ensure, that the spot pattern was wider than the gap. The gap  $d_1$  were varied from  $d_1 = 0$  to  $d_1 = 0.6$  mm. For  $d_1 > 0.4$  mm the weld did not bridge the gap. Figure 45 shows the cross sections for the increased gap. The undercut increased with the gap distance, as no filler material was added.

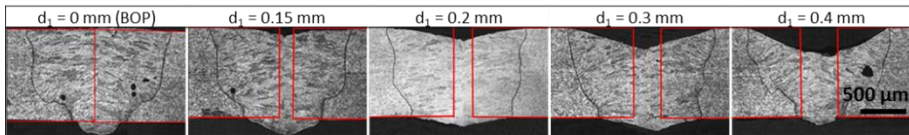


Figure 45 Cross sections from increased gaps and bridging by a five spot pattern, on two sheets in a butt joint configuration.

Figure 46 shows the effect of varying the vertical position of the two centre sheets. Again when  $h_2 = h_3 \leq 0$  undercut occurs, as no filler material is added. Welds in figure 46 all have  $t_1 = t_4 = 1$  mm,  $t_2 = t_3 = 0.5$  mm and  $d_1 = d_2 = d_3 = 0$  mm (or as close as the fixture has allowed, for some tests small gaps can be observed).

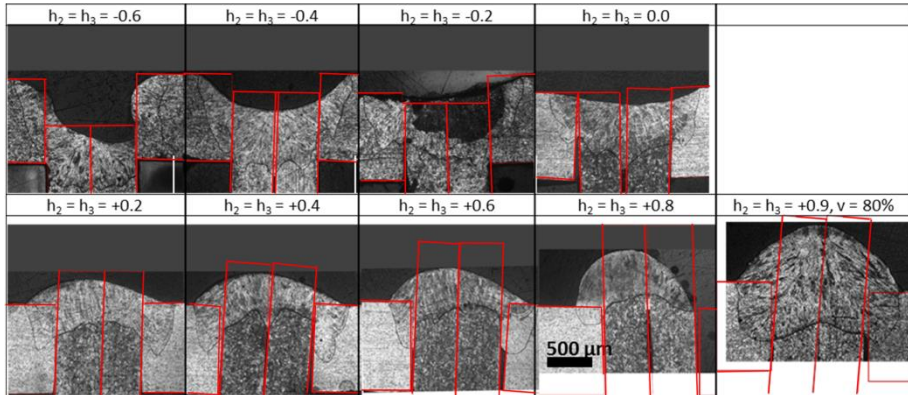


Figure 46 Double butt joints with increasing height of centre sheets. All welds are performed with four or five spots and similar parameters. Initial geometry is outlined.

When  $h_2 = h_3 \geq 0.8$  mm the melt pools from the individual sheets do not bridge. For this bridging to occur, increased power is needed. As the laser was used at maximum power, the speed was reduced instead. An example can be seen for  $h_2 = h_3 = 0.9$  mm.

In terms of quality each weld has been visual evaluated and has been found to be satisfactory in terms of surface roughness, size and angle of head and the absence of pores.

### 5.2.3. CONCLUSION

Welding with multiple laser spots on multiple sheets in a butt-joint configuration in a single pass has been successfully demonstrated using the flexible beam shaping unit at IPU.

The number of spots and the spot distance has been examined along with the more traditional parameters; power, focus and travel speed. This shows that the weld may be widened in steps by using multiple spots. This is answering RQ1, RQ3 and RQ4.

The parameter study shows that the final geometry of the cross-section is similar to a superposition of single spot weld, as long as the spot distance is large enough to keep the keyholes separated. Further the spot distance should not exceed a certain threshold to ensure fusion between the individual keyholes. The threshold (depends on power and spot size, for the shown examples in figure 36 it is approximately 350  $\mu\text{m}$ , thus RQ2 is answered.

RQ5 is a question about how large a gap multispot welding can cover. As shown in figure 46 the ability to bridge gaps and robustness towards tolerances is considered to be higher in multispot laser welding compared to laser welding with a single spot,

which for similar spot sizes would risk passing the gap without being absorbed due to the size of only 85  $\mu\text{m}$ . These experiments have however not made clear the number of spots it might be possible to use. It has made clear, that keyholes are formed at each spot as long as sufficient laser power is available. The use of multiple spots allows bridging in butt joint configurations which is larger than a single spot diameter, as there always will be a spot melting material close to the gap. In this way a robust welding process is ensured as long as the spot pattern is wide enough.

RQ6 is a question about, what kind of vertical tolerances a multispot welding can accommodate. From the achieved results it is concluded, that the process is insensitive to vertical tolerances. As long as enough power to weld material, which is *excessive* ( $h_2 = h_3 > 0$ ), is present. When there is a lack of material ( $h_2 = h_3 < 0$ ), the final weld will have some undercut, but a weld will still be formed, which joins the parts.

The shape of the cross section from each spot in the weld with 100 W in figure 39 is quite triangular. This indicates that for keyhole welding with a spot diameter of 85  $\mu\text{m}$ , the power should be no less than 100-133 W per spot, if the process is to remain a keyhole welding process and not turn into a surface conduction welding process.

From the qualitative quality analysis of the welds no change in quality of welding with spot patterns compared to welding with single spots has been found.

## 5.2.4. FURTHER WORK

To further improve tolerance to gaps a spot pattern design with two rows, where the second row was offset a half spot distance sideways, could be used. See figure 47. This would help ensure that if a single spot “falls into a gap”, there will still be enough energy present in the total weld width. The extra row of spots could maybe increase the tolerances to gaps further, as the melt pool is elongated, and turbulence is changed.

It is not possible just to push the spots closer to each other, as each spot will create its own keyhole, and the material melted in the front of each keyhole needs to flow around the keyhole to the back. If the keyholes are placed too close to each other the flow channels are decreased, and the flow speed must be increased. This is undesirable, as high flow speeds can lead to turbulence, which can lead to porosities, spatters and other welding failures.

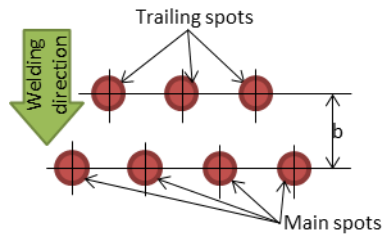


Figure 47 Principle for applying a second row of spots.

It could also be interesting to calculate the melted volume, and compare this to the theoretical maximum melting volume from the added energy, as well as to other welding methods, to see which process which uses the smallest amount of energy.

### 5.3. SUMMARY OF PAPER D: INLINE REPAIR OF BLOWOUTS DURING LASER WELDING

Blowouts during laser welding usually occur when materials are heated beyond their boiling point, or if organic compounds decompose and goes into gas form. This vaporisation happens fast, as both temporal and spatial temperature gradients in laser welding are very high compared to most other thermal processes. This leads to small “local explosions”, which blow away the melt pool.

Blowouts differ from spatters, which usually occurs during high melt velocities and turbulence in the melt. Both phenomena can lead to irregular surfaces and poor weld qualities.

#### 5.3.1. OBJECTIVES

##### Hypothesis:

Blowouts in a butt joint configuration can be repaired inline by use of a multispot pattern with trailing spots as sketched in figure 48.

This raised the following research questions:

##### Research questions (RQ's):

1. How much energy should be in the trailing spots to perform keyholes with the same depth as the main spots in the melt pool?
2. How far should the trailing spots be placed from the main spots to melt new material after a blow out?
3. How can the effect from the blowout be minimized?

### 5.3.2. RESULTS

To answer RQ1 and gain the necessary knowledge for designing spot patterns with respect to power ratios between main spot and trailing spot, a series of initial experiments were performed as bead on plate welding with a three spot pattern. In this two leading spots and a trailing spot is used as shown in figure 48. The energy in the trailing spot (P2) and the trailing spot distance were varied from 100  $\mu\text{m}$  to infinite. The experiments were performed for four different power levels of the main spot with different power ratios.

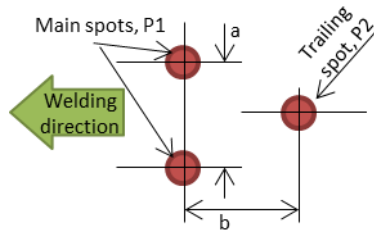


Figure 48 Spot pattern and definitions for experiments to determine power ratios. Individual spots are  $\varnothing 85 \mu\text{m}$ .

In total 180 welds were performed with 36 different transmission phases to find the relation between needed power ratio  $P2/P1$  and trailing spot distance. Figure 49 shows the cross sections from 6 different distances for the trailing spots, a fixed ratio  $P2/P1 = 80\%$  and 260W in each main spot (P1). From the full matrix of experiments it has been possible to establish the different power ratios at which the trailing spot produces the same depth of fusion as the main spots for different distances for the trailing spot.

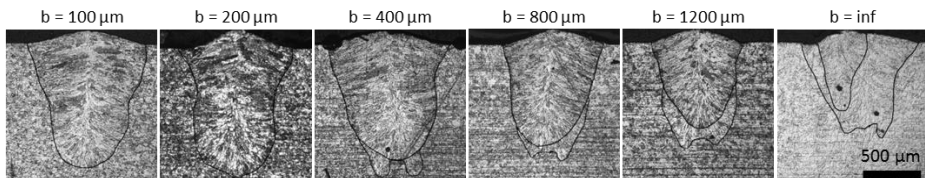


Figure 49 The power ratios for equal depth of fusion for varied distances between main spots and trailing spot for one power level. Performed with  $a = 300 \mu\text{m}$ .

Figure 50 shows the results from the trailing spot experiments in which the power ratio  $P2/P1$  is plotted as function of trailing spot distance. The trailing spot distance ends at infinity. Infinity corresponds to the fact, that the trailing spot has been performed as a secondary weld. This is also the explanation for the small misalignment of the two welds. The curve ends at 115% power in P2 compared to P1. This is due to increased penetration from positive interference from the two main spots. Each spot and error bar in figure 50 is produced from qualitative visual interpretation of the produced cross sections with different power levels and power

ratios, as it is possible to see where the trailing spot produces a keyhole which is just as deep as the two main spots from the weld profile in the cross sections.

In general there has been observed a tendency to small amount of pores on the welds performed with a single trailing spot compared to the experiments performed with only a single row of spots.

The trailing spot needs more power than one of the main spots since the two main spots influence each other and increase the depth of fusion compared to a single main spot. The effect is described further in paper C in appendix C “*Joining of multiple sheets in a butt-joint configuration using single pass laser welding with multiple spots.*”

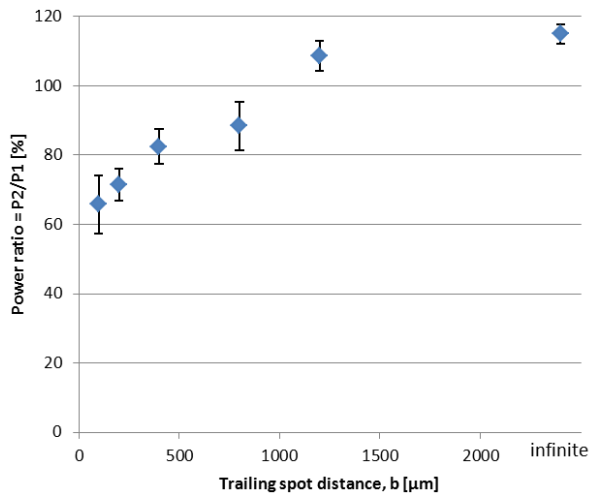


Figure 50 Graph of distance and required power to penetrate weld pool for different power.

To provoke a blowout in the test, a small amount of zinc powder was placed between two discs and the welds performed in a butt-joint configuration.

The used amount of zinc was exaggerated when compared to the amounts of impurities, which are expected to be found in an industrial production. The blowouts are therefore also exaggerated.

To answer RQ2 and 3 several designs of spot patterns were tested. It was found, that a pattern with two leading spots and two trailing spots with 800 μm distance produced the best welds. Figure 51 shows a weld produced with and without two trailing spots, and the spot patterns used to produce them.

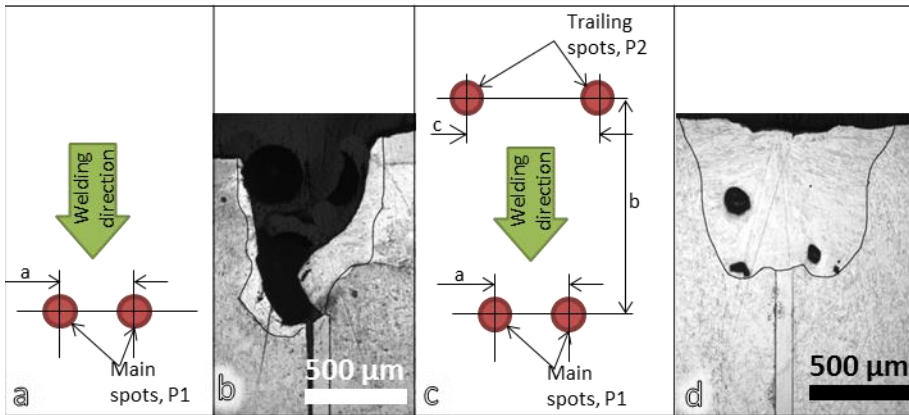


Figure 51 a) Two spot pattern. b) Weld with two spot pattern. c) Four spot pattern. d) Weld with four spot pattern. Both crosssections taken are at the location, where the zinc powder was deposited.

Despite the porosities, in figure 51d, the quality is a large improvement compared to figure 51b, in which the parts are not joined, and the whole melt pool has been blown away.

The welds produced with inline repair welding had a tendency to have some undercut at the position, where the melt pool was blown away. This was caused by the blowout and missing material. The undercut can only be avoided by adding filler material after a blowout.

### 5.3.3. CONCLUSION

The inline repair welding of blowouts caused by zinc powder between sheets in a butt joint configuration were performed using various spot patterns.

The initial trailing spot experiments revealed, that it is necessary to use 60-115% power in a trailing spot, if the desired outcome is to be a penetration similar to when welding with a dual spot pattern perpendicular to the weld direction with a spacing of 200 μm. If the distance between the main spots were increased, so that the keyholes in the main spots did not influence the depth of fusion for each other, it is to expect that the maximum power ratio  $P2/P1$  would be reduced to 100%.

The presence of small amount of pores in the bead on plate experiments were also seen when performing welds with *infinite distance*. In this case the spots cannot affect each other. The presence of porosities can therefore also be from other phenomena, and cannot be concluded to originate from the use of multiple spots in multiple rows. The cause for the porosities could be from differences in the adjustment of the small gas flow placed above the weld, which for these experiments might have caused additional turbulence without being noticed.



The results of the study show that applying multispot laser welding can improve the process stability when welding materials with small impurities in the form of zinc particles. Applying the proposed design does not avoid the melt ejection, but in all experiments during which a repair weld is performed, stability is improved and the foil is welded to the discs.

The tested design suffers from the fact, that there is no degassing gap; therefore, the vaporized zinc needs to pass through the melt pool. This causes porosities, which are not completely removed by the trailing spots. Additional trailing spots will increase the length of the melt pool which may lead to increased degassing and thus less porosity. However, additional spots will require either additional laser power or a reduction of the welding speed.

If the multispot welding should be applied in cases, where a straight weld is not sufficient, the welding geometry also needs to be taken into consideration, so the pattern can be rotated along curvatures with an appropriate radius related to the length of the pattern.

The amount of zinc used in the experiments is heavily exaggerated in order to ensure a local expulsion in all experiments. In a real production the impurities should be smaller; hence the trailing spot will have “less repair work to perform”. Hereby undercut will be minimized, and the surface irregularities will be reduced as well.

### **5.3.4. FURTHER WORK**

The undercut can most likely be reduced by placing additional trailing spots on the edge of the undercut, so this will melt and hereby smoothen out. The technique is similar to the techniques demonstrated by Victor et. al [75] where trailing spots reduce the angle between the weld and the base material.

The weld quality could maybe be further improved by adding additional trailing spots after the first set of trailing spots. In this way the melt pool would be further elongated and gasses causing porosities would have longer time for escaping.

## **5.4. SUMMARY OF PAPER E: MULTISPOT LASER WELDING TO IMPROVE PROCESS STABILITY**

The paper is a summary paper of:

- Paper B: Beam shaping to control of weldpool size in width and depth
- Paper C: Joining of multiple sheets in a butt-joint configuration using single pass laser welding with multiple spots
- Paper D: Inline repair of blowouts during laser welding

The paper does not present any additional results.

### **Summary of examples of multispot fiber laser welding**

It has been shown that a single laser beam can be shaped into multiple spots and in this way provide new options within the field of laser welding.

Basic knowledge on the placement of the beams as well as practical experiments has been carried out with a single mode fiber laser systems and beam shaping equipment.

The results shows that multispot fiber laser welding is a tool, which allows to control the weld pool geometry by adjusting laser power, number of spots and their spacing. Further it has been shown that, when welding with multiple spots, the process is less sensitive to gaps and alignment errors.

The results with inline repair welding shows that it is possible to improve a weld, which has been destroyed by e.g. a blow out of the melt pool, by applying additional spots. Some porosity is though still seen in the welds. Ideas for reducing these further have been presented.

# CHAPTER 6. DISCUSSION & FUTURE WORK

This chapter discusses the effect of power and intensity and relates it to the discussion on welding with high brightness in state-of-the-art.

Implementation of multispot laser welding in industry will require, that specific demands to implementation, these are discussed in relation to the applied techniques in this project.

Examples of other cases in which multi spot fiber laser welding can be applied is suggested besides the two examined in this project.

## 6.1. EFFECT OF SPOT POWER/INTENSITY

In this dissertation most welds are performed with a spot diameter of 85  $\mu\text{m}$  and a maximum of 267 W per spot. The primary lens used has a focal length of  $f_{\text{foc}} = 331$  mm. According to equation 3 in section “2.2.2 *Effects of improved brightness*” the brightness then becomes 454 kW/(mm<sup>2</sup> SR) with a maximum average spot intensity of 47 kW/mm<sup>2</sup>. This is a whole decade from the findings of maximum useful intensity for laser welding defined by Verhaeghe (section 2.1 *Fiber laser technology*), and well within the examined spot diameters of Weberpals, where no maximum is found.

Despite the difference in the results by Verhaeghe and Weberpals, the applied spots and achieved results should be possible to scale to even higher laser power without reaching any process maxima in either spot, before the maximum brightness might be reached at approximately 2 kW of laser power in each spot, which would give same brightness as defined as *maximum brightness* by Verhaeghe.

The use of multispot laser welding from single mode fiber laser should therefore not give any new problems besides those already known from laser welding with single spots.

More extensive analysis with high speed recordings than performed in this project (section 4.5 *High speed photography*) could give information about flow patterns in the specific designs, and in combination with e.g. x-ray monitoring and other process analysis tools, it could give further input and knowledge to design rules and advantages in multi spot laser welding.

## 6.2. IMPLEMENTATION POSEBILITIES

To implement beam shaping in an industrial environment:

- It should be a robust and compact solution with a minimum of maintenance.
- The solution should be able to rotate the pattern to the welding direction.
- Further, it would be beneficial, if the spot pattern can be changed, although this is not the most important, as industrial setups usually run the same product in large quantities.
- However, to enable and use the technology for small series, the ability to change the spot pattern is an absolute demand.

The flexible beam shaping unit used in the project does not comply with these demands. It is large, sensitive to alignment and has not been tested to run continuously. The only industrial requirement it fulfils, is the flexibility to change spot patterns.

To produce the DOE's many different technologies have been presented. All the tested technologies and materials can be used to produce DOE's for an industrial implementation, except the grey scale etched DOE's – but other grey scale technologies exist, which might be used instead. Further tests to ensure minimum focal shift is needed, before it is possible to conclude, which method and material is the best. A manufacturing of DOE's using multi-level etching would allow for changing the pixel size as well as the etching depth. This can be used to further optimise the DOE design to ensure requested intensity in each spot.

The presented rotator for DOE's is fulfilling all the requirements. The size and robustness can most likely be improved by additional product development. The DOE rotator requires a different DOE for each specific pattern to be used, and by additional development a DOE exchanger could most likely be built into the unit.

The method to produce spot patterns with beam splitting or the use of multiple lasers described in section 2.3 *Beam shaping technology* has not been explored in this project. It would in an industrial setup be a large advantage to be able to control the intensity in each spot individually. It could then be possible to do dynamic process control by various feedback loops to accommodate for specific welding problems online. Such a setup would, however, contain many other constraints, as the distance between each spot would be difficult to change.

### 6.3. POSSIBLE WELDING CASES FOR THIS TECHNOLOGY

The work in this project has focussed on multiple spots. It is, however, also possible to develop different beam shapes, where the energy distribution could be an intense center beam surrounded by additional laser radiation, which is less intense and covers a larger area. This would result in a pattern like that produced by the superposition of a Nd:YAG laser and diode laser performed by Kronthaler et al., where it is concluded that the two processes are more than a super imposition, and that improved weld quality in the whole seam is achieved.

This dissertation have shown that two laser welding cases; controlling the weld pool geometry and inline repair of blowouts, achieves better results after applying multiple spots. But there might also be many other laser welding cases, which could benefit from applying multiple spots. Some of these could be:

- Phase distribution in the weld of duplex stainless steel. The cooling rate, when laser welding duplex stainless steel, is often too high, which leads to formation of a weld, where the ferritic phase is overrepresented. The phase distribution is mainly controlled by the time it takes to cool from 800°C to 500°C [111]. By adding additional laser spots in a predefined pattern, where the trailing spots have less and less energy compared to the main spot, it might be possible to control the cooling time from 800°C to 500°C
- Reduction of intermetallic phases when welding of dissimilar materials. It might be possible to affect the phase formation and hereby reduce the amount of intermetallic phases by designing a spot pattern for the specific application
- High speed welding. During high speed welding different phenomena like humping can occur. By adding extra laser spots it might be possible to control the flow in the melt, so it will be less turbulent and hereby less prone to humps and spatters
- Avoiding heat cracks. In some weld designs heat cracks can occur due to uneven cooling. By designing a spot pattern to take this into account, it might be possible to avoid this problem

Other high power laser material processes like laser cutting, laser cladding, hardening and hole drilling would most likely also be able to take advantage of beam shaping. Some of the processes are already using beam shaping in various forms.

## CHAPTER 7. CONCLUSION

In the problem formulation six project research questions were asked. The conclusion is built around these project research questions, and is answering them one by one, including a paragraph about high speed recordings of laser welding.

In PRQ 1 is asked *“how single mode fiber laser beams efficiently be shaped into specific patterns”*. It has been investigated how high quality laser beams from single mode fiber lasers efficiently can be shaped into spot patterns. In the experiments there has not been identified any challenges, which should prevent the technique from being used with other laser types, e.g. a multimode fiber lasers. If a multimode laser is applied the spots and pattern will be larger. This could maybe find use in other applications than those examined in this project.

In section *“4.4 Test of DOE’s”* four different techniques for beam shaping (grey scale etching, multilevel etching, diamond turned and a flexible beam shaping unit) has been examined. All of these change the wavefront and produce a pattern, which resembles the designed pattern. When the pattern is further examined, it is only the diamond turned DOE and the multilevel DOE, which produce satisfactory results, while still being robust enough to be integrated in an industrial setup. Even though the tested DOE’s were designed for cutting, the same results apply for DOE’s designed for welding. It has been shown that these DOE’s can be implemented in traditional laser heads in the collimated part of the beam for fiber laser welding by applying minor changes in the laser head design.

PRQ 2 asks *“how are spot patterns characterized and measured?”* A simple method to evaluate a measured spot pattern compared to its designed pattern has been established and presented in section *“4.3 Summary of Paper A: Design of measurement equipment for high power laser beam shapes”*. The method applies the same principle as the ISO standard, but it is simplified in order to disregard small changes, which easily occur, when either the collimated diameter is unknown or the alignment is imperfect. In this way the measured spot pattern is easily evaluated and compared to the designed spot pattern with respect to energy distribution, spot diameters and distances. Differences, which have no influence on the welding performance, are disregarded. The drawback of the method is, that it is a manual method, and it involves human decision to decide, which details are important, and which details that does not matter.

PRQ 3 asks *“How can design rules be established for a suitable spot pattern meeting the demands of a specific application?”* The flexible beam shaping unit at

IPU has allowed for tests of many different spot patterns. These tests have provided basic knowledge on design rules for applying multiple spots, which would have been difficult to perform, if it should have been performed using physical DOE's etched or milled in optical substrates. The most important knowledge is about using spot spacing for creating a common melt pool. This knowledge was gained in the experiments about beam shaping to control weld geometry in width and depth and in joining of multiple sheets in a butt-joint configuration. Here it was shown, that the weld profile from multiple beams on a row perpendicular to the welding direction to some degree were a superimposing of a series of welds with a single beam. Dependent on the travel speed, spot spacing and laser power, the spots influenced each other. This increased the melting volume and depth of fusion some. For the applied spot size of approximately 85  $\mu\text{m}$  in diameter it was found that a rectangular weld profile could be kept with travel speed of 50 mm/s, a spot distance of 300  $\mu\text{m}$  and still remain rectangular for focus F+2 to F-4. The rectangle could be scaled in incremental steps in width by applying more spots and in depth by adjusting the laser power, or reduce the travel speed. For the tested spots and geometries, power should be  $\geq 167$  W in each spot to achieve a rectangular shape in the profile where the material between each keyhole where melted.

It was possible to produce a significant number of experiments with different spot patterns. In this way it was possible to examine the power ratio for a trailing spot as function of a main spot, in which the trailing spot reaches same depth of fusions as the main spot for different distances of main and trailing spots. With this knowledge it is possible to design and test further spot patterns for specific welding operations.

The experiments with high speed photographing gave only limited results. Al though high speed photographing is a powerful tool, it is difficult to achieve images sequences, where the melt flow can be observed. This is concluded to be due to the high coherence of the illumination, the small scene and the high reflectance of the liquid metal. The achieved results showed a high level of turbulence in the melt with wave speeds approximately 30 times higher than the travel speed. Suggestions for how to improve the quality of the images during high speed photographing by applying the illumination from multiple directions, thus reducing the coherence, has been given.

In PRQ 4 is asked: *“To what extent can multispot welding give better weld qualities than today's state-of-the-art laser welding?”* Two studies, in which multispot welding have been applied presented in section *“5.2 Summary of Paper C: Joining of multiple sheets in a butt-joint configuration using single pass laser welding with multiple spots”* and *“5.3 Summary of Paper D: Inline repair of blowouts during laser welding”*, have shown promising results regarding increased process stability. Welding with multiple spots on a line has shown that it is possible to control the welding width and the depth of fusion independently. The studies have also revealed

## CONCLUSION

a process with increased robustness regarding tolerances compared to welding with a single beam.

It has been demonstrated, that it is possible to bridge a gap, which is larger than a single spot in a multispot pattern, as long as the spots are placed with a distance so that the remaining spots have sufficient energy to melt the material without the spot which passes the gap. The method has proven able to bridge gaps, which are wider than what can be bridged by a single round spot.

Tests with a multispot pattern were carried out in a configuration in which blowouts can occur. Several spot patterns were tested, among these a double dual spot pattern was tested in which trailing spots melted additional material. The additional melted material formed a new melt pool and hereby repaired the weld, where the blowout occurred. This technique has shown promising results for the improvement of process stability compared to state-of-the-art laser welding with a single round spot, even though the resulting weld had some porosity. The porosity is assumed to originate from the exaggerated amount of used zinc powder. It does, however, show the strong turbulence which occurs, when the melt pool is expelled.

In PRQ 5 is asked: *“How is multispot welding technology integrated into the existing production setup?”* The answer is a DOE rotator, as presented in section *“4.2.3 DOE rotator”*, which was developed in cooperation with the Robocut project, which has shown one solution upon how to implement a DOE and hereby make a phase change of the beam, so it can be used in an industrial setup. Hereby is shown a way for a commercial product, which can be developed and used without the need of redesigning the way, a laser weld normally is performed in industry. Only need is an add-on in the welding head and a rotational control. The solution has been developed for a classic laser welding head where the beam is kept stationary with the head. It could also be implemented in a laser scanner system for e.g. remote welding.

The performed industrial cases and examinations have explored new options within laser welding, and they have shown that the market for laser welding can be expanded into areas, where other technologies are still dominant. Further, it has been shown how increased robustness can be implemented in the laser welding process, with respect to both impurities and to tolerances and gaps. The tested cases and achieved results shows, that there is a further potential in the new technology ‘multi beam fiber laser welding’, which is yet to be explored.

In PRQ 6 is asked: *“Can beam shaping of single mode fiber laser beams expand the market for laser welding?”* The answer is yes. Two examples, where multi spot laser welding has improved the final weld quality, have been demonstrated. Further suggestions for other challenges in laser welding, which can be addressed by



applying multispot laser welding is presented in section “*6.3 Possible welding cases for this technology*”

Further tests of DOE’s in various materials and production methods at high power should be performed in order to determine, which material will give the minimum thermal drift in a spot pattern, while still maintaining the produced pattern.

# LITERATURE LIST

1. Dubey, A. K., & Yadava, V. (2008). Laser beam machining – A review. *International Journal of Machine Tools and Manufacture*, 48(6), 609-628.
2. Ion, J. C. (2005). *Laser processing of engineering materials: Principles, procedure and industrial application*. Oxford: Butterworth Heinemann. Retrieved from [www.sciencedirect.com/science/book/9780750660792](http://www.sciencedirect.com/science/book/9780750660792)
3. Kalpakjian, S., & Schmidt, S. R. (2014). *Manufacturing engineering and technology* (7<sup>th</sup> Ed.). Singapore: Pearson.
4. Hilton, P. A. (2002). In the Beginning..... *ICALEO 2002*. Scottsdale, Arizona, USA. Retrieved from [www.twi-global.com/technical-knowledge/published-papers/in-the-beginning-the-history-of-laser-cutting-october-2002/](http://www.twi-global.com/technical-knowledge/published-papers/in-the-beginning-the-history-of-laser-cutting-october-2002/)
5. Shiner, B. (2011). *Fiber lasers for material processing*. Paper presented at New England fiber optic council, 22 June 2013.
6. Hovikorpi, J. (2007, May 9). Disk lasers at TRUMPF. *Paper presented at Lasertekniikan Workshop*.
7. Huang, G. T. (2011). TeraDiode, MIT Lincoln lab spinoff, trying to create the future of laser weapons & welding. *Xconomy*. Boston. Retrieved from: [www.xconomy.com/boston/2011/07/05/teradiode-mit-lincoln-lab-spinoff-trying-to-create-the-future-of-laser-weapons-welding/](http://www.xconomy.com/boston/2011/07/05/teradiode-mit-lincoln-lab-spinoff-trying-to-create-the-future-of-laser-weapons-welding/)
8. International standard ISO. (2000). *Optics and optical instruments — Lasers and laser-related equipment — Test methods for laser beam power (energy) density distribution: Technical Corrigendum 1*. (13694:2000). Technical Committee ISO/TC 172, Optics and photonics, Subcommittee SC 9, Electro-optical systems. Switzerland: International standard ISO.
9. Shiner, B. (2013). *High power fiber laser technology*. Paper presented at DOE LSO workshop, 10 September 2013.
10. Belforte, D (2015). Fiber lasers continue growth streak in 2014 laser market. *Industrial laser solutions*, 30 (1), p. 5-6, 8, 10, 12-13. Retrieved from [www.industrial-lasers.com/articles/print/volume-30/issue-1/features/fiber-lasers-continue-growth-streak-in-2014-laser-market-revenues-increase-despite-mixed-global-manufacturing-growth.html](http://www.industrial-lasers.com/articles/print/volume-30/issue-1/features/fiber-lasers-continue-growth-streak-in-2014-laser-market-revenues-increase-despite-mixed-global-manufacturing-growth.html)
11. Olsen, F. O. (2006). An evaluation of the cutting potential of different types of high power lasers (paper 401). *ICALEO 2006 Congress proceedings*, 188-196.
12. Larsson, J. K. (2009). Appropriate utilization of laser processing in order to stay competitive in the manufacture of world class automotive body structures. *12th NOLAMP*. Copenhagen.
13. Larsson, J. K. (Marts 01, 2013). Laser development at Volvo. *Industrial laser solutions*, 28 (2). Retrieved from [www.industrial-lasers.com/articles/print/volume-28/issue-2/features/laser-development-at-volvo.html](http://www.industrial-lasers.com/articles/print/volume-28/issue-2/features/laser-development-at-volvo.html)
14. Graf, T. & Staufer, H. (2003). *Laser-Hybrid Welding Drives VW Improvements*. Based on a paper presented at the Annual Assembly of the

- International Institute of Welding on June 27, 2002, in Copenhagen, Denmark. Retrieved from [www.aws.org/w/a/wj/2003/01/042/](http://www.aws.org/w/a/wj/2003/01/042/)
15. Graudenz, M., & Baur, M. (2013). 21 - Applications of laser welding in the automotive industry. In S. Katayama (Ed.), *Handbook of laser welding technologies* (1st ed.), (pp. 555-574). Cambridge, United Kingdom: Woodhead Publishing. ISBN: 9780857092649. DOI: 10.1533/9780857098771.4.555
  16. Albert, F., Kilian, A., Franz, C., & Hammer, T. (2014). Laser flange welding - a new method to save weight and to reduce weld defects at zinc-coated steel sheets -. *Proceedings of the LANE 2014*.
  17. Salminen, A., Westin, E. M., Lappalainen, E., & Unt, A. (2012). Effect of gas shielding and heat input on autogenous welding of duplex stainless steel (paper 1701). *ICEO 2012 Congress proceedings*, 524-531.
  18. Shkurikhin, O., Mochalov, D., & Zakharova, A. (2012). *U.S. Patent No. 8160415 B2*. Washington, DC: U.S. Patent and Trademark Office. Retrieved from [www.google.com.ar/patents/US8160415](http://www.google.com.ar/patents/US8160415)
  19. Dausinger, F., Abt, F., & Heß, A. (2007). Focussing of high power single mode laser beams (paper #202). *ICALEO 2007 Congress proceedings*, 77-82.
  20. Abt, F., Heß, A., & Dausinger, F. (2008). Focusing high-power, single-mode laser beams. *Photonics Spectra*, 5 (42). Retrieved from [www.photonics.com/Issue.aspx?PID=5&VID=22&IID=153#38360](http://www.photonics.com/Issue.aspx?PID=5&VID=22&IID=153#38360)
  21. Märten, O., Kramer, R., Schwede, H., Brandl, V., & Wolf, S. (2007). Determination of thermal focus drift with high power disk and fiber lasers. *Proceedings of the 4th international WLT-conference on lasers in manufacturing 2007*, 329-331. Munich, Germany.
  22. Steen, W. M., & Mazunder J. (2010). *Laser material processing* (4<sup>th</sup> Ed.). London: Springer-Verlag. ISBN 1849960615.
  23. IPG Laser (n.d.). *Test results Ytterbium laser system YLS-3000-SM S/N 11076350* (Form 38445, rev. 4). Datasheet.
  24. Rominger, V. (2011). High-performance laser welding. *Laser Technik Journal*, 8 (3), 32-35. Weinheim: WILEY-VCH Verlag GmbH & Co. DOI: 10.1002/latj.201190022
  25. Wandera C. (2006). *Laser cutting of austenitic stainless steel with a high quality laser beam* (master thesis). Lappeenranta University of Technology.
  26. TeraDiode, Inc. (2014). *4kW Direct Diode Laser System at 970nm with 100µm fiber*. Datasheet.
  27. IPG Photonics (2011, September 23). *Specification ytterbium fiber laser - Model YLR-1000-WC-Y11 - 2011 Series* (Spec. G22-15692, rev. 02). Datasheet.
  28. Ream, S. (2006). High-speed fiber laser welding for fuel cell components (paper 1302). *ICALEO 2006 congress proceedings*, 586-594.
  29. Weberpals, J., Dausinger, F., Göbel, G., & Brenner, B. (2006). The role of strong focusability on the welding process (paper #905). *ICALEO 2006 Congress proceedings*, 553-561.

30. Thomy, C., Seefeld, T., Wagner, F., & Vollertsen, F. (2006). Humping in welding with single-mode fiber lasers (paper 903). *ICALEO 2006 Congress proceedings*, 543-552.
31. Miyamoto, I., Park, S.-J., & Ooie, T. (2003). Precision microwelding of thin metal foil with single-mode fiber laser. In I. Miyamoto, A. Ostendorf, K. Sugioka, & H. Helvajian, *Proceedings of SPIE*, 5063, Fourth International Symposium on Laser Precision Microfabrication, (pp. 297-302). DOI: 10.1117/12.541155
32. [0186 book] Katayama, S. (Ed.). (2013). *Handbook of laser welding technologies* (1st Ed.). Cambridge, United Kingdom: Woodhead Publishing. eBook ISBN: 9780857098771. Print Book ISBN: 9780857092649. Retrieved from [www.sciencedirect.com/science/book/9780857092649](http://www.sciencedirect.com/science/book/9780857092649)
33. Vollertsen, F., & Thomy, C. (2005). Welding with fiber lasers from 200 to 17000 W (paper #506). *ICALEO 2005 Congress proceedings*, 254-263.
34. Pekkari, B. (2005). *The welding industry of the world – where are we standing*. Paper presented at Laser Welding Days, 12.-13. April 2005.
35. Fabbro, R. (2010). Melt pool and keyhole behaviour analysis for deep penetration laser welding. *Journal of Physics D: Applied Physics*, 43(44), p. 445501. IOP Publishing. DOI: 10.1088/0022-3727/43/44/445501
36. Kroos, J., Gratzke, U., Vicane, M., & Simon, G. (1993). Dynamic behaviour of the keyhole in laser welding. *Journal of Physics D: Applied Physics*, 26 (3), 481-486. United Kingdom: IOP Publishing Ltd. DOI: 10.1088/0022-3727/26/3/022
37. Olsen, F. O. (2011). Laser cutting from CO<sub>2</sub>-laser to disc- or fiber laser – possibilities and challenges (paper 101-0). *ICALEO 2011*.
38. [0186-k20] NA, S.-J., & Cho, W.-I. (2013). 20 - Developments in modelling and simulation of laser and hybrid laser welding. In S. Katayama (Ed.), *Handbook of laser welding technologies* (1st ed.), (pp. 522-552, 553e-560e). Cambridge, United Kingdom: Woodhead Publishing. ISBN: 9780857092649. DOI: 10.1533/9780857098771.3.522
39. Mackwood, A. P., & Crafer, R. C. (2005). Thermal modelling of laser welding and related processes: a literature review. *Optics & laser technology*, 37, 99-115. Elsevier. DOI: 10.1016/j.optlastec.2004.02.017
40. Fabbro, R., & Poueyo, A. (1994). Plasma in photon matter interaction during laser material processing. *Journal de physique IV*, 4 (C4), p. C4-3 – C4-8. M2P. DOI: 10.1051/jp4:1994401
41. Aden, M., Beyer, E. & Herziger, G. (1989). Laser-induced vaporisation of metal as a Riemann problem. *Journal of Physics. D: Applied Physics*, 23 (6), 655-661. United Kingdom. DOI: 10.1088/0022-3727/23/6/004
42. Kancharla, V. (2006). Applications review: Materials processing with fiber lasers under 1kW (paper #1301). *Icaleo 2006 congress proceedings*, 579-585.
43. Tu, J., Paleocrassas, A. G., Reeves, N., & Rajule, N. (2013). Experimental characterization of a micro-hole drilling process with short micro-second pulses by a CW single-mode fiber laser. *Optics and lasers in engineering*, 55, 275-283. Elsevier. DOI: 10.1016/j.optlaseng.2013.11.002

44. Musiol, J., Luetke, M., Schweier, M., Hatwig, J., Wetzig, A., Beyer, E., & Zaeh, M. F. (2012). Combining remote ablation cutting and remote welding: Opportunities and application areas. In E. Beyer, & T. Morris (Eds.), *Proceedings of SPIE--the International society for optical engineering*, 8239 (1), (pp. 82390Q-14), 2012. DOI: 10.1117/12.908481
45. Liu, Z., Kutsuna, M., & Xu, G. (2006). Fiber laser welding of 780MPa high strength steel (paper #1101). *ICALEO 2006 Congress proceedings*, 562-568.
46. Berend, O., Haferkamp, H., Meier, O., & Engelbrecht, L. (2005). High-frequency beam oscillating to increase the process stability during laser welding with high melt pool dynamics (paper #2206). *ICALEO 2005 Congress proceedings*, 1032-1041.
47. Kinoshita, K., Mizutani, M., Kawahito, Y., & Katayama, S. (2006). Phenomena of welding with high-power fiber laser (paper #902). *ICALEO 2006 Congress proceedings*, 535-542.
48. Vänskä, M., Abt, F., Weber, R., Salminen, A., & Graf, T. (2012). Investigation of the keyhole in laser welding of different joint geometries by means of X-ray videography (paper 1403). *ICALEO 2012 Congress proceedings*, 451-457.
49. Eriksson, I., Powell, J., Kaplan, A., & Ilar, T. (2012). Root humping in laser welding – an investigation based on high speed imaging. *Physics procedia*, 39, 27-32, LANE 2012. Elsevier. DOI: 10.1016/j.phpro.2012.10.010
50. Wang, Z., Zhang, Y., & Yang, R. (2013). Analytical reconstruction of three-dimensional weld pool surface in GTAW. *Journal of Manufacturing Processes*, 15, 34-40. Elsevier. DOI: 10.1016/j.jmapro.2012.08.00
51. Eriksson, I., Powell, J., & Kaplan, A. (2011). High speed video analysis of melt flow inside fiber laser welding keyholes (paper 407). *ICALEO 2011 congress proceedings*, 221-226.
52. Cai, H., & Xiao, R. (2011). Comparison of spatter characteristics in fiber and CO<sub>2</sub> laser beam welding of aluminium alloy (paper #307). *ICALEO 2011 Conference proceedings*, 150-158.
53. Bagger, C. (1991). *Investigations in on-line process control of the laser welding process* (publication no. AP.91-02 / PI.91.1-A), Institute of manufacturing engineering, Technical University of Denmark.
54. L. Romoli, L., Musacchio, A., Franco, A., Fierro, M. C., & Dini, G. (2013). A double-point moving source model for predicting seam geometry in laser welding. *CIRP Annals - Manufacturing Technology*, 62 (1), 219-222. Elsevier. DOI: 10.1016/j.cirp.2013.03.031
55. Gross, M. S., Celotto, S., & O'Neill, W. (2006). Melt flow in narrow thick section kerfs (paper #403). *ICALEO 2006 Congress proceedings*, 206-210.
56. Cho W.-I., Sohail, M., & Suck-Joo, N. (2012). Modeling of keyhole formation in laser and laser arc hybrid welding based on CFD simulations (paper #103). *ICALEO 2012 Congress proceedings*, 34-42.
57. Yang, S., Wang, J., Carlson, B., & Zhang, J. (2012). Zero-gap laser welding of zinc coated steels in a lap joint configuration (paper 1402). *ICALEO 2012 Congress proceedings*, 445-450.

58. Avilov, V., Schneider, A., Lammers, M., Gumenyuk, A., & Rethmeier, M. (2012). Electromagnetic control of the weld pool dynamics in partial penetration laser beam welding of aluminium alloys (paper #701). *ICALEO 2012 Congress proceedings*, 250-256.
59. Vollertsen, F., & Thomy, C. (2006). Magnetic stirring during laser welding of aluminum. *Journal of laser applications* 18 (28). DOI: 10.2351/1.2164477
60. Olsen, F. O. (Ed.) (2009.). *Hybrid laser-arc welding*. Woodhead Publishing. ISBN: 9781845693701. Retrieved from [www.sciencedirect.com/science/book/9781845693701](http://www.sciencedirect.com/science/book/9781845693701)
61. Norman, P., Eriksson, I., & Kaplan, A. F. H. (2009). Monitoring laser beam welding of zinc coated sheet metal to analyze the defects occurring. In E. D. Mortensen (Ed.), *12th NOLAMP conference*, 24.-26. August 2009 in Copenhagen.
62. De Graaf, M., & Aarts, R. (2013). 14 - Applications of robotics in laser welding. In S. Katayama (Ed.), *Handbook of laser welding technologies* (1st ed.), (pp. 401-421). Cambridge, United Kingdom: Woodhead Publishing. ISBN: 9780857092649. DOI: 10.1533/9780857098771.3.401
63. Katayama, S. (2013). 12 - Defect formation mechanisms and preventive procedures in laser welding. In S. Katayama (Ed.), *Handbook of laser welding technologies* (1st ed.), (pp. 332-373). Cambridge, United Kingdom: Woodhead Publishing. ISBN: 9780857092649. DOI: 10.1533/9780857098771.2.332
64. Verhaeghe, G., & Hilton, P. (2005). The effect of spot size and laser beam quality on welding performance when using high-power continuous wave solid-state lasers (paper #507). *ICALEO 2005 Congress proceedings*, 264-271.
65. Tsubota, S., Ishide, T., & Nayama, M. (2004). Improvement of productivity and reliability of welding parts in heavy industry by laser welding process (IIW Doc, IV-861-04). *International welding society annual meeting*. Mitsubishi Heavy Industries, Ltd., Japan.
66. Bergmann, J. P., Bielenin, M., Stambke, M., Feustela, T., Witzendorff, P. v., & Hermsdorf, J. (2013). Effects of diode laser superposition on pulsed laser welding of aluminum. *Physics procedia*, 41, 180-189, Lasers in Manufacturing Conference 2013. Elsevier. DOI: 10.1016/j.phpro.2013.03.068
67. Haglund, P., Powell, J., Kaplan, A., & Eriksson, I. (2013). Surface tension stabilized laser welding (donut laser welding) - A new laser welding technique. *Journal of laser applications*, 25 (3), p. 031501-1 – 031501-2. DOI: 10.2351/1.4798219
68. Miyashita, Y. (2013). Developments in twin-beam laser welding technology. In S. Katayama (Ed.), *Handbook of laser welding technologies* (1<sup>st</sup> ed.), (pp. 434-465e). Cambridge, United Kingdom: Woodhead Publishing. ISBN: 9780857092649. DOI: 10.1533/9780857098771.3.434
69. Müller, A., Goecke, S.-F., Sievi, P., Albert, F., & Rethmeier, M. (2014). Laser beam oscillation strategies for fillet welds in lap joints. *Physics*

- Procedia*, 56, 458-466, LANE 2014. Elsevier. DOI: 10.1016/j.phpro.2014.08.149
70. Wetzig, A. (2013). Developments in beam scanning (remote) technologies and smart beam processing. In S. Katayama (Ed.), *Handbook of Laser Welding Technologies* (1<sup>st</sup> ed.), (pp. 422-433). Cambridge, United Kingdom: Woodhead Publishing. ISBN: 9780857092649. DOI: 10.1533/9780857098771.3.422
  71. Wyrowski, F., & Schimmel, H. (2007). Electromagnetic optical engineering – an introduction. *Photonik international* (1), 48-51.
  72. Alexandrov, O. (2007). *Lens and wavefronts.gif*. Retrieved February 26, 2015, from [www.commonswiki.org/wiki/File:Lens\\_and\\_wavefronts.gif](http://www.commonswiki.org/wiki/File:Lens_and_wavefronts.gif)
  73. Hansen, K. S. (2008). *New strategy for fiber laser cutting* (master thesis, no. L 325, TM 03-08). Technical University of Denmark.
  74. Olsen, F. O., Hansen, K. S., & Nielsen, J. S. (2009). Multibeam fiber laser cutting (paper P156). <http://dx.doi.org/10.2351/1.3184436> / *Journal of laser applications*, 21 (3), 133-138. DOI: 10.2351/1.3184436
  75. Victor, B., Farson, D. F., Ream, S., & Walters, C. T. (2011). Custom beam shaping for high-power fiber laser. *Welding Journal*, 90, p. 113-s – 120-s.
  76. Dankwart, C., Falldorf, C., Kopylow, C. V., Bergmann, R. B., Gläbe, R., & Meier, A. (2010). Design of diamond-turned holograms incorporating properties of the fabrication process. *Applied optics*, 49(20), 3949-3955.
  77. Laskin, A., & Laskin, V. (2012). Controllable beam intensity profile for the tasks of laser material processing (paper 707). *ICALEO 2012 Congress proceedings*, 270-276.
  78. Miklyayev, Y. V., Homburg, O., Krasnaberski, A., Kleinschmidt, L., Pikhulia, D., Ivanenko, M., & Lissotschenko, V. N. (2011). Novel diffractive beam splitters with efficiency above 95% enable multiple beam parallel processing with highest throughput (paper #C103). *ICALEO 2011*.
  79. Miklyayev, Y. V., Imgrunt, W., Pavelyev, V. S., Kachalov, D. G., Bizjak, T., Aschke, L., & Lissotschenko, V. N (2010). Novel continuously shaped diffractive optical elements enable high efficiency beam shaping. In M. V. Dusa, & W. Conley (Eds.), *Proceedings of SPIE, Optical Microlithography XXIII*, 7640, (pp. 764024-1 - 764024-7). San Jose, California. DOI: 10.1117/12.846573
  80. Li, L., Yi, A. Y., Huang, C., Grewal, D. A., Beater, A., & Chen, Y. (2006). Fabrication of diffractive optics by use of slow tool servo diamond turning process. *Optical engineering*, 45 (11), p. 113401-1 - 113401-9. DOI:10.1117/1.2387142
  81. O'Shea, D. C., Pulaski, T. J., Kathman, A. D., & Prather, D. W. (2004). *Diffractive optics design, fabrication, and test*. SPIE press, ISBN-13: 9780819451712
  82. Schweitzer, H. (2012). *VirtualLab Training material from LightTrans GmbH*.
  83. Falloff, C., Dankwart, C., Copilot, C. v., Bergmann, R. B., Globe, R., & Lineman, B. (2009). Holographic projection based on diamond-turned

- diffractive optical elements. *Applied optics*, 48 (30), 5782-5785. DOI: 10.1364/AO.48.005782
84. G. J. Swanson, & Veldkamp, W. B. (1992). *U.S. Patent No. 5161059 A*. Washington, DC: U.S. Patent and Trademark Office. Retrieved from [www.google.com/patents/US5161059](http://www.google.com/patents/US5161059)
  85. Christophersen, M., & Philips, B. F. (2008). Gray-tone lithography using an optical diffuser and a contact aligner. *Applied physics letters*, 92, p. 194102-01 – 194102-3. DOI: 10.1063/1.2924314
  86. Henke, W., Hoppe, W., Quenzer, H. J., Staudt-Fischbach, P., & Wagner, B. (1995). Simulation assisted design of processes for gray-tone lithography. *Microelectronic engineering*, 27, 267-270. Elsevier.
  87. Henke, W., Hoppe, W., Quenzer, H. J., Staudt-Fischbach, P., & Wagner, B. (1994). Simulation and experimental study of gray-tone lithography for the fabrication of arbitrarily shaped surfaces. *Proceedings of the IEEE Micro electro mechanical systems*, 205-210. DOI: 10.1109/MEMSYS.1994.555624
  88. Hamamatsu photonics k.k. (n.d.). *LCOS-SLM – X10468 series*. Datasheet. Hamamatsu city, Japan. Retrieved February 26, 2015 from [www.hamamatsu.com](http://www.hamamatsu.com)
  89. Wyrowski, F., & Schimmel, H. (2008). Electromagnetic optical engineering – shaping light through design. *Photonik international* (1), 80-83.
  90. Ploshikhin, V., Prikhodovsky, A., Makhutin, M., Zoch, H.-W., Heimerdinger, C., & Palm, F. (2004). Multi-beam welding: advanced technique for crack-free laser welding. In M. Geiger & A. Otto (Eds.), *Laser assisted net shape engineering* (4), (pp. 131-136), Proceedings of the LANE 2004.
  91. Bagger, C., Olesen, S., Roos, S.-O., & Olsen, F. O. (2001). Diffractive optics for reduction of hot cracking in pulsed mode nd:YAG laser welding. In F. O. Olsen, & J. K. Kristensen (Eds.), *8th NOLAMP conference*, (pp. 223-234). ISBN 8790855329.
  92. Trautmann, A., Roeren, S., & Zaeh, M. F. (2004). Welding of extruded aluminium profiles by a hybrid bifocal laser system. In M. Geiger, & A. Otto (Eds.), *Laser assisted net shape engineering 4*, (pp. 169-180), Proceedings of the LANE 2004.
  93. Seefeld, T., Beren, J. v., Vollertsen, F., Piontek, D., & Dilthey, U. (2004). CO2 laser welding with double beam optics. *ICALEO 2004 congress proceedings*.
  94. Kronthaler, M. R., Braunreuther, S., & Zaeh, M. F. (2011). Bifocal hybrid laser welding – more than a superposition of two processes. *Physics Procedia* (12), 208–214. Elsevier. DOI: 10.1016/j.phpro.2011.03.027
  95. Kell, J., Tyrer, J. R., Higginson, R. L., Jones, J. C. & Noden, S. (2012). Laser weld pool management through diffractive holographic optics. *Materials Science and Technology*, vol 25, no 3 p 354-362, Maney Publishing.
  96. Olowinsky, A. (2012, May 9). Extending the process limits of laser polymer welding with high-brilliance beam sources - POLYBRIGHT project overview. *Proceedings of the EU FP7, POLYBRIGHT consortium*.
  97. Vogler, D. (2014). Beam shaping for enhanced laser plastic welding. *Industrial laser solutions*, 29 (3). Retrieved from [www.industrial-](http://www.industrial-)



- lasers.com/articles/print/volume-29/issue-3/features/beam-shaping-for-enhanced-laser-plastic-welding.html
98. Kaplan, A. F. H. (2012). Absorptivity modulation on wavy molten steel surfaces: The influence of laser wavelength and angle of incidence. *Applied Physics Letters*, 101, p. 151605-1 – 151605-4. AIP Publishing. DOI: 10.1063/1.4759126
  99. Hu, J., Tsai, H. L., & Lee, Y. K. (2003). Modeling of weld pool dynamics during dual-beam laser welding process (paper 11688). *Faculty Research & Creative Works*. ICALEO 2003 Congress proceedings. Retrieved from scholarsmine.mst.edu/faculty\_work/11688
  100. Hansen, K. S., Olsen, F. O., Kristiansen, M., & Madsen, O. (2013). Design of measurement equipment for high power laser beam shapes. In A. Kaplan, & H. Engström (Eds.), *Proceedings of The 14th Nordic Laser Materials Processing Conference NOLAMP 14*, (pp. 293-304). Luleå Tekniska Universitet.
  101. Hansen, K. S., Olsen, F. O., Kristiansen, M., & Madsen, O. (2015). Joining of multiple sheets in a butt-joint configuration using single pass laser welding with multiple spots. *Journal of Laser Applications* 2015.
  102. Dickey, F. M., & Holswade, S. C. (Eds.) (2000). *Laser beam shaping theory and techniques*. New York, US: Marcel Dekker. ISBN: 0824703987.
  103. SCHOTT (2010, April 19). *Optical glass – Data sheets*. Datasheet. Duryea, USA. Retrieved February 26, 2015, from [www.schott.com/advanced\\_optics/us/abbe\\_datasheets/schott\\_datasheet\\_all\\_us.pdf](http://www.schott.com/advanced_optics/us/abbe_datasheets/schott_datasheet_all_us.pdf)
  104. II-VI INFRARED (n.d.). Zinc Sulfide (ZnS). Retrieved February 26, 2015, from [www.iiviiinfrared.com/Optical-Materials/zns.html](http://www.iiviiinfrared.com/Optical-Materials/zns.html)
  105. Ream, S., Zhang, W., Walters, C., & Firestone, G. (2007). Zinc sulfide optics for high power laser applications (paper #1609). *ICALEO 2007 Conference proceedings*.
  106. Polyanskiy, M. (2008-2015). *refractiveindex.info* (database). Retrieved from refractiveindex.info
  107. Dickey, F. M., Holswade, S. C., & Shealy, D. L. (Eds.) (2005). *Laser beam shaping applications*. Boca Raton, FL: Taylor & Francis. ISBN: 0824759419.
  108. Hansen, K. S., Olsen, F. O., Kristiansen, M., & Madsen, O. (2015). Inline repair of blowouts during laser welding. *World of Photonics Congress - Lasers in Manufacturing*. Article submitted for publication in February 2015.
  109. Zhao, C. X., Steijn, V. v., Richardson, I. M., Saldi, Z., & Kleijn, C. R. (2008). Experimental characterization of GTA weld pool surface flow using PIV. In S. A. David, T. Debroy, J. N. Dupont, T. Koseki, & H. B. Smartt (Eds.), *Trends in welding research*. Proceedings of the 8<sup>th</sup> International conference, (pp. 201-210). DOI: 10.1361/cp2008twr201
  110. Hansen, K. S., Olsen, F. O., & Kristiansen, M. (2014): Beam shaping to control of weldpool size in width and depth. *Physics Procedia*, 56, 467–476, Lane 2014. Elsevier. DOI: 10.1016/j.phpro.2014.08.150

## CONCLUSION

111. Elmesalamy, A. S., Li, L., & Francis, J. A. (2012): Narrow gap laser welding of thick section stainless steel (paper #1501). *ICALEO 2012 Congress proceedings*, 474-479.
112. LWT (2013, Oktober 29). *Trumpf dual disc-laser system*. Demonstration at Dansk-svensk lasermøde, Munkebo, Denmark.
113. Optoskand (2012, December 21). *Prealigned External Optics D50 1237*. Product catalogue. Mölndal, Sweden.
114. International standard ISO. (2005). Lasers and laser-related equipment — Test methods for laser beam widths, divergence angles and beam propagation ratios - Part 1: Stigmatic and simple astigmatic beams. (11146:2005). Technical Committee ISO/TC 172/SC 9, Optics and photonics, Subcommittee SC 9, Electro-optical systems. Switzerland: International standard ISO.
115. ROFIN-SINAR Laser GmbH (2015, May). *CO2-Slab-Laser, Cutting and welding without break*. Data sheet. Hamburg, Germany. Retrieved November 04, 2015, from [www.rofin.com/en/products/co2-laser/slab-lasers/dc-series/](http://www.rofin.com/en/products/co2-laser/slab-lasers/dc-series/)
116. Hansen, K. P., & Broeng, J. (2006, May). High-Power Photonic Crystal Fiber Lasers. *Photonics Spectra*, Feature, 1-9. Retrieved November 22, 2015, from [www.photonics.com/Article.aspx?AID=25277](http://www.photonics.com/Article.aspx?AID=25277)
117. Olsen, F. O. (2011, September-Oktober). Laser metal cutting with tailored beam patterns. *Industrial Laser Solutions for Manufacturing*, 26(5), 17-19. Retrieved June, 26, 2008, from [www.industrial-lasers.com](http://www.industrial-lasers.com)
118. Photron “Fastcam SA5 – worlds fastest high speed camera” datasheet. Retrieved November 04, 2015 from [www.photron.com](http://www.photron.com)



# APPENDICES

Appendix A: Design of measurement equipment for high power laser beam shapes

Appendix B: Beam shaping to control of weldpool size in width and depth

Appendix C: Joining of multiple sheets in a butt-joint configuration using single pass laser welding with multiple spots

Appendix D: Inline repair of blowouts during laser welding

Appendix E: Multispot laser welding to improve process stability



# APPENDIX A: DESIGN OF MEASUREMENT EQUIPMENT FOR HIGH POWER LASER BEAM SHAPES

Published: 12 November 2012

Conference: NOLAMP 14

Published by: Universitetsstryckeriet, Luleå 2013

ISBN: 978-91-7439-688-1 (print)

ISBN: 978-91-7439-689-8 (pdf)

Edited by: Alexander Kaplan and Hans Engström

DOI: N/A

# DESIGN OF MEASUREMENT EQUIPMENT FOR HIGH POWER LASER BEAM SHAPES

**K. S. Hansen<sup>1</sup>, F. O. Olsen<sup>1</sup>, M. Kristiansen<sup>2</sup>, O.  
Madsen<sup>2</sup>**

*<sup>1</sup>IPU Technology Development, Denmark.*

*<sup>2</sup>Department of Mechanical and Manufacturing Engineering, Aalborg University, Denmark University,  
Fibigerstræde 16, 9220 Aalborg, Denmark*

---

## Abstract

To analyse advanced high power beam patterns, a method, which is capable of analysing the intensity distribution in 3D is needed. Further a measuring of scattered light in the same system is preferred. This requires a high signal to noise ratio.

Such a system can be realised by a CCD-chip implemented in a camera system. Most available CCD-based systems do however suffer from a low maximum intensity threshold. Therefore attenuation is needed.

This paper describes the construction of such a beam analysing system where beam patterns produced by single mode fiber laser on a diffractive optical element can be evaluated using a CCD based camera.

The system is tested with various DOE's for evaluation of efficiency and measurement of scattered light with success. Also tests with capturing beam caustics of focused laser beams from which beam parameters has been fitted and compared with measurements by a commercial product has been done.

The realised system might suffer from some thermal drift at high power; future work is to clarify this.

**Keywords:** Laser caustic, camera, high power high brightness, laser beam diagnostics

---

## 1. Background

In recent years high power high brightness fiber lasers has emerged. These has led to ideas about reshaping the beam into application specific patterns for cutting [1], welding [2] [3] and other macro laser processes.[12]

IPU and Aalborg University has two on-going projects, which utilise a 3 kW single mode fiber laser and beam shaping using Diffractive Optical Elements (DOE's) [1].

The system should be able to verify beam patterns produced by DOE's, evaluate scattered light and perform measurements of beam parameters, such as diameter and the beam quality factor. Furthermore flexibility should be considered, so that the system is open and allows access to raw data and automation.

|   |                                       |
|---|---------------------------------------|
| A/D conversion  | 10 bit                                |
| Signal to noise ratio (SNR)   | 1000:1                                |
| Maximum intensity threshold (when analysing round beam, $f=200$ )                 | 3.6 MW/mm <sup>2</sup>                |
| Minimum intensity detectable (when analysing round beam, $f=780$ )                | 2.3 kW/mm <sup>2</sup>                |
| Minimum intensity detectable (when analysing beam pattern, $f=780$ ) <sup>1</sup> | 37 W/mm <sup>2</sup>                  |
| Dynamic range (beam / pattern)  | 93 dB                                 |
| Total required dynamic range (Dynamic + SNR)                                      | 153 dB                                |
| Total power up to   | 3 kW                                  |
| Resolution  | 1.7 $\mu\text{m}$ x 1.7 $\mu\text{m}$ |
| Scan area   | 2.0 mm x 2.0 mm                       |
| Focal length of analysed optical system   | 200-800 mm                            |
| Clear aperture  | 16 mm                                 |
| Flexibility   | High / open system                    |

<sup>1</sup>Beam pattern assumed to be up to 8 times larger than a round beam

*Table 1. Minimum demands for the system. All dB values are  $\text{dB (volts)} = 20 \times \log_{10}(\text{measuring-ratio})$*

In table 1 is shown the minimum requirements for the system. The numbers are based on design considerations for the requirements for the constructed beam patterns, and the theoretical minimum beam diameter that can be formed with the available equipment. ISO 11146-1:2005 specifies that any detail to be measured in the design should be resolved by minimum 20 pixels in any direction [9]. The system should also be able to measure the intensity distribution in different planes within +/- 2 times the Rayleigh length [9].



## 2. Commercial systems

To fulfil the requirements a product search in the market were performed. In table 2 is shown a small amount of available systems and techniques

Based on this market/product analysis, it was decided to produce a “low cost” system, where beam is attenuated before imaged on a camera chip, instead of buying a turnkey system.

It is not expected, that the produced system will be better than any system, that can be bought; it is expected to save some money and gain some flexibility in the final design compared to the commercial systems.

|                                 | Primes<br>HighPower<br>MSM [4] | Primes<br>FocusSpotMonitor<br>[4] | Spiricon<br>SP620<br>[11]   | Gentec<br>Beamgage<br>CCD-12 [10] | Spiricon<br>Pyrocam<br>™ [11] |
|---------------------------------|--------------------------------|-----------------------------------|-----------------------------|-----------------------------------|-------------------------------|
| Principle                       | CCD /<br>CMOS                  | Rotating needle                   | CCD                         | CCD                               | Thermal<br>chip               |
| Product<br>type                 | Ready to<br>use                | Ready to use                      | OEM                         | OEM                               | OEM                           |
| A/D<br>conversio<br>n           | 12 bit?                        | 12 bit                            | 12 bit                      | 14 bit                            | 14 bit                        |
| Signal to<br>noise ratio        | High                           | High                              | 1000:1                      | 1000:1                            | 1000:1                        |
| Dynamic<br>range                | >130 dB<br>(system)            | ?                                 | 62 dB                       | 42 dB                             | 43 dB                         |
| Minimum<br>intensity            | -                              | -                                 | 0.025<br>nW/mm <sup>2</sup> | -                                 | 0,3<br>nW/mm <sup>2</sup>     |
| Maximum<br>intensity<br>(focus) | 127<br>MW/mm <sup>2</sup>      | 0.1 MW/mm <sup>2</sup>            | 0.022<br>μW/mm <sup>2</sup> | -                                 | 32<br>μW/mm <sup>2</sup>      |
| Max<br>power                    | 10 kW                          | >10 kW                            | ~1 mW                       | ~1 mW                             | ~100 mW                       |
| Resolutio<br>n                  | ~1 x 1 μm                      | ~8 x 8 μm                         | 4.4 x 4.4<br>μm             | 4,7 x 4,7 μm                      | 100 x<br>100μm                |
| Scan area                       | 8 x 8 mm                       | 8 x 8 mm                          | 7.1 x<br>5.4mm              | 6.3 x 4.8 mm                      | 12.4 x<br>12.4mm              |
| Price                           | Very high                      | High                              | Medium                      | Medium                            | Unknown                       |

Table 2. Some of the different systems and principles considered

On the market there exist several systems capable of analysing laser beams, and beam patterns [12]. Most of these systems have a low maximum beam intensity threshold compared to the intensity in focus by a 3 kW single mode fiber laser.

One of the few products capable of performing the measurements directly in focus with a 3 kW SM-fiber laser is the Primes FocusSpotMonitor. But the Primes FocusSpotMonitor still has two problems: it has a limited resolution, which is too large compared to the specification in table 1, and it is quite expensive [4].

Another option is to split the beam and only perform the measurement on a fraction of the beam. One of the systems, which operate with this technique, is Primes HighPower MicroSpotMonitor [3]. In this system, there is an option to add a lens after attenuation which increases the beam, before it is imaged on a CCD chip. This increases the resolution and combines it with the ability to measure high power and high intensities. The product is however quite expensive and suffers from some thermal drift. [4].

The two camera systems are in many ways similar to the Primes HighPower MSM. They are just OEM products with software to perform some measurements.

Pyrocam is also a pixelbased measurements system. However the way to capture data is different, as it is the heat which is measured. Pixels are much bigger and the dynamic range is on 43 dB, which gives a signal to noise ratio of 141. This would be way too little for detecting scattered light. The Pyrocam has its largest advantages spectral areas where traditional CCD/CMOS in various designs don't have any response.

### 3. System design

First step in the construction of a measurement system is to decide on a measuring principle. Following principles were considered:

- Scanning aperture techniques (integral measurements)
- A rotating needle
- Thermal chips
- CMOS / CCD chips

The scanning aperture technique can also do measurements with micron resolution and excellent signal to noise ratio. The technique was considered and abandoned, due to difficulties in calculating more complex structure patterns from integrated measurements. [13]

The principle with the rotating needle was abandoned due to the system is quite complex to produce, and that available commercial tends to have a minimum resolution of  $8 \times 8 \mu\text{m}$ . [4]

The choice of measuring principle fell on a CCD based solution, as this is the technique identified with the best available resolution without introducing lenses. A

CCD solution is preferred over a CMOS as the spectral response from most CMOS chips at the laser wavelength is quite low or non-existing as shown in fig 1.

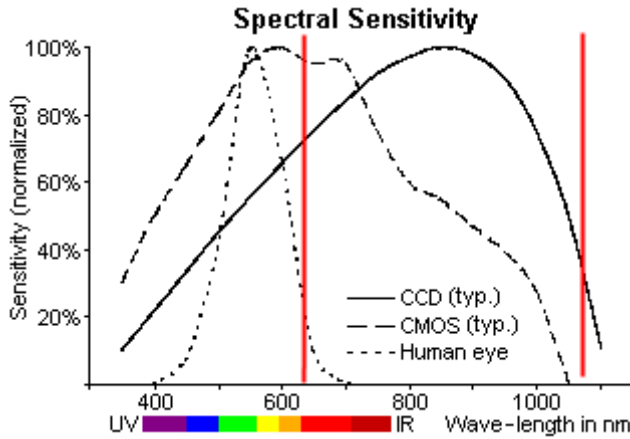


Fig. 1. Spectral response for CCD, CMOS and human eye with laser wavelength (1075 nm) and wavelength for measured camera response (633 nm). [6]

The final choice of product fell on Laser Beam Analyser SP620 U from Ophir-Spiricon, as it was the camera identified in the search with best spatial resolution and highest dynamic range. The camera does not fulfil the requirements for spatial resolution given. This demand is disregarded, as choice has been made on the best available technique and camera which were identified. Also it is considered to be important not to introduce lenses in the beam path to enlarge the beam. This has been important for avoiding further aberrations in the beam. The 1.7  $\mu\text{m}$  resolution demand originates from the necessary resolution with a 200 mm focus lens. Using a 500 mm lens the demand is met.

The SP620 U camera comes with beam analysis software, BeamGage, with functions to correct for average background noise, diameter calculations etc.

|                                       |   |
|---------------------------------------|---|
| Spectral Response                     | 190 - 1100nm                            |
| Maximum beam size                     | 7.1mm x 5.4mm                           |
| Pixel spacing                         | 4.40 $\mu\text{m}$ x 4.40 $\mu\text{m}$ |
| Number of effective pixel             | 1600 x 1200                             |
| Frame rate                            | 7.5 fps @ full resolution               |
| Camera dynamic range                  | 62 dB                                   |
| Saturation intensity <sup>1</sup>     | 2.2 $\mu\text{W}/\text{cm}^2$           |
| Lowest measurable signal <sup>1</sup> | 2.5 nW/cm <sup>2</sup>                  |
| Damage threshold                      | 0.15 W/ cm <sup>2</sup>                 |
| Image depth                           | 12 bit                                  |

<sup>1</sup> @632.8nm wavelength

Table 3. Data for the SP620 camera [5]

The chip in the camera is a silicon based CCD chip. The response for a CCD chip is shown in fig. 3. The two red lines indicate the laser wavelength (1075 nm) and the wavelength, for which Ophir-Spiricon has given the saturation and lowest measurable signal (633nm). From the curve it can be seen, that the expected signal for a laser with 1075 nm wavelength is about half of the signal at 633 nm. This means that the lowest measurable signal and saturation is about twice as high as given in table 3.

Transferring the 12 bit A/D conversion gives 72 dB. The spec is however 62 dB. This is due to some natural noise on the chip and in the digitizer. To keep the signal to noise ratio during measurements high, the noise must be kept low. To do this the gain should be kept low, and no light from surroundings must enter the camera.

The beam needs to be attenuated before entering the camera. To do this a series of beamsplitters and ND-filters are introduced in the beam path. In fig. 2 the unwrapped beam path is shown in one plane.

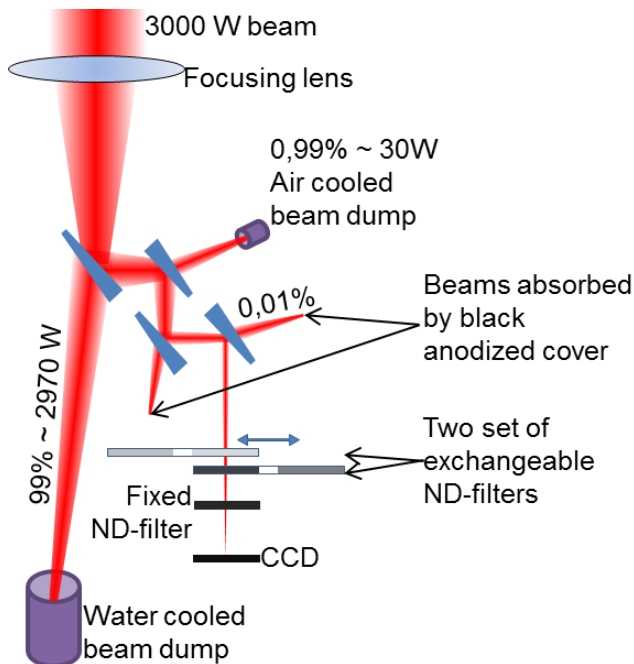


Fig. 2. Sketch of unwrapped beam path. The 4 blue wedges are wedge shaped beamsplitters.

The beam splitters are wedge shaped, and the rear side are AR-coated. The wedge shape further result in that the transmissive part of the beam is bent a little as shown on fig. 2 and 3.

The beam dump is placed far away from the beam splitters and camera to allow the beam to expand again before being absorbed, so the intensity is reduced to below the damage threshold. As beams with focal length up to 780 mm are to be analysed with the system a large distance from camera to beam dump is needed.

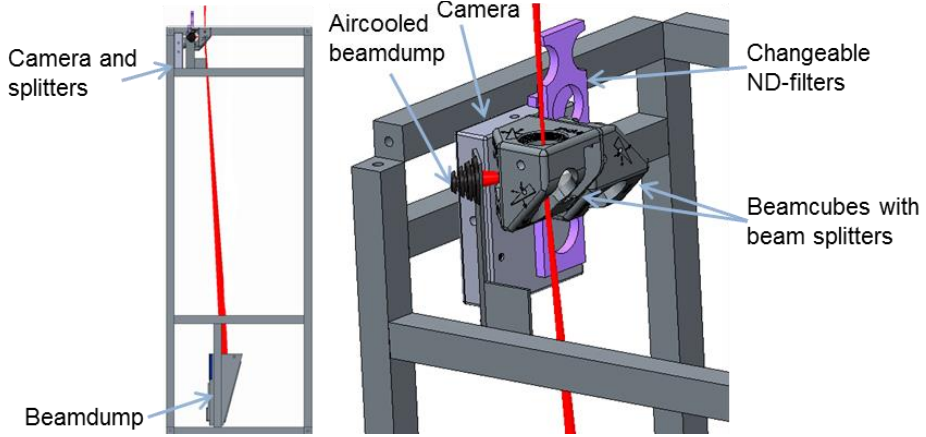


Fig. 3. CAD-model of the constructed setup shown with no cover plates.

To attenuate the maximum intensity from the laser beam to “saturation intensity”, a set of beam splitters and ND-filters is applied. For minimising problems with alignment two beam cubes from Ophir Spiricon is used. These are manufactured to align the beam splitters wedges with only little work and no need for adjustment off each splitter and align with the camera entrance. This gives four beam splitters before the beam passes the ND-filters.

At the setup at Aalborg University two different focussing heads is applied, both with a collimating focal length of 200 mm and each with two different focussing modules ranging from 200 to 780 mm focal length. This gives focus spot sizes from 34 to 134  $\mu\text{m}$  when applying the focussing heads without DOE's, and center intensities as given in Table 4, when applying the full 3 kW. Since the full power is not allowed to enter the chip, attenuation is needed. This is given as ND-values and is calculated from eq. 1

$$\text{ND} = -\log_{10}(T) \quad \text{eq. 1}$$

T is the percentage of the beam, which continues towards the chip.

| <b>Focal length</b> | <b>D<sub>min</sub></b> | <b>Z<sub>R</sub></b> | <b>I, center<sup>1</sup></b> | <b>Round beam 3 kW</b> | <b>Round beam 30 W</b> | <b>Beam pattern 30 W</b> |
|---------------------|------------------------|----------------------|------------------------------|------------------------|------------------------|--------------------------|
| mm                  | μm                     | mm                   | MW/cm <sup>2</sup>           | ND-value               | ND-value               | ND-value                 |
| 200                 | 34                     | 0.71                 | 6.6                          | 15.3                   | 13.3                   | 11.5                     |
| 300                 | 51                     | 1.6                  | 2.9                          | 15.0                   | 13.0                   | 11.2                     |
| 470                 | 80                     | 3.9                  | 1.2                          | 14.6                   | 12.6                   | 10.8                     |
| 780                 | 133                    | 10.8                 | 0.43                         | 14.2                   | 12.2                   | 10.4                     |

<sup>1</sup>The center intensity for a Gaussian beam is two times as high as the average intensity

Table 4. Data for beam to camera system and required attenuation.

In table 4 is also given the minimum spot diameter in focus when the focussing heads are applied without DOE's, D<sub>min</sub> and the Rayleigh length, Z<sub>R</sub>. The different focal lengths give a need for different ND-values. The intensity in focus also depends if a pattern is generated or not, and at which power level the laser is set. Only the extremes are shown in table 4. These gives that the attenuation should be changeable from ND 10.4 to ND 15.3, giving a ratio of  $97.344 = 99.7$  dB. This dynamic is built into the system by fixed beamsplitters and changeable ND-filters. Values are given in table 5.

The minimum diameter and Rayleigh length are calculated from eq. 2 and 3

$$D_{min} = \frac{4\lambda M^2 f}{\pi D_0} \quad eq. 2$$

$$Z_R = \frac{D_{min}^2 \pi}{4\lambda M^2} \quad eq. 3$$

f is the focal length, M<sup>2</sup> is the beam quality factor, D<sub>0</sub> is the collimated beam diameter on the focusing lens and λ is the wavelength.

| <b>ND-value Options</b> |  |
|-------------------------|--|
| Splitter 1              | 2 Fixed  |
| Splitter 2              | 2 Fixed  |
| Splitter 3              | 2 Fixed  |
| Splitter 4              | 2 Fixed  |
| Variable ND-filter      | 0 to 3.9 0 – 0.4 – 0.8 – 1.0 – 2.0 – 3.0 – 3.9 |
| Variable ND-filter      | 0 to 3.9 0 – 0.4 – 0.8 – 1.0 – 2.0 – 3.0 – 3.9 |
| <b>Sum</b>              | <b>8 to 15.8</b>                               |

Table 5. Realised damping of beam and selectable options of ND-filters

#### 4. Tests

To test the system a HighYag BIMO focussing head is applied, and the beam is directed through the attenuation system to the camera where images are recorded and stored.

Two types of tests were performed: Beam caustics at different power levels and evaluation of patterns created by DOE's.

#### 4.1 Measurements of beam patterns

When producing beam patterns with DOE's there will often be some scattered light. Results and measurements from one DOE are shown in fig. 4. Image is only evaluated within a certain area of the CCD. This area is set so that areas which contain scattered light and beam pattern is included, but areas which cannot be distinguished from the background noise is excluded. Further a process zone is defined. This is light, which is not in the pattern, but still is in the area which will be melted or removed during cutting or welding. This is chosen because this light will still be absorbed in the process zone.

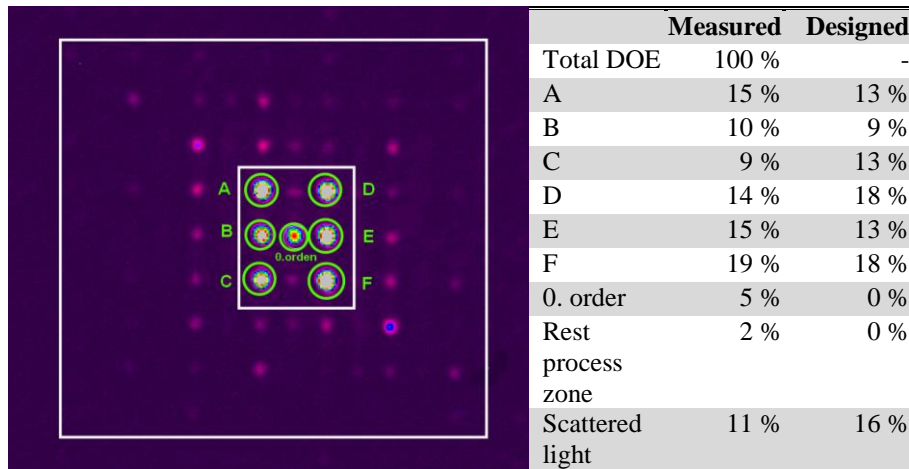


Fig. 4. Image and results from a measurement of a beam splitting DOE.

As seen on figure 4 and the corresponding table the evaluation of patterns produced by DOE's can be performed. The results do also show some difference of design compared to measurements. This gives feedback to the manufacturing and designing process.

## 4.2 Measurements of beam caustics

Two sets of measurements are shown in fig. 4. The corresponding caustics calculations are shown in fig. 5.

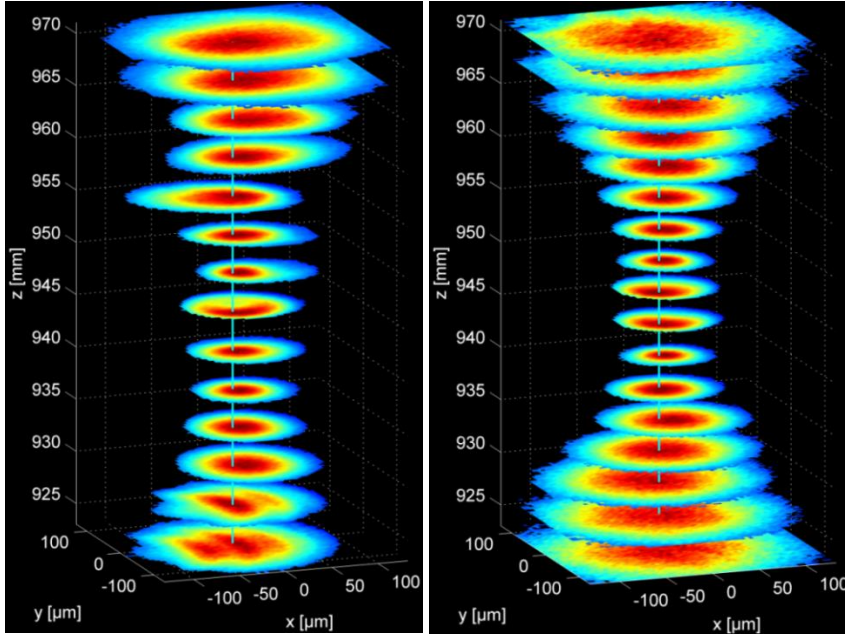


Fig. 5. Left: Profile with 1.3 kW. Right profile done with 60 W. Both with 780 mm focal length  $\Delta Z = 3$  mm between each image.

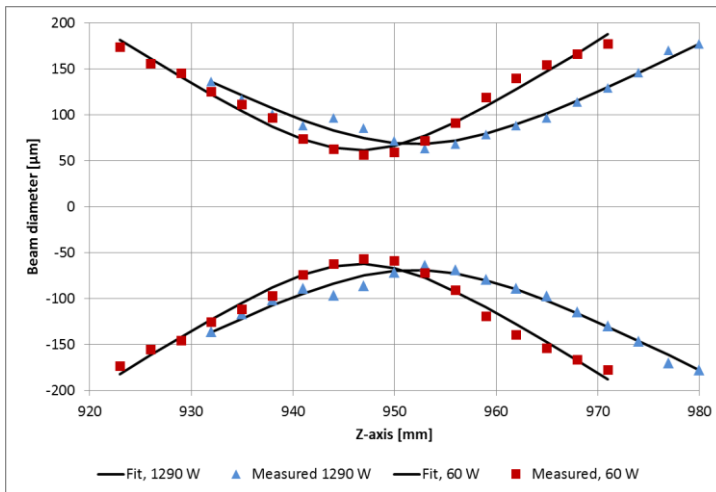


Fig. 6. Caustic for fig. 4. Diameter measurements according to ISO 13694. [8]



From fig 6 some difference between focus position and focus diameter are observed.

### 4.3 Comparisons

The diameter measurements in fig 6 have been fitted using eq. 4 [7] by least square method. This gives information on the focus position, focus diameter and the beam quality factor.

To evaluate the goodness of the coefficient of determination –  $R^2$ , is calculated

$$D(z) = D_{min} \sqrt{1 + \left( 4M^2 \lambda \frac{z_{focus} - z}{\pi D_{min}^2} \right)^2} \quad eq. 4.$$

Least square method is used instead of ISO 13694, despite ISO 13694 recommends not to give equal weight to central region and wings of caustic. [8] The purpose is here just to compare the two measurements with 780 mm focus lens, and evaluate the measurement system and stability.

In connection to the acceptance test of the laser source a set of beam measurements where performed with a different HighYag BIMO focussing head, using a Primes FocusSpotMonitor at different power levels. These measurements are shown on fig. 6.

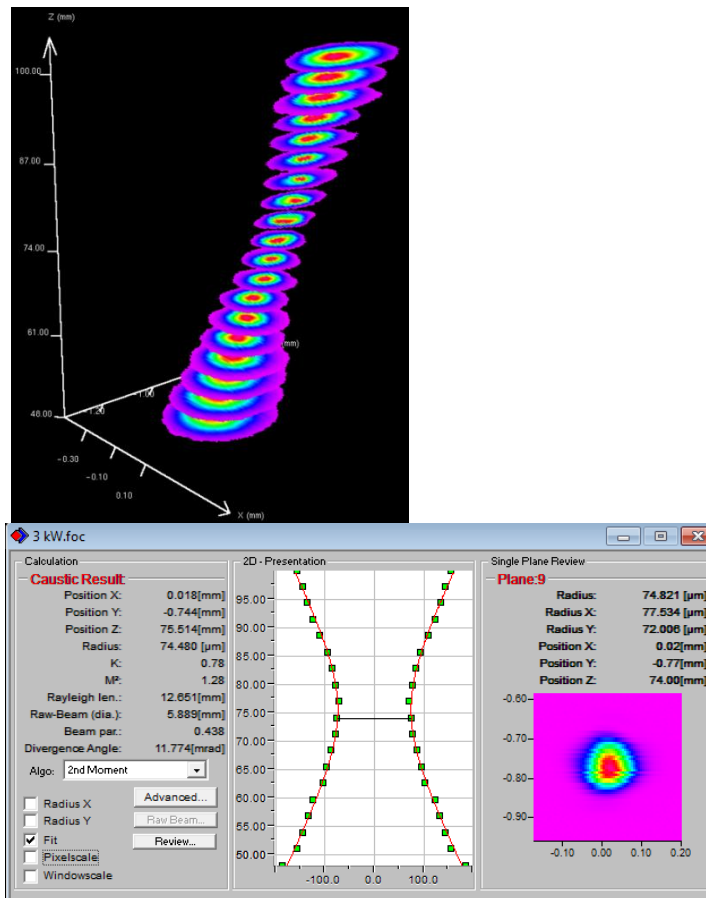


Fig. 6. Profile done with Primes FocusSpotMonitor with F500 and 3 kW. Screen dumps from Primes measurement software.

In table 6 results from the fit of eq. 4 to the measurements in fig. 6, and caustic with f300 (Optoscand focusing system) combined with the acceptance test measurements done with Primes FocusSpotMonitor are collected.

| Measurement system           |               | SP620 | SP620 | SP620 | Primes | Primes |
|------------------------------|---------------|-------|-------|-------|--------|--------|
| Focussing head magnification |               | 3.9   | 3.9   | 1.5   | 4.2    | 4.2    |
| Laser power                  | W             | 60    | 1.290 | 550   | 1.000  | 3.000  |
| Beam quality factor. $M^2$   |               | 1.32  | 1.18  | 1.35  | 1.3    | 1.28   |
| $D_{\text{focus}}$           | $\mu\text{m}$ | 124   | 137   | 53    | 138    | 150    |
| Relative focus difference    | mm            |       | +5.5  | -     |        | +0.8   |
| $R^2$                        |               | 0.97  | 0.97  | 0.99  | -      | -      |

*Table 6. Results from the two caustic measurements*

As can be seen there is two very different focus positions and focus diameters for the two measurements done with the 780 mm lens (magnification 3.9). This is most likely due to some thermal drift of either the optical head or the measurement system. It has not been possible to distinguish, whether this is coming from the optics in the camera or from the optics in the head itself.

Measurements done with the Primes FocusSpotMonitor and a different optical head do also give a little difference in the focus diameter and focus position. The Primes FocusSpotMonitor cannot have any thermal drift in the measurement system due to the way it is constructed, so here the difference must originate from either the laser or the processing head. The processing head is unfortunately not the same, so no conclusion can be made from this.

The measurement of  $M^2$  gives values which all are close to each other, and close to the value promised by laser manufacturer. The  $M^2 = 1.18$  differs slightly, but is within what could be expected.

The acceptance test where done with a different laser head, with different focal and collimation lenses. The magnification is however almost the same. Therefore the focus diameter should also be close to each other, which table 6 also show.

The focus diameter,  $M^2$  and focus position should be independent of power. This does however not seems to be true for the measurements. Further there is a change in the focus position from low to high power. This might be due to thermal drift in the laser head, or the measuring system. However the Primes FocusSpotMonitor cannot have any thermal drift due to way it performs the measurement with no optics.

## 6. Future work

To examine how much of the thermal drift that originates from the laser head and how much coming from the measurement system there is planned a set of measurements. In these measurements the beam is left on with high power for a long period away from the camera system and then quickly moved onto the camera. This shall be compared to experiments, where the beam is on for a long period directly on the camera. In this way it should be possible to isolate long term thermal drift from the laser head and the measurement system.

Also the calculations of beam parameters by curve fitting are planned to be done with a closer link to ISO 13694. This requires an update of the algorithms used.

## 7. Conclusion

The ability to measure scattered light and evaluate DOE's has been demonstrated.

The spatial resolution of the system are sufficient for most cases, only evaluation of focused beams with magnification of less than 2.5 is a problem according to the ISO-standard. Smallest magnification available is 1.0. In this case the beam will only fill 8 pixel in any direction. Measurements can still be performed so operator can verify if the beam looks reasonable, just not according to standard.

The chosen CCD based camera from Ophir Spiricon was the best camera identified on the market with a high dynamic range without introducing possible aberrations and alignment problems from lenses.

Even though the demand for 20 pixels in any direction from ISO 13694 is not met for magnifications below 2.5 the system can be used to quick information on the produced pattern. If measurements in accordance to the standard are needed, then a switch to longer focal length or shorter collimation length is needed.

Further work is necessary to evaluate if the system suffers from thermal drift. It has so far not been possible to decide whether this drift comes from the measurement system or the laser head.

## 8. References

- [1] Olsen, F.O.; Hansen, K.S. and Nielsen J.S.:  
**Multibeam fiber laser cutting**, Journal of Laser Application 2009, vol 21.Issue 3, p. 133-138. ISSN 1042-346X (2009)
- [2] Hansen, K.S.: Project description of industrial Ph.D. project: Multi fiber laser welding technology.
- [3] Brian, M. Victor, B.S.:  
**Custom beam shaping for high-power fiber laser welding**, Master thesis, Graduate School of The Ohio State University (2009)
- [4] Primes online **Product catalogue** accessed 14<sup>th</sup> April 2013
- [5] Ophir-Spiricon **manual for SP620 U**
- [6] Preiss, Walter:  
**Sensor techniques** <http://www.fen-net.de/walter.preiss/e/slomoinf.html>, accessed 15<sup>th</sup> May 2013 (2012) (Skiftet)
- [7] Steen, W.M., Mazunder, J.:  
**Laser Material Processing**, Springer, 4<sup>th</sup> edition, ISBN 1849960615 (2010)
- [8] ISO 13694:2000  
“**Optics and optical instruments — Lasers and laser-related equipment — Test methods for laser beam power (energy) density distribution**”
- [9] ISO 11146 :2005  
“**Lasers and laser-related equipment — Test methods for laser beam widths, divergence angles and beam propagation ratios**”
- [10] Gentec **product catalogue 2011**, 2011
- [11] Ophir-Spiricon online **product catalogue** accessed. 3<sup>rd</sup> January 2011
- [12] Dickey, F.M., Holswade, S.C.:  
**Laser Beam Shaping Theory and Techniques**, Marcel Dekker., ISBN: 0824703987 (2000)
- [13] ISO Standard 11554:2008  
“**Optics and photonics – Lasers and laser-related equipment – Test methods for laser beam power, energy and temporal characteristics.**”

## **APPENDIX B: BEAM SHAPING TO CONTROL OF WELDPPOOL SIZE IN WIDTH AND DEPTH**

Published: 2014

Conference: 8th International Conference on Laser Assisted Net Shape  
Engineering LANE 2014

Published by: Physics Procedia 56 ( 2014 ) 467 – 476

ISSN: 1875-3892

Edited by: M. Schmidt, F. Vollertsen and M. Merklein

DOI: [http://dx.doi.org/10.1016/S1875-3892\(14\)00349-6](http://dx.doi.org/10.1016/S1875-3892(14)00349-6)

8<sup>th</sup> International Conference on Photonic Technologies LANE 2014

## Beam shaping to control of weldpool size in width and depth

K.S. Hansen<sup>a</sup>, M. Kristiansen<sup>b</sup>, F.O. Olsen<sup>a</sup>

<sup>a</sup>*IPU Technology Development, Produktionstorvet 425, 2800 Kgs. Lyngby, Denmark*

<sup>b</sup>*Department of Mechanical and Manufacturing Engineering, Aalborg University, Fibigerstræde 16, 9220 Aalborg, Denmark*

### Abstract

---

The introduction of high power single mode fiber lasers has given deeper and narrower laser welds than seen previously. In some cases the weld becomes too narrow and must be expanded to fit the geometrical shape of a given weld task. It was suggested that instead of using only one beam, the beam was split into multiple beams placed in a pre-specified pattern. In this way the dimensions of the weld pool could be controlled. This gave the ability to control the final weld face width and penetration depth independently of each other with minimum heat input.

Practical implementation of splitting a beam into a beam pattern with a diffractive optical element (DOE) is presented with results on splitting a beam from a single mode fiber laser into either three or seven individual beams on a row. Basic design rules for controlling the weld pool dimensions are developed. Results show that it is possible to control weldpool in size.

© 2014 The Authors. Published by Elsevier B.V.

Selection and blind-review under responsibility of the Bayerisches Laserzentrum GmbH.

**Keywords:** Beamshaping; laser welding; diffractive optical element (DOE); weld geometry.

---

### 1. Introduction – motivation

Traditional laser welding is performed with a single beam. This creates a single keyhole, where the resulting welding face width and penetration depth is controlled by the geometry of the keyhole. The geometry of the keyhole is a function of the process parameters.

In this paper a new method for applying a specific weld face width and penetration depth is suggested and demonstrated. A single mode fiber laser was used with a diffractive optical element (DOE). The DOE was inserted just above the lens and transforms the beam into several beams on a line perpendicular to the welding direction in the focus area. In this way the face width could be chosen by designing the DOE to split the (main) beam into a specific number of sub-beams. The penetration depth can be adjusted by the laser power and travel speed, as in traditional keyhole welding, for specific combinations of focus adjustment and lens configurations. [11] [9] [10]

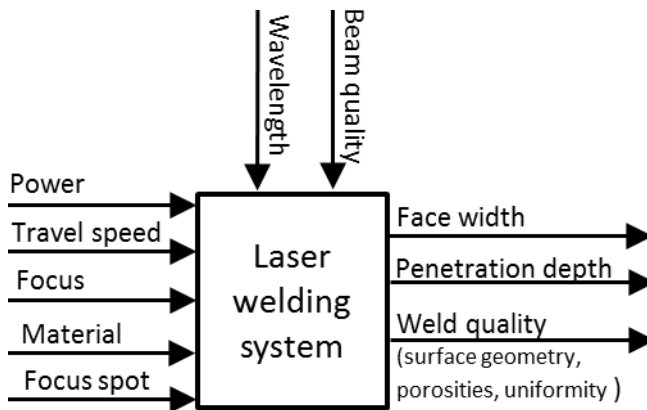


Figure 1 Laser welding system. Horizontal input variables, vertical fixed input parameters and process output parameters.

In figure 1 the most relevant parameters for designing a weld to a specific face width and penetration depth are shown.

In general, laser welding produces deep and narrow welds, and is often chosen as production method when deep narrow welds are needed. However, if a wider weld is required, it can be difficult to realise it with lasers. First, the keyhole has to be increased. This can be realised by a larger beam diameter. However, when increasing the diameter, the intensity drops. When the intensity gets low enough, the keyhole is no longer formed, and the welding then changes from a keyhole welding to a laser surface conductive welding. The differences are sketched in figure 2a and 2b.

A laser conductive welding does not have the ability to allocate the energy in a nearly line down through the material. Instead the energy is absorbed on the surface of the material. It is therefore difficult to transport the energy deep into the material, or to penetrate more than the top sheet which is needed in overlap joints. Overlap joints are therefore difficult to perform as laser surface conductive welding, since no keyhole is formed.



In figure 2a and 2b the difference in melt pool for overlap joints and a double butt joint with different beam diameter is sketched. The double butt joint can be difficult to realise, as the demands for alignment increases, so the heat input should be limited. In this case it could be an advantage with two small keyholes placed in the interface instead.

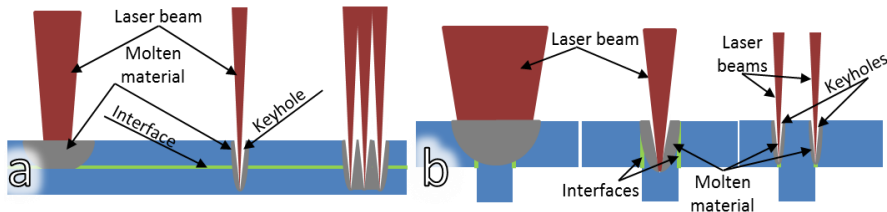


Figure 2 Difference between laser surface conductive welding (wide beam), laser keyhole welding with one beam (single narrow beam) and multiple simultaneous beams (multiple narrow beams): a) for overlap joints, b) for double butt joints.

Several researches have focused on improving laser welding techniques and to expand the process window in laser material processing. Some of the applied techniques include oscillation of the beam in the keyhole for larger gap tolerances or to lower the cooling rate in welding of duplex steel [15], applying more than one laser beam in the same weld pool [13] [17], pulse shaping [12], beam shaping to smoothen out the edge on the top of the weld [14] and crack free welds [16].

The role of focus ability has been examined to see if there is an “optimum beam” for a specific material regarding intensity and welding depth [20] [19]. Also focus shift and its effects have been studied to see how a beam and the resulting weld are affected over time on real welding installations [18].

Welding with single mode fiber lasers has been demonstrated by several researchers [11] [9] [10] with penetration depth up to several millimetres and narrow deep welds. In most cases focus is on narrowing down the total welding width, which in some real cases can be unpractical as showed in figure 2b. If the vertical plate is more than just a half millimetre thick, it becomes difficult to create a wide enough melt pool by keyhole welding with a single beam.

A new approach for designing weld geometries has been proposed. By applying more beams in the same melt pool it was expected that the face width and penetration depth could be controlled, as sketched in figure 2b. A series of experiments with multiple beams were performed to verify this hypothesis.

### 1.1. Laser development

For many years laser welding has been dominated by the Nd:YAG laser. This has been faced with competition from the multimode fiber or disc laser. The new lasers

has a better beam quality and is typically also cheaper, has less maintenance and can be scaled to higher powers [19]. In recent years the single mode fiber laser has entered the market. The single mode fiber laser has a nearly perfect beam quality. [18] This high quality beam allows for narrow and deep welds [11] [9]. These narrow beams gives the option to place multiple beams next to each other without making the overall weld width wider than a weld produced by a multimode fiber or YAG laser.

## **1.2. Beam shaping techniques**

To produce multiple single mode laser beams focused close to each other there are several strategies. Multiple lasers could be used and focused through the same lens, or it could be one laser where the beam is split and each beam again placed close to each other and focused through the same lens. The third option is to reshape the wavefront.

To change the form of electromagnetic radiation, which essentially is what a laser beam is, it is necessary to change the wavefront of the beam. A traditional lens is changing the wavefront of the beam in a rotational symmetrical way. Instead of using rotational symmetric elements the lens can be changed to a free form surface. In this way distortions and more free formed patterns can be created. Production of free form lenses is, however, a complicated and expensive process. Since the beam still needs to be focused to a small area, the effect of the lens is necessary.

It is also possible to reshape the wavefront by making local changes in a substrate, where the wave front is delayed with up to one wavelength. In this way it is possible to make complicated patterns of the resulting beam. This is referred to as a diffractive optical element – a DOE. The individual beams can furthermore be tailored with an individual power level by proper DOE design.

It is even possible to overlay the effect of the lens in the DOE. In these experiments the focussing effect is excluded from the DOE design. This makes it possible to do experiments with different focal lengths by only changing the lens, thus reducing the demand for different costly DOE's.

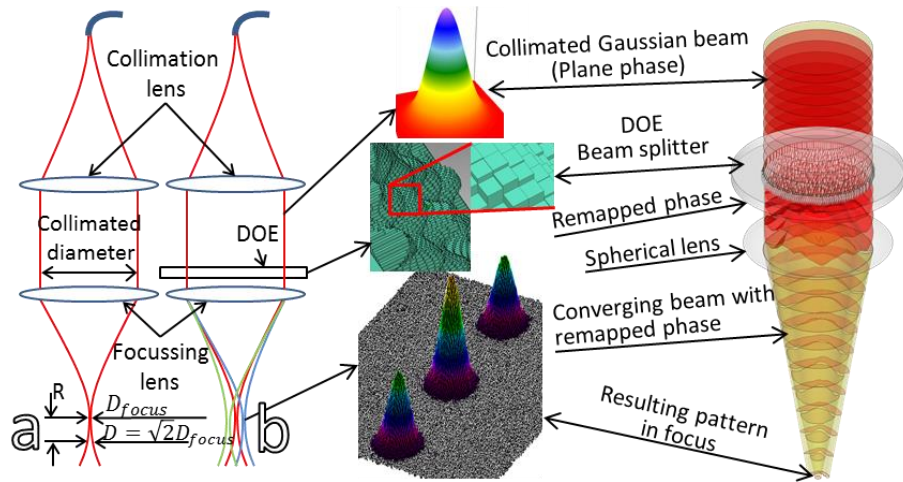


Figure 3 Focussing of a traditional laser beam with fiber transmission: a) with basic definitions, where  $R$  indicates the Rayleigh length, b) with a DOE, which splits the beam into three beams Indicated by green, red and blue colours.

In figure 4 a summation of beam shaping techniques is shown, where the beam is changed from its natural round form to more complicated geometries.

The aim of this work is to control the weld pool size by applying multiple keyholes in a pattern. It was therefore chosen to use the beam splitting design strategy. It is also in this strategy that the highest conversion efficiencies for DOE's are generally found together with robustness against alignment errors of the DOE in the optical path.

|   | Advantage   | Disadvantage   | Pattern types possible   | Depth of field                                    | Transformation efficiency | Alignment tolerances  |
|---|---|--|--|---|---------------------------|---|
| <b>DOE - Shapers</b><br>[8] [22]            | High transformation efficiency                                  | Difficult to get a good depth of field                     | Simple shapes, round, square, top hat                                | Medium to high (difficult)                        | High                      | High  |
| <b>DOE - Splitters</b><br>[8] [22]          | Automatic conserves nearly same depth of field as original beam | Can only do copies of input beam                           | Repeats of beam in pattern   | Nearly the same as input beam                     | High                      | Low   |
| <b>DOE - Diffusers</b><br>[8] [22]          | Complex patterns  | Zero order beam in middle of pattern, speckles in pattern  | Arbitrary shapes, like logos etc.                                    | Low   | Medium-High               | Low   |
| <b>Beam splitting of a single laser</b> [4] | For two beams it is simple                                      | Complicated to do more than two beams                      | Two beams in arbitrary positions                                     | Same as input beam                                | Nearly 100 %              | Unit built into laser head, and it is typically easy to change distance |
| <b>Multiple lasers</b> [6]                  | Power can be changed freely between spots                       | Expensive, loss of beam quality in complex delivery fibers | Dots in same pattern as fiber bundle arrives to collimator           | Same as input beam                                | 100 %                     | None - built into collimator  |
| <b>Field mappers</b><br>[7] [8]             | Industrial unit ready to integrate                              | Limited transformation possibilities                       | Top hat and line profiles, inverse gauss and other simple geometrics | Depends on size of pattern compared to input beam | Nearly 100 %              | Low   |

Figure 4 Beam shaping options

## 2. Experiments

Experiments were performed with an optical setup as sketched in figure 3a and 3b. First reference experiments were performed with a single round beam as sketched to the left in figure 3a. Later a DOE were introduced before the focusing lens which was designed to split the beam into sub-beams on a line transverse to the welding direction. Two different DOE designs were tested.

The welding were performed using three different single mode fiber lasers. Parameters and details are listed in figure 5.

|                                 |                   | IPG YLR-400-SM           | IPG YLS-3000-SM          |
|---------------------------------|-------------------|--------------------------|--------------------------|
| Power levels                    | [W]               | 100 - 400                | 100 - 3.000              |
| Beam quality, $M^2$             |                   | 1.05                     | 1.25                     |
| Collimated diameter             | [mm]              | 12.5                     | 9.6                      |
| Focal length,<br>focussing      | [mm]              | 200, 331, 552            | 780                      |
| Travel speeds                   | [mm/s]            | 5 - 150                  | 5 - 150                  |
| Fiber core diameter             | [ $\mu\text{m}$ ] | 20                       | 37                       |
| $D_{\text{focus}}$ , calculated | [ $\mu\text{m}$ ] | 23, 40, 63               | 139                      |
| Gas                             |                   | Nitrogen, Argon, Mison18 | Nitrogen, Argon, Mison18 |

*Figure 5 Lasers and parameters*

Initial reference experiments were performed with maximum 400 W using IPG YLR-400-SM laser. To have enough power in each beam when it was split, experiments were also performed with an IPG YLS-3000-SM laser with maximum power of 3 kW. Not all combinations of power, focus, travel speed and lenses have been performed. The experimental strategy was to determine the influence of the input variables on the resulting welding geometry (and quality) by adjusting parameters on achieved results.

Experiments were performed as bead-on-plate experiments on two different materials: Mild steel (EN DC01) and Stainless Steel (EN 1.4301).

In all cases the laser head was held steady perpendicular to the plate performing upside down welds and the plate was moved linearly. Shielding gas was delivered perpendicularly to the welding either through a large flat nozzle approximately 40 mm from the welding process, or by a coaxial nozzle with a diameter of 10 mm approximately 13 mm from the welding process. Gas flow where kept at 20-25 l/min.

## 2.1. Reference experiments

The goals of the experiments were to establish a reference database to make best designs of DOE's to build up design rules for future pattern design. Therefore, the following research questions are to be answered:

- When is a keyhole formed?
- What is the weld geometry made with a single beam?
  - What is the effect of travel speed?

- What is the effect of power?
- What is the effect of focus position?
- What is the effect of spot size?

To evaluate the penetration depths and face widths, polished and etched cross-sections were produced of each weld, and measured with an optical microscope.

From the polished cross-section the penetration depth, face width and middle width were measured. In figure 6a a typical keyhole weld is seen, and in figure 6c a typical surface conduction weld. Figure 6b shows a weld which has formed a small keyhole penetration in the middle resulting in a small bulge downwards, but mostly just is a surface conductive welding.

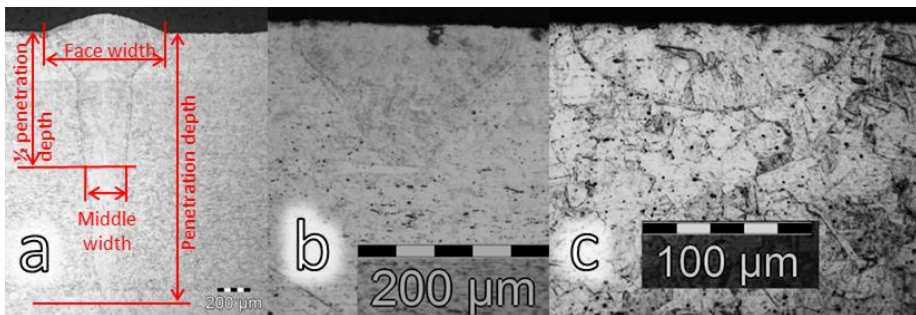


Figure 6 a) A classic keyhole welding. b) A weld which has just started to form a deep keyhole in the middle. c) A surface conductive welding performed with  $\varnothing 23 \mu\text{m}$  spot 1 mm from ideal focus position.

During examination in microscope welding defects like porosities, hot cracking etc. were noted if seen.

## 2.2. Experiments with beam patterns

The aim of the experiments with beam patterns was:

- To control the weld profile by applying a number of single beams on a line transverse to the welding direction.
- To establish design rules with respect to beam spacing and power distribution for pattern designs.

By placing a number of beams on a line, it was the goal to form a common melt pool which would have several keyholes, and in this way control both the welding face width and penetration depth, as an almost cross square section. To do this two DOE's were designed which spitted the beam into three and seven individual keyholes.

Experiments were made in the same way as for single beams, with the difference that the DOE is introduced in the collimated beam before the lens as shown in figure 3b.

After evaluation of the bead on plate experiments welding experiments were performed on a double but joint as showed in figure 2b.

### 2.3. Pattern designs

Spacing of the beams was calculated as the middle width of a single keyhole welding plus additional 20%. The 20% is added since the cooling effects to the sides are expected to be lower, because there is a neighbouring beam that heats the material on each side. The edge beams were set to be 50 % more intense than the centre beams, to take the extra cooling towards the sides into account.

The total weld face width was expected to be close to the distances between the edge spots and two weld radii. The penetration depth was expected to be the same as for single welds with same lens and power.

Therefore the weld profile produced by a DOE was not expected to be significantly different from the ones of a series of single welds which were placed next to each other with the same distance as the DOE spaces the beams.

Both DOE's were produced with grayscale etching with a pixel size of 100  $\mu\text{m}$  and 250 pixels in each direction. The grey scale etching technique applied was causing errors due to manufacturing problems.

For the three spot DOE the distance was set at 200  $\mu\text{m}$  using the lens creating the 40  $\mu\text{m}$  spot. Both spacing between the spots and the individual spot sizes vary linearly with the focal length of the used focusing lens in the laser head.

The patterns produced by the DOE's were analysed using a CCD based beam analysing system with suitable beam splitters and filters in front of the CCD chip, with both low and high power [21].

For both DOE's the focus diameter were increased in both the transverse and longitudinal directions with respect to the welding direction. Transverse to the welding direction, it was nearly doubled. In the longitudinal direction it grew up to 70 % for the seven spot DOE and 10 % for the three spot DOE. This increase in spot and hereby keyhole size was not taken into account during the DOE design.

The introduction of the DOE also changed the focus position several millimetres. Testing with up to 1 kW and analysis using the CCD camera showed no significant thermal drift, caused by the DOE during the time in which a weld was performed.

The three spot DOE was designed with less intensity in the centre spot, but came out with more energy in the centre spot. The seven spot DOE almost ended as a six spot DOE, as the centre beam almost disappeared.

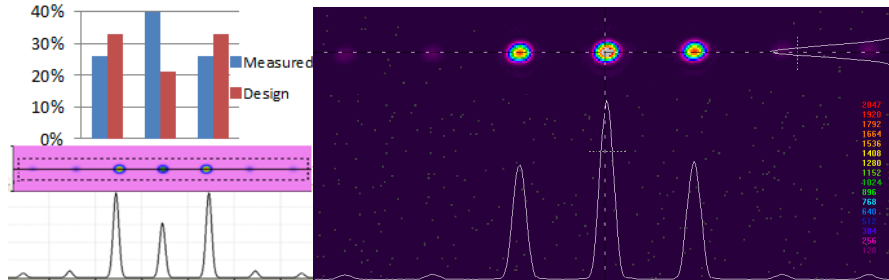


Figure 7 Bottom left: Pattern design. Top left: Energy distributions in design and measurement. Right: Measured profile from three spot DOE.

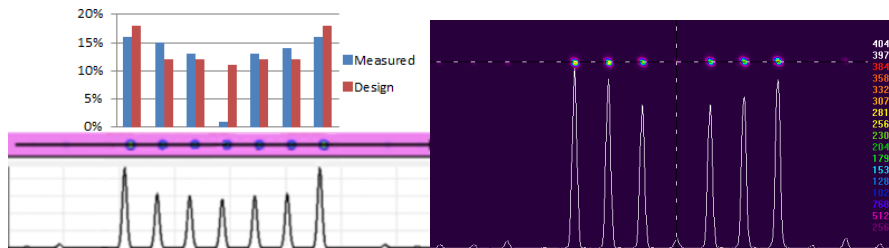


Figure 8 Bottom left: Pattern design. Top left: Energy distributions in design and measurement. Right: Measured profile from seven spot DOE.

In figure 7 and 8 simulation and measurement results from the two DOE's are shown. For the three spot DOE the measured scattered light outside the three spots was 8 %, which were less than the 13 % expected from the design. For the seven spot DOE the measured scattered light was 12 % and 5 % in the design.

During examination of the two DOE's it was found that they both were under-etched with approx. 15-20 %. To evaluate the effect of this, a simulation with an under etched DOE was performed. This gave results similar to those measured on the manufactured DOE's, with a higher intensity in the middle for the three spot DOE, and no energy in the middle for the seven spot DOE. Also most of the differences in scattered light could be explained from the under etching.

## 2.4. Results of reference experiments

By studying the polished cross sections it was found that the welds which only have formed a small bulge in the middle of the weld had a penetration depth/ face width ratio of minimum 0.5-0.7. The actual value depends on travel speed, focus spot, laser power and focus position.



In figure 9 the penetration depths for different travel speeds and laser powers for three of the different spot sizes are seen. There is a clear nonlinear change when going from 300 to 400 W for an  $\varnothing 63 \mu\text{m}$  spot, when going down in spot size the keyhole is formed at lower laser power. When looking at the polished cross sections for 300 W laser power, it was seen that the bulge on the bottom came at travel speeds from 50 mm/s and lower.

To create a keyhole with a single beam with  $\varnothing 23 \mu\text{m}$  spot, 100 W is enough even though the graph for  $\varnothing 23$  spot might indicate differently. For  $\varnothing 40$  spot 300 watt is needed to form a keyhole, and for the  $\varnothing 63$  spot more than 300 W is needed to form a keyhole.

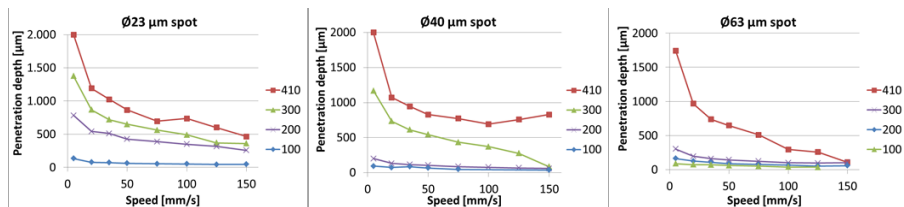


Figure 9 Comparison of penetration depth in stainless steel for different values of travel speed, laser power and spot size.

- Deepest penetrations were found when focus was placed between the surface and one Rayleigh length into the material. In general half a Rayleigh length into the material gave the deepest welds.
- The narrowest welds were found when focus is placed between 0.5 and 1 Rayleigh length into the material.
- In general, penetration depths were found to be 10 % deeper in stainless steel compared to mild steel.
- It were found that the shorter the focal length, the deeper the welds became with the same power.
- The middle widths at half penetration depth were found to be almost independent of power for keyhole welding.
- When focus was moved one Rayleigh length for welds were the power was only sufficient for forming a keyhole, the weld became a laser surface conduction weld instead. At higher powers this sensitivity to focus position became less. It did, however, still affect the penetration depth in all cases, when the focus was moved.
- Tests with different shielding gasses and no shielding gas were also performed. It was found that it is not important for the weld profile, only for surface oxidation. This has previously been reported for fiber laser welding. [22] [20]

## 2.5 Results of experiments with beam patterns

In figure 10 are shown cross sections from the experiments with the three spot DOE and 400 W laser power. With the  $\varnothing 40\mu\text{m}$  spot and travel speed of 50 mm/s this configuration produces rectangular welds.

Looking on the cross sections, we see in (a) and (b), that when the line energy is high and the penetration depth is over a certain depth, then the melt pools of the individual spots are totally integrated. When the line energy is small, we see in (c), that the three spots creates separate keyholes in the lower section of the weld.

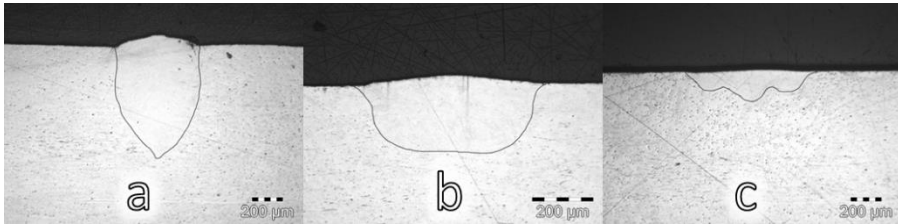


Figure 10 Welds with the three spot DOE, 50 mm/s travel speed, 400 W power and focus at the surface performed with three different lens configurations:.

a)  $\varnothing 23\mu\text{m}$  spot, b)  $\varnothing 40\mu\text{m}$  spot and c)  $\varnothing 63\mu\text{m}$  spot.

Penetration depths for the three spot DOE with 50 mm/s are shown on figure 11 together with the penetration depths for a single round beam. This shows that the penetration depth of the three spot DOE is a little higher than one third of the penetration depth of the single spot penetration for the similar beam diameter and laser power.

In figure 11 left is shown the typical appearance of the weld surface of a weld performed with the three spot DOE with parameter combinations where the three keyholes were creating one melt pool. It is seen that in such cases there were no visible topographical structures from the three spots.

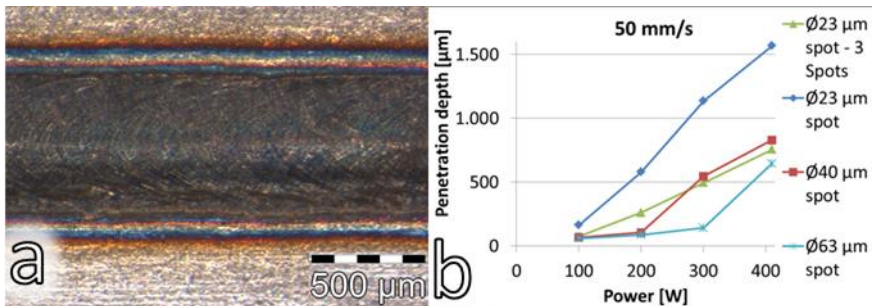
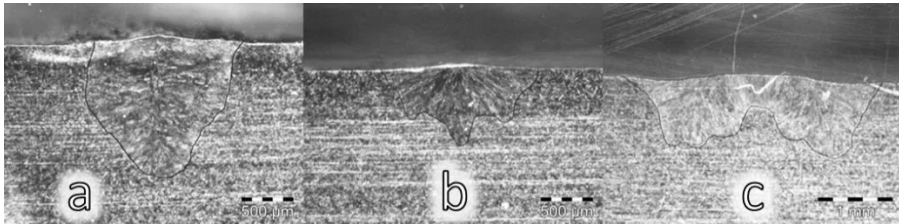


Figure 11 a) Surface of the weld with cross section seen in figure 10b.

b) Relation between power, penetration depth and focus spot size for the individual beams in the pattern for stainless steel and three spot DOE.

The power of the 400 W laser was not high enough to create keyhole welding with the seven spot DOE. Further experiments were therefore conducted with higher power on the 3 kW laser with both the three and seven spot DOE.

Figure 12 shows three cross sections of welds performed with the 3 kW laser and the 780 mm focal length. The obtained individual spot diameters of the DOE-patterns were here 139  $\mu\text{m}$ . The two examples of welding with the three spot DOE (Figure 12a and 12b) shows results of similar structure as in figure 10a and 10c: When the line energy is high (figure 12a), the penetration is over a certain depth, then the melt pools of the individual spots are totally integrated with a deep central region as result. When the line energy is smaller (figure 12b) the three spots creates separate keyholes in the lower section of the weld. Figures 12b and 12c show the the individual keyholes, which are reflecting the power distribution between the individual spots, see figures 7 and 8. The apperance of keyholes indicates that the line energy is not sufficiently high to create totally integrated melt pools.



*Figure 12 Cross sections of welds with 139 $\mu\text{m}$  spot performed; a) with three spot DOE, 800 W, 20 mm/s., b) with three spot DOE, 800 W, 50 mm/s. and c) with seven spot DOE, 50 mm/s, 1500 W.*

After evaluation of the bead-on-plate welds a few preliminary experiments were performed on a double butt joint geometry as showed in figure 2b.

For comparison bead on plate welds were performed with one laser beam, defocussed to obtain the same face width with the same travel speed as obtained with the three spot DOE. Cross sections of the two types of welds are shown in figure 13. These cross sections shows that for the same weld face width and travel speed, the penetration depth obtained applying the three spot DOE and 400 W was slightly larger than the penetration depth obtained when applying 1050 W with a single defocussed laser beam.

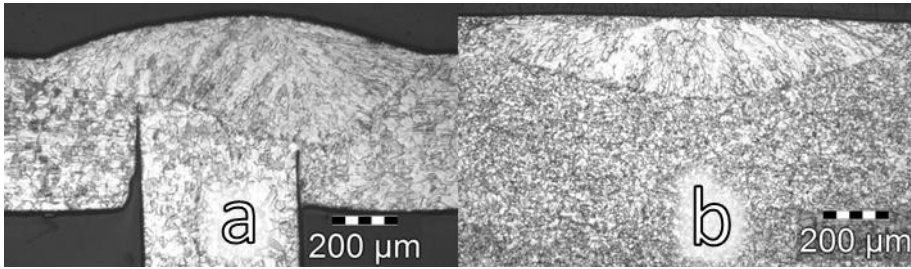


Figure 13 a) A weld performed with the three spot DOE as a double butt joint. Total power 400 W. and travel speed 50 mm/s.  
 b) Defocussed beam which produces nearly the same face width as the three spot DOE. Power 1050 W and travel speed 50 mm/s.

### 3. Discussion and outlook.

Looking on the results, it is important to define the distances between the individual beams in the beam pattern carefully. This can be affected by DOE-design and scaled by scaling the F# (where F# is focal ratio, being the focal length of the lens divided with the collimated beam diameter) for example by changing the focal length of the focussing optics.

In this study, the beams have been placed a little too close to each other on the three spot DOE when applying the low F#, i.e. the focussing systems with focal lengths of 200 mm, 331 mm and 552 mm. With focal length of 780 mm, creating 440 µm spacing the keyholes separate clearly. In this case, each of the spots grows to above 200 µm in the direction transverse to the welding direction.

It has not been possible to verify how much extra laser power is needed for the edge beams compared to the other beam spots to obtain rectangular weld seams. However when comparing the weld with the seven spot DOE it looks as if the 15 % difference in amount of laser power realized in the manufacturing is a reasonable starting point for design.

On the other hand the results with the three spot DOE and high line energy shows, that the thermal interaction in between the different keyholes increases, which results in deeper penetration in the centre and a fuzzy weld pool shape.

Besides shaping of the weld profile, the technique, where a pattern of high brightness beams is directed into the same melt pool, could be applied in a number of dissimilar applications such as:

- Improvement of surface quality – more hygienic welds
- Welding of duplex steel – control of cooling to ensure enough austenite is formed
- High speed welding – avoiding humping beads

- Welding of dissimilar materials – control of energy distribution to each material
- Robustness in welding – decreasing the effect from surface pollution and inaccuracies.
- Cladding – control of mixing

#### 4. Conclusion

This paper describes an experimental study of laser welding with single mode fiber lasers, applying two different line patterns of intense laser beams across the work pieces with small distances in between the individual beams to create one wider weld pool.

It has been shown that the face width and penetration depth can be controlled by applying a pattern of laser spots each forming a keyhole. It is shown that the process can be scaled to any desired welding width.

By applying a row of high intensity beams instead of one large defocussed or multimode laser beam, higher melting efficiency is obtained compared to welding of the same profile with a defocussed laser beam. This is resulting in lower overall laser power requirement with multi beam welding compared to welding with one larger laser beam.

For implementation in real applications it is important to produce a specific beam pattern design for the specific task and adapt the laser power and the travel speed, like in welding with a single round laser beam.

A set of design rules has been established from which penetration depth and face width can be deducted approximately and a basis for future work within has been established.

#### References

1. Steen, W.M., Mazunder, J.: Laser Material Processing, Springer, 4th edition, ISBN 1849960615 (2010)
2. Kristiansen, M. Selchau, J., Olsen, F.O., Hansen, K.S.: Quality and performance of laser cutting with a high power SM fiber laser, NoLamp14 (2013)
3. Petring, D., Schneider, F., Wolf, N., Nazery, V.: The relevance of brightness for high power laser cutting and welding, ICALEO2008 (2008)
4. OptoSkand product catalogue “Prealigned External Optics D50 1237”, Optoscand (2012)
5. ISO 11146-1 Lasers and laser-related equipment — Test methods for laser beam widths, divergence angles and beam propagation ratios (2005)
6. Demonstration at LWT of a Trumpf dual disc-laser system, okt 2013 ”Dansk-svensk lasermøde”.

7. Laskin, A., Laskin, V.: Controllable Beam Intensity Profile for the Tasks of Laser Material Processing, ICALEO2012, (2012)
8. Dickey, F.M., Holswade, S.C.: Laser beam shaping theory and techniques, Marcel Dekker, New York, ISBN: 0824703987 (2000)
9. Precision microwelding of thin metal foil with single-mode fiber laser
10. Vollertsen, F., Thomy, C.: Welding with fiber lasers from 200 to 17000 W, ICALEO2005 (2005)
11. Thomy, C., Seefeld, T., Wagner, F., Vollertsen, F.: Humping in welding with single-mode fiber lasers, ICALEO2006(2006)
12. Zhongjie, J., Katsuna, M., Xu, G.: Fiber laser welding of 780MPa high strength steel, ICALEO2006 (2006)
13. Tsubota, S., Ishide, T., Nayama, M.: Improvement of productivity and reliability of welding parts in heavy industry by laser welding process,
14. Brian, M., Victor, B.S.: Custom beam shaping for high-power fiber laser welding, Master thesis Ohio State University (2009)
15. Salminen, A., Westin, E., Lappalainen, E., Unt, A.: Effect of Gas Shielding and Heat Input on Autogenous Welding of Duplex Stainless Steel, ICALEO2012 (2012)
16. Ploshikhin, V., Prikhodovsky, A., Makhutin, M., Zoch, H.W., Heimerdinger, C., Palm, F.: Multi-beam welding: advanced technique for crack-free laser welding, Laser Assisted Net Shape Engineering 4, LANE2004 (2004)
17. Trautmann, A., Roeren, M., Zaeh, M.F.: Welding of extruded aluminium profiles by a hybrid bifocal laser system, Laser Assisted Net Shape Engineering 4, LANE2004 (2004)
18. Abt, F., Hess, A., Dausinger, F.: Focusing of high power single mode laser beams, ICALEO2007 (2007)
19. Verhaeghe, G., Hilton, P.: The effect of spot size and laser beam quality on welding performance when using high-power continuous wave solid-state lasers, ICALEO2005 (2005)
20. Weberpals, J., Dausinger, F., Göbel, G., Brenner, B.: The role of strong focusability on the welding process, ICALEO2006 (2006)
21. Hansen, K.S., Olsen, F.O., Kristiansen, M., Madsen, O.: Design of measurement equipment for high power laser beam shapes, NoLamp14 (2013)
22. Ream, S.: High-speed fiber laser welding for fuel cell components, ICALEO 2006 (2006) O'Shea, D.C., Suleski, T.J., Kathman, Alan, D., Prather, D.W.: Diffractive Optics design, fabrication, and test, SPIE PRESS (2004), ISBN-13: 9780819451712

# **APPENDIX C: JOINING OF MULTIPLE SHEETS IN A BUTT-JOINT CONFIGURATION USING SINGLE PASS LASER WELDING WITH MULTIPLE SPOTS**

Published: 3<sup>rd</sup> June 2015

Journal: Journal of Laser Applications

ISSN: N/A

Published by: Laser Institute of America,

DOI: <http://dx.doi.org/10.2351/1.4922222>

Copyright is not cleared, article is therefore not reprinted in this version.

# APPENDIX D: INLINE REPAIR OF BLOWOUTS DURING LASER WELDING

Published: Submitted

Journal: Welding in the World

ISSN: N/A

DOI: N/A

Copyright is not cleared, article is therefore not reprinted in this version.



## **APPENDIX E: MULTISPOT LASER WELDING TO IMPROVE PROCESS STABILITY**

Published: 2015

Conference: LiM 2015 – Lasers in Manufacturing

Venue: International Congress Center Munich, Germany As a part of the  
World of Photonics Congress 2015

Published by: WLT e.V.

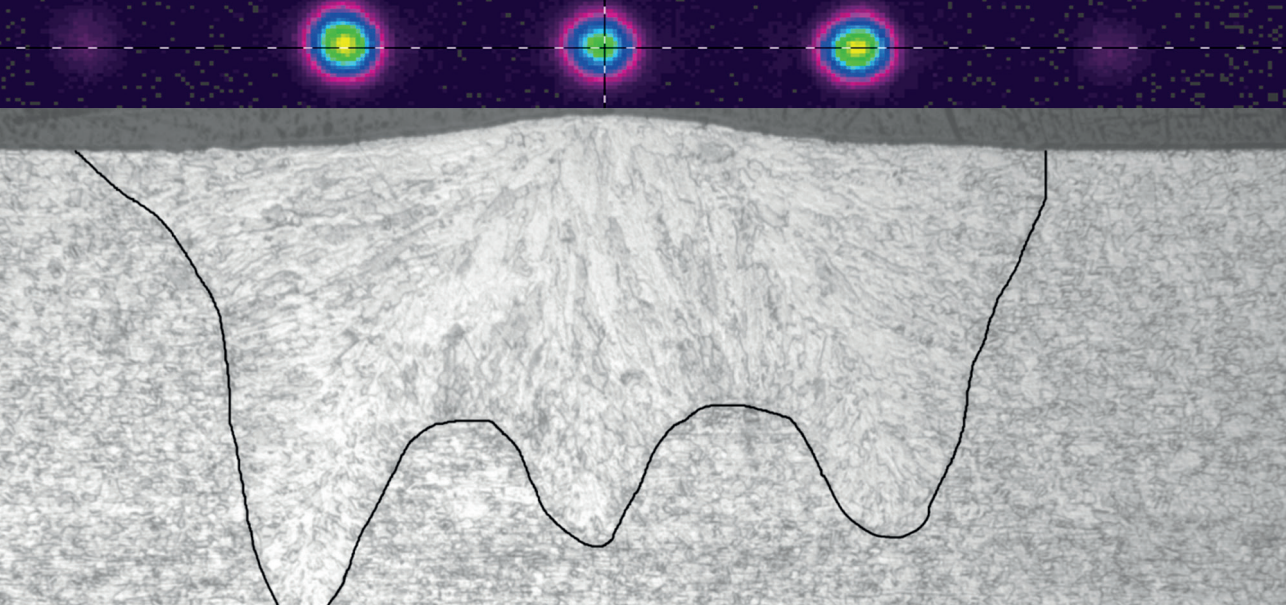
ISSN: N/A

Edited by: Prof. Thomas Graf - Prof. Claus Emmelmann - Prof. Ludger  
Overmeyer - Prof. Frank Vollertsen

DOI: N/A

Copyright is not cleared, article is therefore not reprinted in this version.





## SUMMARY

This dissertation presents work and results achieved in the field of multi beam fiber laser welding. The project has had a practical approach, in which simulations and modelling have been kept at a minimum. Different methods to produce spot patterns with high power single mode fiber lasers have been examined and evaluated. It is found that both diamond turned DOE's in zinc sulphide and multilevel etched DOE's (Diffractive Optical Elements) in fused silica have a good performance. Welding with multiple beams in a butt joint configuration has been tested. Results are presented, showing it has been possible to control the welding width in incremental steps by adding more beams in a row. The laser power was used to independently control the keyhole and consequently the depth of fusion. An example of inline repair of a laser weld in butt joint configuration was examined. Zinc powder was placed in the weld causing expulsion of the melt pool. Trailing beams were applied to melt additional material and ensure a melt pool. The method showed good results for increasing tolerances to impurities and reduction of scrapped parts from blowouts during laser welding.